INVESTIGATION OF VOC REACTIVITY EFFECTS USING EXISTING REGIONAL AIR QUALITY MODELS

Report to
American Chemistry Council
Contract SC-20.0-UCR-VOC-RRWG

William P. L. Carter, Gail Tonnesen and Greg Yarwood[1]
Co- investigators

April 17, 2003

Center for Environmental Research and Technology
College of Engineering
University of California
Riverside, California 92521

---

[1] ENVIRON International Corporation, 101 Rowland Way, Novato, CA 94945

ABSTRACT

The CAMx grid model was used to assess ozone reactivity effects for Carbon Bond (CB4) VOC species and ethane using the CRC-NARSTO database for the July 12-15, 1995 NARSTO-NE episode in the Eastern United States. The ozone sensitivities to emissions changes in NO_x, total VOCs, total anthropogenic VOCs, CO, ethane and the 8 CB4 species used to represent major anthropogenic VOC emissions were calculated using DDM sensitivity analysis. A number of different ozone reactivity scales were derived using various methods to quantify the ozone impacts of the VOC species on the regional scale. These were based on effects of VOCs on daily maximum 1-hour averages in four different episode days, on effects on daily maximum 8-hour averages in three different episode days, and on using six different methods or metrics to derive regional reactivity scales from the varying impacts throughout the modeling domain. The results were compared to relative reactivities calculated with the same chemical mechanism in an EKMA box model used previously to derive the Carter reactivity scales.

The CAMx DDM results showed that there are differences in relative ozone impacts of VOC species with time and location, and that these differences are reflected in the effective ranges of the reactivity scales derived by the various methods. The effective range is the ratio of relative reactivities for the most reactive VOC species to ethane, the compound currently used by the EPA to define “negligible” reactivity. This varies from ~60 (on a carbon basis) for MIR and other scales that represent primarily urban impacts to ~20 to for regional average ozone and other scales that weigh impacts over large regions more equally. However, except for the CB4 TOL model species, whose relative O_3 impacts are much more sensitive to NO_x conditions than comparable model species in other mechanisms, the ordering of reactivity rankings are generally preserved regardless of which region of the domain or quantification method are employed. The relative reactivities derived from regional model results were generally consistent with the results using the EKMA scenarios when derived using comparable metrics. Using 8-hour vs. 1-hour ozone averaging time does not significantly affect relative reactivity scales.

A series of large-scale substitution calculations also were carried out where all anthropogenic VOC emissions were removed or replaced with varying amounts of ethane. The results were generally consistent with expectations based on the DDM first-order sensitivities. Replacing all anthropogenic VOCs (AVOCs) with equal mass or moles of ethane resulted in ozone reductions comparable to, but somewhat less than, removing all AVOCs. If ethane was added back to replace the AVOCs on a “reactivity neutral” basis, ozone tended to increase in the non-urban regions but decrease in VOC-sensitive areas dominated by urban emissions.

ACKNOWLEDGEMENTS AND DISCLAIMERS

The authors wish to acknowledge the many helpful discussions with the active members of the Reactivity Research Working Group (RRWG) that resulted in the design of this project and assisted in the interpretation of the results. We also thank Amir Hakami of Georgia Institute of Technology for providing us with an advance copy of a manuscript on a related project, and Bo Wang of CE-CERT for assistance in data processing.

The opinions and conclusions expressed in this report are entirely those of the authors and to not necessarily reflect the views of the American Chemistry Council or any other participant in the RRWG. Mention of trade names or commercial products does not constitute endorsement or recommendation for use.

TABLE OF CONTENTS

LIST OF TABLES

LIST OF FIGURES

INTRODUCTION

Background

Ground level ozone is formed in a complex series of gas-phase reactions involving the interactions of volatile organic compounds (VOCs) and NO_x in the presence of sunlight. Until recently, the focus of VOC controls has been reducing mass emissions without regard to differences among ozone formation potentials of different types of VOCs, except for exemptions of selected classes of compounds on the basis of "negligible" reactivity. However, VOCs can differ significantly in their impacts on ozone formation, and taking these differences into account in VOC regulations may provide a means to achieve ozone reductions in a more cost-effective manner than regulating all reactive VOCs equally. Indeed, reactivity-based VOC regulations have already been implemented in the state of California (CARB, 1993, 2000). However, there are a number of scientific and policy issues that need to be addressed before reactivity-based regulations can be more widely implemented.

A fundamental problem with reactivity-based VOC regulations is the fact that the effect of a VOC on ozone formation depends significantly on the environment where it is emitted, which means that no single reactivity quantification will be applicable for all conditions. The determination of which quantification to use in regulatory applications that will be applied over widely varying regions therefore involves policy as well as scientific considerations. The current reactivity-based regulations in California are based on the concept that it is most appropriate to quantify VOC reactivity under conditions where ozone formation is most sensitive to VOC emissions (CARB, 1993). This is the basis of the Maximum Incremental Reactivity (MIR) scale (Carter, 1994a, 2000a) that has been adopted in California (CARB 1993, 2000). However, the MIR scale does not represent all conditions where ground level ozone pollution is a problem, particularly regional and long-range transport scenarios where ozone is more sensitive to NO_x controls. In addition, this scale was calculated using highly simplified physical models of ambient airshed conditions. Because of these and other concerns, the EPA believes that more research is needed before reactivity-based regulations should be implemented (RRWG, 1999).

The Reactivity Research Working Group (RRWG) has been organized to coordinate policy-relevant research related to VOC reactivity. In developing a research plan, a consensus was reached that a near-term research priority is to use existing models to address the effectiveness of reactivity-based controls and substitutions on multiple scales, particularly regional model scenarios where many believe that reactivity effects have not been adequately evaluated. A particular concern is whether reactivity-based controls and substitutions may be ineffective or even counter-productive in multi-day transport or stagnation scenarios where low reactivity compounds have longer times in which to react and affect ozone formation. The primary objective is to give policymakers an indication of whether reactivity-based policies are really as potentially effective in reducing ozone on multiple scales as it is hoped, and if so what type of reactivity quantification should be used. An additional objective is to determine what constitutes "negligible" reactivity if current VOC exemption policies are to be continued. Input by policymakers is critical to these assessments, since results must have both relevance and credibility from their perspective in order to be useful in their decision-making.

Objectives

In order to address these research needs, the American Chemistry Council (ACC), an active supporting member of the RRWG, contracted the University of California at Riverside (UCR) and ENVIRON corporation to carry out a study to investigate VOC reactivity effects using an existing regional air quality modeling database available at ENVIRON. Although funded by the ACC, his work was carried out with the oversight and approval of the RRWG as a whole. The proposal for this project listed several possible ENVIRON databases that could be used, but after discussion with the RRWG membership it was decided to focus on the CRC-NARSTO database for the July 7-15, 1995 episode in the Eastern United States. Use of an eastern U.S. scenario is chosen for this initial study because transport is believed to be important in this region, because the effectiveness of reactivity-based substitutions in such scenarios has not been adequately assessed and is considered to be quite uncertain.

This UCR/ENVIRON project for the RRWG include the following specific objectives when assessing reactivity effects in this Eastern U.S. scenario:

- Assessing the extent to which relative ozone impacts of various types of VOCs vary within the regional modeling domain, which includes a wide variation of source and receptor areas.
- Assessing the effects of using different reactivity metrics[2] when quantifying regional ozone impacts. This includes assessing effects of using different methods to quantify ozone impacts at a given location, and using different methods to derive a single reactivity measure that appropriately reflects the multiple impacts in multiple locations.
- Comparison of relative ozone impacts of various types of VOCs derived for this regional modeling domain with their impacts calculated using the EKMA models used to derive the Carter (1994a) reactivity scales.
- Assessing the effects of selected large-scale reactivity based VOC substitutions and the extent to which the effects of large-scale substitutions can be predicted by incremental reactivity scales.
- Assessing alternative approaches for deriving a general reactivity scale representing regional ozone impacts.

Overall this project, whose results are described in this report, was able to address most of these objectives. Relevant policy issues of interest to the RRWG are discussed at the conclusion of this report in light of the results obtained.

---

[2] In the context of this discussion, the term “reactivity metric” refers to a method for deriving a single number that quantifies the reactivity, or relative ozone impact, of a VOC species based on the results of the model calculations of O_3 changes resulting from changes of emissions of the VOC. To derive a metric, one needs to specify how O_3 impacts are quantified at a given location (e.g., by maximum O_3, average O_3, maximum 1- or 8-hour average O_3, etc.), and how to obtain a single number from the distribution of impacts in different locations (e.g., by averaging the impacts, using the impacts in the most sensitive regions, etc.) A “reactivity scale” consists of the set of relative reactivity quantification numbers for the full set of model species or VOC species represented in the calculation.

METHODS

Modeling Database

The modeling database used for this study was the CRC-NARSTO database for the July 7-15, 1995 episode in the Eastern United States. The CRC-NARSTO episode was developed by ENVIRON and is being used in studies sponsored by the Coordinating Research Council[3] (ENVIRON, 2002a). It is not a SIP model, but it has the advantages of having higher resolution than the corresponding SIP models and offering the SAPRC-97 mechanism (Carter et al, 1997a) as an alternative to CB4 (Gery et al, 1988; ENVIRON, 2002b), though as discussed below only CB4 is used in the current study. The database uses 36, 12, and 4-kilometer 2-way nested grids, with the highest resolution grids being centered on New Jersey and the New York Metropolitan area. The emissions data were prepared using EPA Net96 and the meteorological data were prepared using the PSU/NCAR mesoscale model, version 5 (MM5) (Dudhia, 1993). The model domain indicating the grid sizes employed is indicated on Figure 1.

The first five days of the simulation were used for initialization, and the simulation data for those days were not used in the reactivity analysis discussed in this report. Therefore, the episode days used in the analysis in this report are restricted to July 12-15.

Separate analyses of reactivity results are presented for each of the three nested domains indicated on Figure 1. Note that when we refer to the lower resolution 36K or 12K domains we are referring to the entire area within those domains, including the portion that have embedded higher resolution domains, with the data in the lower resolution cells in the areas overlapping the higher resolution domains

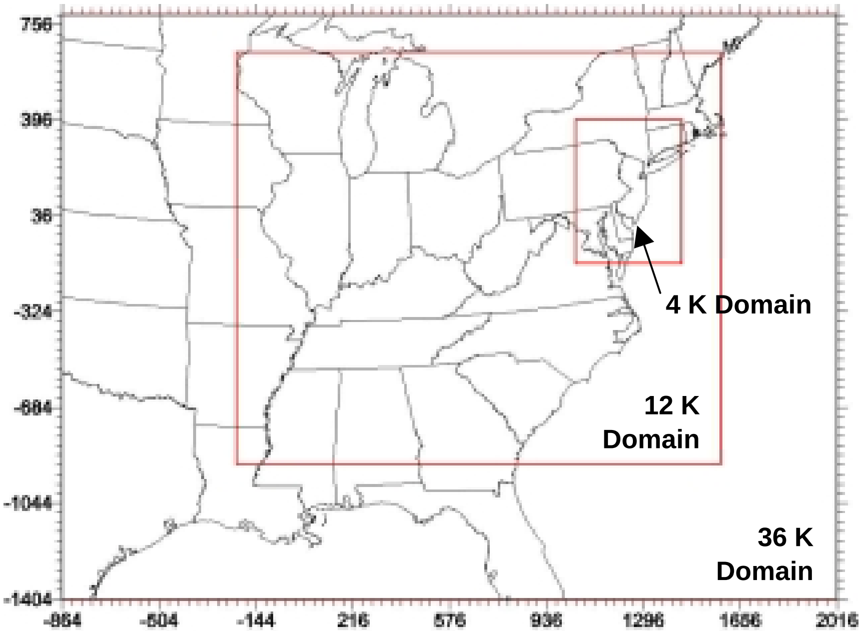

Figure 1. CRC-NARSTO modeling domain used for this study for the July 7-15, 1995 episode.

---

[3] Information about the Coordinating Research Council is available at www.crcao.com.

consisting of averages of data in the higher resolution cells. For example, the data for a 36 km cell in the 36K domain that is also within the 12K domain consists of averages of the data calculated for the 9 12 km cells it overlaps. Likewise, the data for a 12 km cell within the 4K domain consist of averages of the data for the 9 4 km cells it overlaps. Therefore, the data given for the lower resolution domains incorporate the results of the higher resolution calculations for the applicable regions, in the form of averages. This aggregation of fine grid information to overlapping coarser grids is a normal part of the 2-way grid nesting algorithm in CAMx, and is the same approach used in other 2-way nested atmospheric models such as MM5.

Several tables and figures from the report describing the development of the CRC-NARSTO modeling database (ENVIRON, 2002b) are included here to provide an overview of the modeling. Figure 2 summarizes the contributions of major emission categories to the VOC and NOx emission inventories for the entire modeling domain. Figure 3 shows the modeled daily maximum ozone concentrations on July 14th and 15th, 1995 for the 4 km grid covering the Northeast Corridor and using CAMx version 2. Figure 4 shows scatter plots of daily maximum predicted and observed ozone for monitoring sites in the 4 km grid on July 14th and 15th, 1995.

The airshed model, chemical mechanism and the reactivity calculation and data analysis approach used with this modeling database are discussed in the following sections. More detailed information concerning aspects of this modeling domain not discussed here are given elsewhere (ENVIRON, 2002a).

Airshed Model

This CRC-NARSTO database is implemented for the CAMx model, which was developed at ENVIRON and is widely used. CAMx has been used in a number of SIP applications and is fully publicly

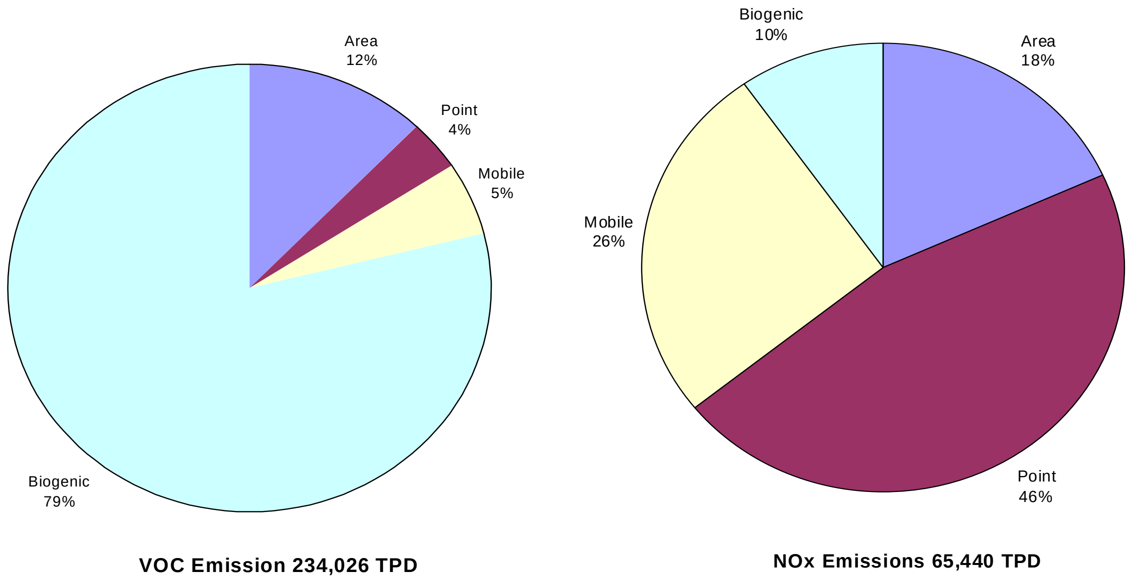

Figure 2. Total VOC and NOx emissions by source category on July 7, 1995 for the CMAQ/CAMx eastern US LCP modeling domain. (From ENVIRON, 2002b).

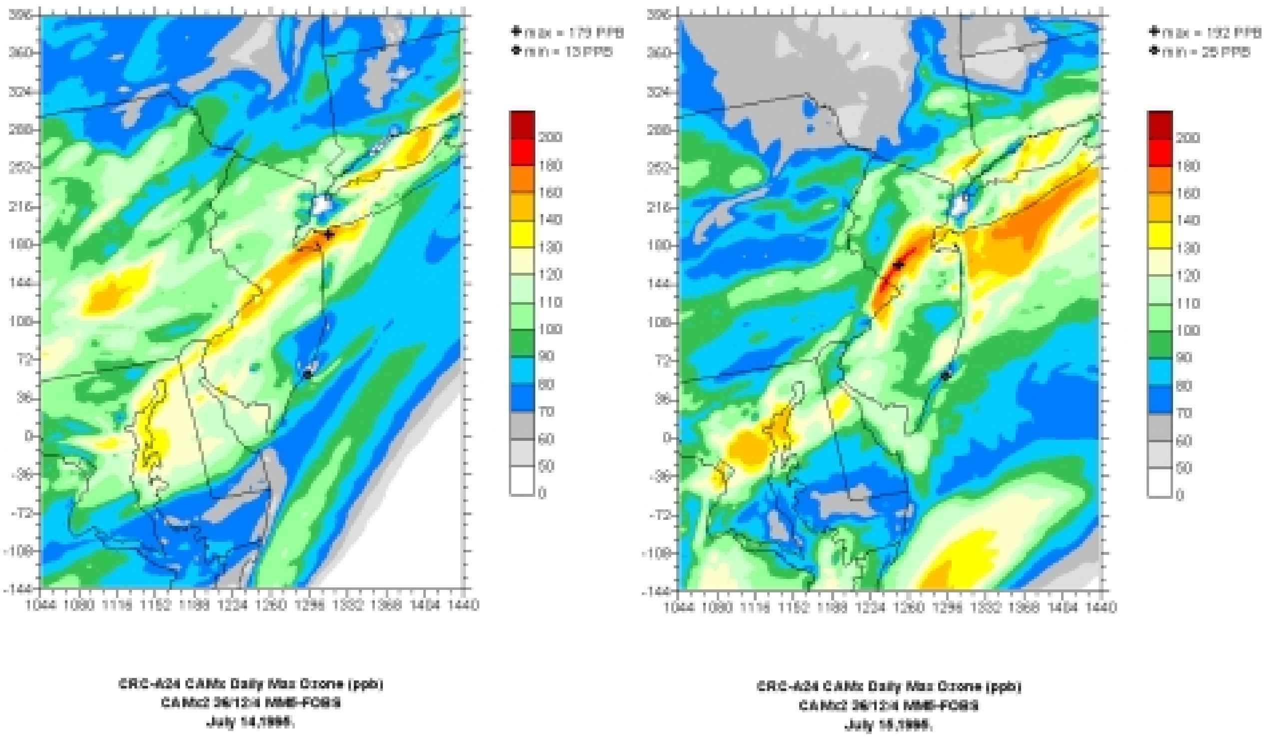

CRC-A24 CAMx Daily Max Ozone (ppb)
CAMx2 36/12/4 MM5-FOBS
July 14,1995.

CRC-A24 CAMx Daily Max Ozone (ppb)
CAMx2 36/12/4 MM5-FOBS
July 15,1995.

Figure 3. Modeled daily maximum ozone concentration on July 14, 1995 (left) and July 15, 1995 (right) for the CRC-NARSTO simulation. (From ENVIRON, 2002b).

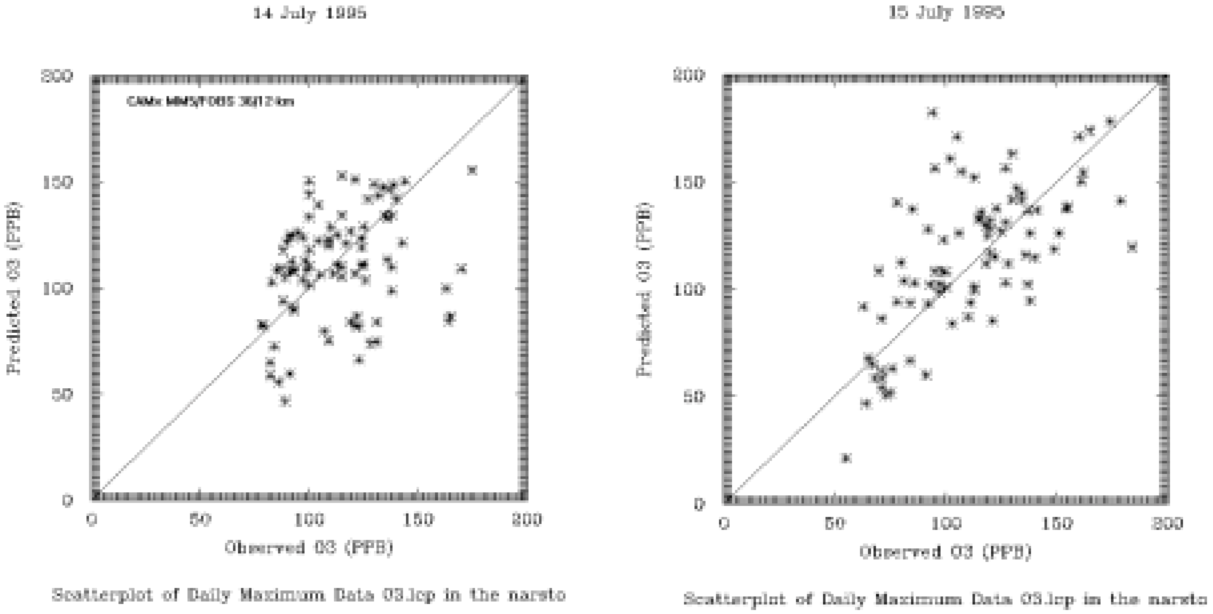

Figure 4. Scatter plots of predicted and observed daily maximum ozone concentrations (ppb) on July 14, 1995 (left) and July 15, 1995 (right) for sites in the Northeast Corridor for the CRC-NARSTO simulation. (From ENVIRON, 2002b).

available[4]. In addition, it includes valuable diagnostic capabilities such as the decoupled direct method (DDM) for sensitivity analysis (Dunker et al, 2002 and references therein) and a detailed chemical process analysis system that has been implemented in CAMx by CE-CERT and ENVIRON (ENVIRON 2002b). The DDM capability was the key to this study, as discussed below. The process analysis capability may be useful in a follow-on study to by potentially providing chemistry-based explanations for the reactivity results obtained. The implementation of DDM in CAMx was funded by the Coordinated Research Council.

A more complete description of the capabilities, operation, and algorithms of the current version of CAMx is provided elsewhere (ENVIRON, 2002b). The chemical mechanism and DDM outputs, which are particularly relevant to this study, are discussed further below.

Chemical Mechanism

Although the database and CAMx model for this episode can support use of either the SAPRC-97 or the CB4 mechanism, it was decided that CB4 would be used in the current project. This is because of the significantly lower cost and because CB4 represents most (though not all) of the important classes of reactive VOCs, allowing reactivity trends for the major classes to be assessed with the minimum number of species and computational overhead. As discussed below, this is considered to be appropriate for the objectives of the current project.

However, use of the Carbon Bond mechanism does have some disadvantages that must be taken into account when assessing the results of this study. It was developed in the late 1980's (Gery et al, 1988) so it does not represent the current state of knowledge of atmospheric chemistry. Some modifications were made to correct for problems in its representation of peroxy + peroxy reactions at low NO_x conditions, and to update the isoprene mechanism to be consistent with the isoprene mechanism of Carter (1996) (ENVIRON, 2002b). It is highly condensed, which means that it cannot be used to predict the impacts of most individual VOCs, except in an approximate manner. It has inappropriate or no representation of some important types of VOCs, as discussed below. In addition, comparison of box model reactivity results suggest that the Carbon Bond mechanism may be more sensitive to radical initiation and termination effects than current mechanisms (Jeffries and Crouse, 1991; Hales et al, 1993), which may affect the spatial variability of the reactivity results.

Nevertheless, the CB4 mechanism was considered suitable for at least an initial and qualitative assessment of variability of reactivity effects within a regional modeling domain, which is a major objective of this study. Calculations to verify the reactivity trends using this mechanism can be conducted using the more up-to-date and chemically detailed mechanisms in a later phase of this project, if appropriate, or by comparison with results of SAPRC-99 simulations of this same episode being carried out by Russell and co-workers for other RRWG projects.

Because of the importance of ethane in the current EPA reactivity policy (Dimitriades, 1999), a model species representing this compound explicitly was added to this mechanism for this work. The ethane mechanism is based on that used in SAPRC-99, using the appropriate CB4 species, ALD2, to represent the formation of acetaldehyde, its major photooxidation product. A complete listing of the reactions and rate constants in the mechanism is given in Appendix A to this report.

---

[4] Documentation and source code for CAMx are available at http://www.camx.com.

Table 1 lists the VOC model species in the version of the CB4 mechanism used in this project, and the types of compounds whose reactivity characteristics they represent. The table also indicates the types of compounds that are either not represented or (in our opinion) not appropriately represented in the current version of the mechanism. It also indicates the distribution of species used to represent the base ROG composition for the purpose of relative reactivity assessment, as discussed later in this report.

Table 1 indicates that the Carbon Bond 4 mechanism represents the major classes of reactive VOCs that must be considered when modeling ozone formation, though with two major exceptions. These are internal alkenes, whose emissions are represented only by the emissions of their reactive products, and radical inhibiting compounds, which are not represented at all. These omissions are probably not significant when representing entire emissions because the initial reactions of the internal alkenes are probably not as important in terms of overall impacts as the reactions of their products, and because the overall contribution of radical inhibiting compounds in current emissions profiles is relatively small. However, this means that the reactivity characteristics of these types of compounds are not represented in the model simulations in this work.

Toluene is an important compound in the emissions, and the TOL model species used to represent it is also used for other monoalkylbenzenes and lower reactivity aromatics. However, as indicated on Table 1, the TOL model species in the current mechanism may not appropriately represent the reactivity characteristics of these compounds. In particular, the CB4 TOL model species is calculated to have O_3 reactivities that are much more sensitive to NO_x conditions than is calculated for toluene in the SAPRC mechanism (Jeffries and Crouse, 1991; Hales et al, 1993). This is probably primarily because the CB4 mechanism uses a very high (36%) cresol yield, while currently accepted product data indicate that the yield is more likely in the ~20% range (Carter, 2000a and references therein). However, the atmospheric chemistry of aromatics contains many uncertainties (Calvert et al., 2002) and, since both the CB4 and SAPRC mechanisms for toluene contain parameterization of unknown processes with adjustments to fit chamber data, it is possible that no current mechanism appropriately predicts the ozone impacts of this compound. Mechanism differences other than the cresol yield may also contribute to the significantly different reactivity characteristics predicted for toluene by the CB4 and SAPRC mechanisms.

It is possible that the reactivity characteristics of toluene, in terms of dependences on environmental conditions is better represented by those predicted for the CB4 XYL (xylene) model species, though the magnitude of the impacts would be greater than is the case for toluene because of the greater reaction rate and higher yields of radical initiators. The reactivity characteristics of the CB4 TOL model species is probably more indicative of those of styrenes or phenols, whose reactivities are calculated to be highly dependent on NO_x conditions in the SAPRC-99 mechanism (Carter, 2000a). Since a comprehensive reactivity assessment should include considerations of such compounds, the reactivity characteristics calculated for the TOL model species is still of interest in this study.

Base ROG Mixture

The impacts of VOCs on ozone formation are known to be highly dependent on environmental conditions, particularly availability of NO_x (Carter and Atkinson, 1989, RRWG, 1999 and references therein). However, since the purpose of this project is assess the effects of VOC substitutions, the quantities of interest in this study are *relative* reactivities, i.e., ratios of incremental reactivities of the VOCs to some standard compound or VOC mixture. These would be expected to be less variable with conditions because the effects of variability of sensitivities of O_3 to VOCs in general are factored out. It is the variability of the relative reactivities that must be considered when assessing impacts of reactivity-based VOC substitution policies.

Table 1. List of Carbon Bond 4 VOC model species, indicating those whose ozone sensitivities were studied for this project. The types of compounds whose reactivity characteristics that are not represented by this mechanism are also indicated.

Species	Compounds Represented	Base ROG contribution (millimoles/ mole C)
	<u>CB4 species whose ozone sensitivities were calculated</u>	
PAR	Primarily $C_4 - C_6$ alkanes (one PAR for each carbon). Also used in the model to represent extra carbons on other molecules. Mechanism based on $C_4 - C_6$ alkanes (1 carbon)	547
ETH	Ethene (represented explicitly) (2 carbons)	21
OLE	Propene and other 1-alkenes (mechanism based on propene) (2 carbons)	20
TOL	Used to represent toluene and monoalkylbenzenes in emissions, but gives reactivity results that may be inappropriate for these compounds. However, its reactivity characteristics may be indicative of those for styrenes and phenols. See text. (7 carbons)	12
XYL	Xylenes and other polyalkylbenzenes (8 carbons)	8
FORM	Formaldehyde (represented explicitly) (1 carbon)	10
ALD2	Acetaldehyde and higher aldehydes (mechanism based on acetaldehyde) (2 carbons)	19
ETOH	Ethanol (represented explicitly) (2 carbons)	21
ETHA	Ethane (represented explicitly). Not represented in the standard CB4 mechanism but added for the purpose of this study. (2 carbons)	
CO	Carbon Bond (explicitly represented) (1 carbon)	
	<u>CB4 species whose ozone sensitivities were not calculated</u> <u>(reactivity contribution to the base ROG neglected)</u>	
ISOP	Isoprene (represented explicitly)	0.4
MEOH	Methanol (represented explicitly)	5
UNR	Unreactive compounds (has reactivities of zero by definition).	124
	<u>Chemical Compounds not adequately represented by available CB4 species</u>	
	Internal alkenes. (Only their products are represented; effects of initial OH and O_3 reactions are ignored.)	
	Toluene. (Reactivity characteristics of the TOL model species not considered representative of this compound. See text.)	
	Radical inhibiting VOCs such as benzaldehyde or high molecular weight alkanes. (No model species in the mechanism with strong radical inhibiting characteristics.)	

In this work, relative reactivity is defined as the ratio of the incremental reactivity of the compound or model species to the incremental reactivity of a standard mixture designed to represent the composition of anthropogenic VOC emissions from all sources. This is referred to as the "base ROG mixture" in the subsequent discussion. Defining relative reactivity in terms of base ROG mixture is a useful definition from a policy perspective because it gives a measure of the relative benefit (or disbenefit) of regulating or increasing emissions of this compound alone compared to regulating or increasing emissions from all VOC sources equally. For example, if a compound has a relative reactivity of 2 it means that a control strategy that reduces emission of that compound alone will have twice the O_3 reduction of a control strategy that reduces all VOC emissions by the same amount.

The base ROG mixture should approximate the composition of the total mixture of all non-methane anthropogenic VOC emissions into the models. Although the total emissions composition should generally be very similar for current regional models using the same generation of emissions inventories, there may be slight differences among the modeling databases used in the RRWG studies. To facilitate comparisons with other studies, it is more important that the same mixture be used as the standard than that they necessarily exactly represent the emissions inventory used in each simulation, which may differ in some respects among the models, provided that the standard mixture is reasonably representative.

Because the RRWG modeling studies are national in scope, the base ROG mixture to be used for this study consists of the mixture of VOCs from the total emissions profile that was provided by the EPA to represent total anthropogenic emissions into regional models (EPA, 1998). This composition was used to derive the fixed parameter version of the SAPRC-99 mechanism for Models-3 (Carter, 2000b). Although this may not be exactly the same as the composition of the total anthropogenic emissions profiles used in the specific model in this study, and may not necessarily reflect the current state of the EPA's emissions databases (see comments in the EPA, 1998 reference), it is considered to be a sufficiently close approximation for the purpose of this study.

The composition of the base ROG is specified in terms of moles of model species per mole carbon of base ROG. The data provided by the EPA (1998) were provided in terms of mass emissions of EPA SAROAD classes. Methane was removed from the mixture, and the non-methane composition was converted into molar emissions of SAPRC-99 and other mechanism model species using emissions assignments made for use with a comprehensive emissions database that is in preparation (Carter, 2002a). Note that some of the compounds that were not assigned to SAPRC-99 species have assignments to carbon bond species, either from previous emissions assignments or made by Carter (2002a). Approximately 99% of the mass of the emitted non-methane organics in the EPA emissions profile could be assigned to Carbon Bond species using this approach. The emissions were normalized to give moles of model species per mole carbon of base ROG.

The base ROG composition in terms of moles carbon bond species is given on Table 1, and Figure 5 shows the distributions in terms of carbon and reactivity. The reactivity distributions were derived using EKMA MIR scale, derived for this version of the Carbon Bond mechanism as discussed below. In terms of carbon distributions (which approximates mass), more than half of the base ROG is PAR and approximately 2/3 are PAR + unreactive VOCs, about 15% are aromatic species and the remainder are the various other species. When weighted by reactivity contribution, the various reactive species become more comparable in their contributions, with no single species contributing more 20% of the overall ozone impact as estimated using the MIR scale.

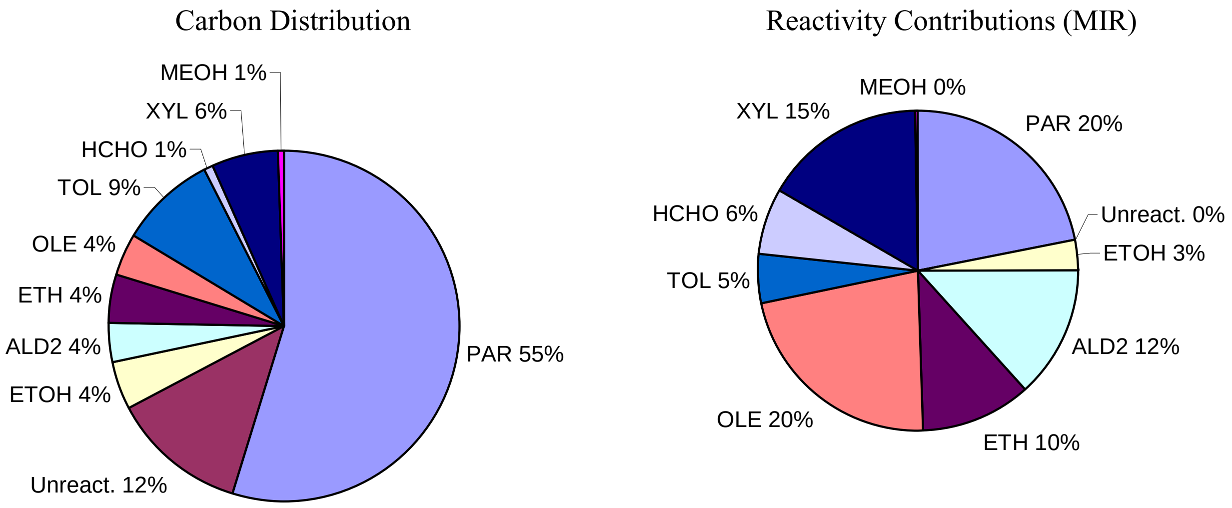

Figure 5. Relative carbon and reactivity distributions of the carbon bond species used for the base ROG surrogate used to compute relative reactivities.

DDM Calculations

For the current phase of this project, the changes in ozone formation caused by incremental changes of various types of model species were calculated using the decoupled direct method (DDM) as implemented in CAMx (Dunker et al, 2002, ENVIRON, 2002b). These sensitivities were calculated as a function of time and space and output as hourly averages for all the ground level cells. Three separate DDM calculations were carried out, using the same episode as the base case. Sensitivities of other model species besides O_3 to changes in the emissions were also calculated, but in this work we will consider O_3 sensitivities.

Note that even though the discussion here characterizes the DDM simulations as calculating the effects of changes of emissions, technically the DDM simulations do not involve actually changing any emissions. Instead, the DDM method involves calculating derivatives with respect to emissions or other inputs by appropriate differentiation of the model equations (Dunker, 1980; Dunker et al, 2002, ENVIRON, 2002b). However, since the results should be the same as one would obtain by actually varying emissions [and test calculations have shown this to be the case (Dunker et al, 2002)], for simplicity this is how they will be referred to in the discussion in this report. The DDM method implemented in CAMx has advantages of accuracy and efficiency compared to the "brute-force" approach of varying emissions inputs. The DDM can be used to calculate sensitivities for model species other than ozone simultaneously.

In the first DDM calculation, the sensitivities to changes in total VOC and NO_x emissions were computed. The results gave ppm changes in ground-level O_3 per fractional change in emissions, e.g., an ozone sensitivity to total VOC of 10 ppb means that a 10% increase in all VOC emissions would cause a 1 ppb increase in ozone. Note that the VOC emissions that were varied in this calculation included biogenic as well as anthropogenic VOCs, so the results of the VOC sensitivity calculations were not the same as the results of the base ROG sensitivity calculations, which represent variations in anthropogenic emissions derived from the second DDM calculation. This is discussed further below.

In the second DDM calculation, the sensitivities to changes in surface emissions of CO and the VOC model species listed in Table 1 were calculated. The emissions varied had the same time and space distribution of the total anthropogenic VOCs. Note that this is different than the time and space variation of the total VOC used in the first DDM calculation because biogenics were not included in the second calculation. The results give the ppb changes in ozone relative to fractional changes in total anthropogenic VOC emissions, with the added anthropogenic VOC emissions represented by the single model species with the same number of carbons. For example, an ozone sensitivity to OLE of 10 ppb means that increasing the total anthropogenic VOC emissions by 10%, and representing all of this increase by the same number of carbons of OLE, will cause O_3 to increase by 1 ppb. Note that because OLE has two carbons the number of moles of OLE added to cause this change is half as much as the number of carbons, which means that the impact on a molar basis is twice as much (since the amount added is in the denominator). This method gave the sensitivities of ozone to the model species to the model species on a per carbon basis. These were multiplied by the carbon numbers of the model species to get the sensitivities on a mole basis, which are the units used in this report. Table 1 indicates the carbon numbers that were used for this purpose.

In the third DDM calculation, the sensitivities to changes in emissions of various types of anthropogenic VOCs were computed. Note that this is not the same as the total VOC sensitivities that were computed in the first DDM calculation where the total VOC sensitivities included the significant contribution of biogenics. In addition to sensitivities to total anthropogenic VOC, sensitivities were also computed for changes in emissions of the three major anthropogenic VOC classes, namely mobile, area, and point sources. The units of the results were the same as for the first series of calculations, i.e., the results gave ppm changes in O_3 per fractional change in anthropogenic emissions. Note that the sum of the sensitivities for the three classes of anthropogenic emissions should exactly equal the total anthropogenic VOC sensitivities that were calculated, and this indeed was found to be the case.

These DDM sensitivities of ozone with respect to the model species as derived in the second calculation provided the *incremental reactivities* of these species, which is defined as the change in O_3 caused by adding the model species to the emissions, divided by the amount added. The amount added is relative to the total anthropogenic VOC emissions, which is the same for all of the VOC model species. Since in this work we are concerned with relative reactivities only, no attempt was made to convert these into absolute incremental reactivity units such as moles O_3 per mole of model species. This is because the conversion factor of the molar DDM sensitivities to absolute incremental reactivities is the same for all species, so it cancels out when computing relative reactivities.

The incremental reactivity of the base ROG mixture that was used as the basis of deriving the relative reactivities was calculated from the incremental reactivities of the model species and the emissions weighted contribution of the model species to one mole carbon of the base ROG, as given on Table 1, i,e.,

$$\begin{aligned}\mathrm{IR(Base\ ROG)} = {} & 0.547\ \mathrm{IR(PAR)} + 0.021\ \mathrm{IR(ETH)} + 0.020\ \mathrm{IR(OLE)} + 0.012\ \mathrm{IR(TOL)} + \\ & 0.008\ \mathrm{IR(XYL)} + 0.010\ \mathrm{IR(FORM)} + 0.019\ \mathrm{IR(ALD2)} + 0.021\ \mathrm{IR(ETOH)}\end{aligned}$$

where IR(Base ROG) is the incremental reactivity of the base ROG in terms of ozone formed per carbon of base ROG mixture, IR(PAR) is the incremental reactivity of the PAR species in terms of ozone formed per mole PAR, etc.

As indicated on Table 1, DDM sensitivities and therefore incremental reactivities were not calculated for all CB4 species used to represent the base ROG. The contributions of these species were not counted when computing the base ROG reactivity. The contributions of these species are small, so neglecting them should have no significant effect.

Note that an alternative to using the sensitivities to the base ROG mixture as the standard for deriving relative reactivities would be to use the sensitivities to the total anthropogenic VOC emissions as derived in the third DDM calculation. This approach was not used in order to provide a more straightforward comparison to results of the EKMA model reactivity calculations, and of other regional reactivity modeling studies being carried out for the RRWG. However, as discussed later, the sensitivity to the total anthropogenic VOCs was found to be very close to those to the base ROG mixture, as one might expect.

Reactivity Metrics Used

In order to derive reactivity quantifications using regional models, it is necessary to specify the time period being covered, the portions of the domain that are included in the analysis, the method used to quantify the ozone impact in a given cell, and the method used to derive a single reactivity metric from the results throughout the domain. The specific approaches employed in this study are described below.

Episode Days Used

For the purpose of this study, each 24-hour period of the multi-day simulation is treated as a separate "episode" for the purpose of deriving a regional reactivity metric using the various ozone impact and multi-cell reactivity quantification methods. This is appropriate because even though the ozone on a given day is affected by ozone formed on previous days, the meteorology, and thus the transport phenomena and the resulting spatial pattern of where the highest ozone occurs, can be quite different on each day. The episode day is defined as being from midnight to midnight, Eastern Standard Time. Since the data from the calculations are stored as 1-hour averages given for the ending hour, this means that the data used for a given day are the hourly averages associated with 1 AM to midnight. Note that the "midnight" (Hour 24) data go with the day that ended and not the day that is beginning because it is the average for the previous hour.

As indicated above, because of the desire to remove the influences of initial and boundary conditions, and because the high-resolution simulations did not begin until July 11, the results from the first five days of the simulation (July 7-11) are not used in the analysis. In addition, the CAMx simulations ended at 1800 EST on July 15, so July 15 could not be used for computing the 8-hour averages (see below). Therefore, the episode days considered in this study were July 12-15 for the 1-hour average metrics and July 12-14 for the 8-hour metrics derived from 8-hour averages. As shown below each of these days had differences in ozone spatial patterns, indicating that they represent different conditions of meteorology and transport.

Quantification of Ozone Impact in a Cell

Ozone impacts can be quantified in a number of ways, and the most appropriate method depends on the objectives of the analysis. Since the RRWG studies are ultimately aimed at guiding policies aimed at achieving the ambient air quality standards for ozone, the most appropriate quantification is probably in terms of the quantification used in the standards. These are daily maximum 1-hour and 8-hour average ozone levels. Since effects of VOCs on 8-hour averages may be different than affects on 1-hour levels, both methods are considered in this study.

The metrics based on 1-hour ozone impacts were derived by determining the hour in the simulated day that had the highest average ozone for that hour, and using the DDM sensitivities for that hour to derive the incremental reactivities of the model species and the base ROG associated with this cell for this episode day. These give the relative impacts of the VOCs on the peak 1-hour ozone concentration in that cell.

Likewise, the metrics based on 8-hour ozone impacts were derived by determining the hour in the simulated day that had the highest 8-hour average associated with it, and using the averages of the DDM sensitivities for those 8 hours to determine the incremental reactivities for that cell and episode day. (The averages of the DDM sensitivities reflect the sensitivities for the average because averages are essentially sums, and derivatives of sums are sums of derivatives.) Since the regulatory definition of 8-hour averages associates the average with the *beginning* hour of the averaged data, for this study the 8-hour averages associated with a given hour are derived by averaging the data for that hour and the 7 following hours. Note that the 8-hour averages assigned to hours after 1600 involve averaging in data for the following day. Therefore the morning data for July 15 were used when computing the 8-hour average metrics for July 14, the last day for which 8-hour reactivity metrics could be computed.

Computation of Global Reactivity Metrics

The procedures discussed above will in effect give thousands of relative reactivity scales for each of the two impact metrics, one for each grid cell for each day. This provides useful information on how reactivities by these metrics vary with location for the different types of episode days, which addresses one of the objectives of this study. However, most types of quantitative reactivity-based analyses require derivation of a single scale (or at least a manageable number of scales) that appropriately represents the distribution of impacts throughout the episode. There are many alternative approaches that can be used to derive such a global reactivity metric, and the seven alternative approaches examined in this study are only a subset of the many other possibilities that might be considered. These are summarized in Table 2 and discussed in more detail below.

Table 2. Summary of alternative global reactivity metrics examined in this report

Designation	Description
Regional Average Ozone	Average of incremental reactivities (absolute O_3 impacts) throughout the entire domain. Same as effect of the VOC on the domain-wide average ozone.
Regional Maximum Ozone	Relative reactivities at the grid cell where the domain-wide maximum O_3 concentration occurs.
Regional Average O_3 Over the Standard	Average of incremental reactivities (absolute O_3 impacts) for all grid cells where the ozone levels exceeds the specified standard (120 ppb for daily 1-hour maximum, 80 ppb for daily 8-hour maximum).
Minimum Substitution Error (two methods)	Relative reactivity that minimizes the change in ozone (substitution error) resulting from reactivity-based substitutions. (Two alternative methods are examined based on the types of substitution, but the preferred method is that based on substitutions of the base ROG for the model species)
Regional MIR	Relative reactivities at the grid cell where the incremental reactivity (O_3 impact) of the base ROG mixture (total anthropogenic VOC emissions) are the highest.
Regional MIR to MOIR	Average of incremental reactivities (absolute O_3 impacts) for all grid cells where NO_x emissions have a negative impact on O_3 formation. Note that these cells represent MIR to MOIR conditions according to the definition of Carter (1994a).

Regional Average Ozone Metric

Perhaps the simplest of the true global reactivity metrics is to use the effects of the VOCs on the average or total amount of ground-level ozone formed in the modeling domain. This reflects the effects of the VOCs on ozone formation in all locations, weighting ozone at all locations equally. Since incremental reactivities are derivatives, and derivatives of sums are sums of derivatives, the incremental reactivities of a VOC species with respect to average and total ozone in the domain are given by

$$\mathrm{IR(Species)}^{\mathrm{Total\ O3}} = \Sigma_{\mathrm{cells}}\ \mathrm{IR}_{\mathrm{cell}}\mathrm{(Species)}$$

$$\mathrm{IR(Species)}^{\mathrm{Average\ O3}} = \Sigma_{\mathrm{cells}}\ \mathrm{IR}_{\mathrm{cell}}\mathrm{(Species)}/\mathrm{N}_{\mathrm{cells}} = \mathrm{IR(Species)}^{\mathrm{Total\ O3}}/\mathrm{N}_{\mathrm{cells}}$$

where $\mathrm{IR}_{\mathrm{cell}}$(Species) is the ozone sensitivity for the species in a cell, and $\mathrm{N}_{\mathrm{cells}}$ is the number of cells in the domain. Since the relative reactivities are ratios of incremental reactivities of the species to the incremental reactivities of the base ROG, these are given by

$$\mathrm{RR(Species)}^{\mathrm{Average\ O3}} = \mathrm{RR(Species)}^{\mathrm{Total\ O3}} = \Sigma_{\mathrm{cells}}\ \mathrm{IR}_{\mathrm{cell}}\mathrm{(Species)}\ /\ \Sigma_{\mathrm{cells}}\ \mathrm{IR}_{\mathrm{cell}}\mathrm{(Base\ ROG)} \qquad \mathrm{(I)}$$

Note that the relative reactivities with respect to total and average O_3 are the same, since the only difference between the incremental reactivities is the factor reflecting the number of cells, which is a constant that factors out when taking the ratio for computing the relative reactivities.

This metric does give somewhat greater weight to cells with higher sensitivities of O_3 to the VOC species or the base ROG, because the cells with the higher incremental reactivities (O_3 sensitivities) contribute more to the sums in Equation (I) than those with lower IR values. However, this weighting of the sensitive cells is not as great as is the case for the minimum substitution error metrics, discussed below.

One problem with this metric is that it weighs the contribution of the VOCs to O_3 formation in the many low O_3 cells equally with the cells where O_3 approaches or exceeds the air quality standards. This can be addressed by not including the low O_3 cells in the averages in Equation (I). The effects of using different O_3 cutoff levels in computing the regional average O_3 metric is examined in this work, and two special cases of this are considered. The most extreme case of this is the "Regional Maximum Ozone Metric," which counts only the cell with the very highest ozone levels. A second, less extreme example is the "Regional Average Ozone O_3 Over Standard Metric," which counts only the cells where O_3 is above the 1-hour or 8-hour standard. These alternative metrics are discussed below.

Regional Maximum O_3 Metric

An alternative metric that might be appropriate if the policy is to reduce the highest O_3 levels is to base the global metric on the impacts of the VOCs on the maximum ozone concentration throughout the domain. This is given by

$$\mathrm{RR(Species)}^{\mathrm{Max\ O3}} = \mathrm{IR}_{\mathrm{cell\ with\ highest\ O3}}\mathrm{(Species)}\ /\ \mathrm{IR}_{\mathrm{cell\ with\ highest\ O3}}\mathrm{(Base\ ROG)} \qquad \mathrm{(II)}$$

This is one of the metrics that was examined in the regional reactivity modeling studies carried out by Russell and co-workers (e.g., Hakami et al, 2002). If each episode day is treated separately, this would involve finding the hour and cell that has the highest maximum O_3 concentration (either 1-hour or 8-hour averages, depending on the quantification used), and using the relative reactivities in that hour in that cell as the global reactivity metric. It should be noted that this is not a true global metric because it reflects impacts in only a single cell. However, comparing maximum ozone reactivities on different days give an indication of how ozone impacts are affected in different regions, since the location of the ozone maximum, and the meteorological conditions giving rise to it, are different in the different episode days.

Hakami et al (2002) refer to this metric as the "3-D MOIR," since it refers to conditions where the maximum ozone occurs. However, it should be pointed out that the cell where the O_3 maximum occurs may not necessarily represent MOIR conditions according to the definition used by Carter (1994a) when deriving the MOIR scale. Carter (1994a) defines MOIR conditions where NO_x levels are optimum for ozone formation, which means that a true MOIR cell is one where either increasing or decreasing NO_x emissions would reduce the O_3 concentration. This is mathematically equivalent to the cell having a local NO_x sensitivity (derivative) of zero. In fact the results of our calculations indicate that the maximum ozone concentration usually (but not always) occurred in quite NO_x sensitive cells, as indicated by relatively large and positive sensitivities to NO_x emissions in those cells. This may be due to the highest O_3 being formed as a result of long-range transport into NO_x limited regions.

Regional Average O_3 Over Standard Metric

As discussed below in the Results section, the regional maximum O_3 metric tends to give highly variable results because the chemical conditions of the highest O_3 cell can vary significantly depending on the meteorology of the episode day, and in some cases the domain-wide maximum O_3 can be relatively insensitive to anthropogenic VOCs. This suggests that the regional maximum O_3 metric is not particularly robust and probably not suitable for deriving general reactivity scales. An alternative approach that still reflects the effects of the VOCs on the highest O_3 levels is to use a special case of the regional average O_3 metric where only the cells where O_3 exceeds the air quality standards. This is given by

$$\mathrm{RR(Species)}^{\mathrm{Avg\ O3 > Std}} = \Sigma_{\mathrm{cells\ with\ max\ O3>O3std}}\ \mathrm{IR_{cell}(Species)} / \Sigma_{\mathrm{cells\ with\ max\ O3>O3std}}\ \mathrm{IR_{cell}(Base\ ROG)} \quad \mathrm{(III)}$$

Where "O3std" is the ozone air quality standard, which is 0.12 ppm for if the maximum 1-hour average quantification is used, or 0.08 ppm if the metric is based on the 8-hour average quantification. Because this reflects impacts over a number of cells, this should yield a somewhat more robust and less variable metric than the regional maximum O_3 metric, yet give results of similar utility from a policy perspective.

Minimum Substitution Error Metrics

One of the applications of reactivity-based regulatory policies might be to use reactivity scales to predict effects of substitution of one type of VOC for another. If a global reactivity scale were perfect, i.e., if relative ozone impacts of VOCs were the same in all cells and the scale used reflected these impacts, then a substitution of one type of VOC for another using an appropriate reactivity adjustment would result in no change in ozone in any of the cells. Since relative impacts indeed vary, any substitution, no matter what weighting factor is used, would cause ozone changes in at least some of the cells. The total ozone change in all the cells, quantified by some appropriate method, is referred to as the "substitution error" in this discussion. The best one could hope for would be to obtain optimum weighting factors that minimize substitution errors that result when reactivity-based substitutions are made. The reactivity scale that yields these optimum weighting factors are referred to as minimum substitution error scales.

A useful way to quantify substitution error is the sum of squares of the ozone change in all the cells being considered. Sum of squares is appropriate because it counts positive and negative errors equally, and weighs larger errors more than smaller ones by increasing factors. It is generally the approach used in optimizations such as line fits, etc.

The substitution errors will depend on the type of substitution being considered. Since we are interested in relative reactivities, the relevant substitutions are replacing the VOC by the base ROG, or vise-versa. It turns out that in general different results are obtained depending on which is being substituted for what, so alternative global metrics are derived based on the two possibilities, discussed in the following two sections.

Minimum Substitution Error Method 1 (MSE 1): Base ROG for VOC

In the first minimum substitution error option, we consider the effect of removing the VOC whose relative reactivity is being assessed (test VOC) and replacing it by the base ROG by a factor equal to the amount of test VOC removed times the test VOC's relative reactivity. Since the relative reactivity of the test VOC is the ratio of the change in O_3 caused by adding the VOC to that caused by adding the base ROG, the net change in O_3 in a cell caused by this substitution should be zero if the appropriate relative reactivity value for that cell were employed. For all the cells, the sum of squares substitution error would be given by

$$\text{Sum of Squares Substitution Error} = \Sigma_{\text{cells}}\ [\text{RR(test VOC)}\cdot\text{IR}_{\text{cell}}(\text{Base ROG}) - \text{IR}_{\text{cell}}(\text{test VOC})]^2 \quad \text{(IV)}$$

where RR(test VOC) is the relative reactivity of the test VOC the global reactivity scale, $-\text{IR}_{\text{cell}}$(test VOC) is the ozone reduction in the cell caused by removing one unit of the species from the emissions, and RR(test VOC)$\cdot\text{IR}_{\text{cell}}$(Base ROG) is the ozone increase caused by replacing it by the reactivity-adjusted amount of base ROG. Note that this is based on a linear approximation for estimating effects of substitutions from incremental reactivities, and is strictly speaking valid only for small substitutions. However, this is still appropriate because this is an incremental reactivity scale.

The value of RR(test VOC) that minimizes this sum of squares substitution error is given by

$$\text{RR}^{\text{MSE 1}}(\text{test VOC}) = [\Sigma_{\text{cells}}\ \text{IR}_{\text{cell}}(\text{test VOC})\ \text{IR}_{\text{cell}}(\text{Base ROG})]\ /\ [\Sigma_{\text{cells}}\ \text{IR}_{\text{cell}}(\text{Base ROG})^2] \quad \text{(V)}$$

Note that this is the same as the slope of a least squares fit line, forced through zero, of plots of IR_{cell}(test VOC) vs. IR_{cell}(Base ROG). Examples of such plots are given in the Results section, below. Note, however, that the line has no intrinsic meaning beyond the fact that its slope is mathematically equivalent to the least squares substitution error relative reactivity.

Minimum Substitution Error Method 2 (MSE 2): VOC for Base ROG

Although substituting the base ROG for the test VOC may be considered as a rough analogue to reactivity-based strategies aimed at reducing emissions of highly reactive compounds, much of the interest in reactivity-based controls in recent years has been on substituting current emissions with VOCs with low reactivity. A better analogue to this would be substituting the test VOC for the base ROG. An appropriate reactivity scale for this type of substitution may be one based on minimizing the substitution error caused by removing the base ROG and replacing it by the test VOC by an appropriate reactivity adjusted factor. This factor would be the ratio of the ozone formed by the base ROG to the ozone formed by the test VOC, which is the reciprocal of its relative reactivity. Under this scenario, the sum of squares substitution error is given by

$$\text{Sum of Squares Substitution Error} = \Sigma_{\text{cells}}\ [\text{IR}_{\text{cell}}(\text{Base ROG}) - \text{IR}_{\text{cell}}(\text{test VOC})/\text{RR(test VOC)}]^2 \quad \text{(VI)}$$

and the RR(Species) that minimizes this is given by

$$\text{RR}^{\text{MSE 2}}(\text{test VOC}) = [\Sigma_{\text{cells}}\ \text{IR}_{\text{cell}}(\text{test VOC})^2]\ /\ [\Sigma_{\text{cells}}\ \text{IR}_{\text{cell}}(\text{test VOC})\ \text{IR}_{\text{cell}}(\text{Base ROG})] \quad \text{(VII)}$$

Note that in this case the global relative reactivity is the same as the slope of a least squares fit line, forced through zero, of plots of IR_{cell}(Base ROG) vs. IR_{cell}(test VOC). This is *not* necessarily the same thing as the RR(test VOC) that minimizes the base ROG for VOC substitution error, though they are close if the data are well fit by a line forced through zero.

Although in some respects this aggregation approach seems like a more realistic type of substitution upon which to base a reactivity scale (for low reactivity VOCs, at least), in practice it does not give well-defined values for VOCs whose reactivities are zero or scattered around zero, i.e., or are negative in some conditions and positive in others. Relative reactivities cannot be derived if the incremental reactivity of the species is zero because it is in the denominator in Equation (VI), and mathematical instability occurs when the species incremental reactivities are scattered around zero. As discussed below, this problem can be seen in the results obtained for the TOL model species, which has this characteristic.

Note that both of these minimum substitution error metrics weigh the impacts by approximately the square of the incremental reactivities of VOCs in the individual cells, as indicated by Equations (V) and (VII), above. This means that this metric is more influenced by the reactivities in the VOC-sensitive cells than is the case for the regional average O_3 metric, which weighs the impacts by the incremental reactivities themselves, as indicated by Equation (I).

Regional MIR Metric (MIR)

An alternative method that was used in the regional reactivity modeling studies of Russell and co-workers (e.g., Hakami et al, 2002) is to base the global metric on the impacts of the VOC in the cell where VOCs have the highest incremental reactivities. This would involve first finding for each cell the time of the peak O_3 levels (either as 1-hour or 8-hour averages), determining the incremental reactivities for the times of the ozone peaks in each cell, and then using the relative reactivities in the cell that has the highest incremental reactivity of the base ROG as the global metric. This is of interest because it is an analogue to the widely used MIR scale of Carter (1994a), which is based on quantifying ozone impacts for conditions that are most sensitive to VOC emissions, as measured by the base ROG incremental reactivity. Again this is not a true global metric because it is based on relative impacts in only a single cell. However, the results of this study indicate that relative impacts under MIR or near-MIR conditions tend not to be highly variable, so the relative impacts in this single cell should give a fair approximation to the impacts in other cells with approximately MIR-like conditions.

In some episode days and domains, the cell with the highest incremental reactivity of the base ROG had relatively low ozone levels. Since sensitivities in low O_3 cells are probably not appropriate for deriving global reactivity metrics, cells with O_3 below given cutoff levels were not considered when deriving the regional MIR metric. This, the relative reactivity in the regional MIR metric is given by

$$\mathrm{RR(Species)^{Regional\ MIR}} = \mathrm{IR_{cell\ with\ highest\ IR(Base\ ROG)\ and\ O3>O3cutoff}(Species)} \,/\, \mathrm{IR_{same\ cell}(Base\ ROG)} \qquad \text{(VIII)}$$

where O3cutoff is 0.08 ppm when using the 1-hour average quantification, and 0.06 ppm when using the 8-hour average quantification. These are respectively 40 and 20 ppb lower than the current standards of 120 and 80 ppb, and appear to be reasonable margin for the purpose of this analysis. Using too high of a cutoff may result in a metric that is similar to the regional maximum O_3 or regional average O_3 over standard metrics.

Regional MIR to MOIR Metric

As with the regional maximum O_3 metric the regional MIR metric reflects the impacts only in a single cell, which may not necessarily be representative of other cells with high O_3 or high incremental reactivity. Although the regional MIR relative reactivities were found not to be as variable as the regional maximum O_3 reactivities, a more robust metric would be a regional average O_3 metric that includes only cells with MIR or near MIR-like conditions. As discussed previously (Carter, 1994a), MIR conditions are characterized not only by high incremental reactivities of the base ROG but also by highly negative sensitivities of O_3 to NO_x. This can be contrasted by MOIR conditions, which refer to cells where any change in NO_x emissions will result in less O_3 formation, i.e., to cells where the sensitivity to NO_x emissions are zero (Carter, 1994a, see also the discussion of categorization of reactivity characteristics, below). Therefore, cells where the sensitivity of O_3 to NO_x is negative can be considered to represent MOIR to MIR conditions for the purpose of categorizing cells for total VOC and NO_x sensitivity.

With this in mind, relative reactivities in the regional MIR to MOIR metric are defined as regional average ozone reactivities (i.e., calculated using Equation I), except that only cells with negative O_3 sensitivities to NO_x, and positive incremental reactivities of the base ROG, are included. This is given by

$$\mathrm{RR(Species)}^{\mathrm{MIR\ to\ MOIR}} = \Sigma_{\mathrm{cells\ with\ IR(NOx)<0}}\ \mathrm{IR_{cell}(Species)}\ /\ \Sigma_{\mathrm{cells\ with\ IR(NOx)<0}}\ \mathrm{IR_{cell}(Base\ ROG)} \qquad \mathrm{(IX)}$$

where $IR(NO_x)$ is sensitivity of the daily maximum O_3 in the cell to total NO_x emissions. Note that derivations of this metric may include cells where O_3 sensitivities to anthropogenic VOCs are low because the VOCs are dominated by biogenic emissions. However, the general reactivity characteristics of these cells should be the same in terms of the general effects of VOCs and NO_x on ozone formation.

EKMA Reactivity Scales

For comparison purposes, incremental reactivities of the Carbon Bond model species were also calculated using the modeling approach and scenarios employed by Carter (1994a) to derive the MIR and the other box model, NO_x-adjusted incremental reactivity scales. The scenarios and methods employed were as discussed by Carter (1994a), with some minor modifications to the methodology as described by Carter (2000a). The only difference was that the Carbon Bond mechanism as implemented in the CAMx model used in this study (and listed in Appendix A) was employed, and reactivities were calculated only for the Carbon Bond model species. The approach was essentially the same as used by Carter (1994b) when deriving these scales for an earlier version of the Carbon Bond mechanism.

These scales are referred to as “EKMA” reactivity scales to refer to the fact that EKMA-type box models were used rather than a regional model such as discussed in the rest of this report. The starting point was 39 EKMA scenarios developed by the EPA (Baugues, 1990). As discussed by Carter (1994a,b), some reactivity scales were derived based on averages of incremental reactivities of the carbon bond model species in the 39 scenarios with NO_x inputs adjusted to yield specified reactivity characteristics, and others were derived based on results of the base case (i.e., unadjusted NO_x) scenarios. The specific scales used in this study were as follows:

- The MIR scale was derived by adjusting the NO_x inputs in the 39 EKMA scenarios to yield the highest incremental reactivity of the base ROG. The base ROG used for this purpose was actually based on a somewhat different composition (see Carter, 1994b), but this should have minor or essentially no effect on the MIR scenarios that were derived. This represents the relatively high NO_x conditions where O_3 is most sensitive to VOCs, and where NO_x has a negative effect on O_3 formation.
- The MOIR scale was derived by adjusting the NO_x inputs to yield the highest peak ozone concentration. This represents NO_x conditions that are optimum for ozone formation.

- For the purpose of comparisons with the regional MIR to MOIR metric, The EKMA MIR to MOIR relative scale was derived by averaging the EKMA MIR and EKMA MOIR relative reactivities.
- The average O_3 scale was derived using incremental reactivities in the 39 base case, using the same approaches as employed when deriving regional average O_3 scale, except in this case each base case EKMA scenario was treated as a separate cell.
- Likewise, the two minimum substitution error scales were derived using incremental reactivities in the 39 base case, using the same approaches as employed when deriving regional model minimum substitution error scales, with each EKMA base case scenario was treated as a separate cell.

In all these cases, the incremental reactivities are derived in terms of the effects of the VOC species on the peak O_3 concentration, which, because of the nature of the box models, was the final O_3 level in the one-day simulations. This makes them comparable to the calculations using the maximum 1-hour average O_3 quantification.

Note that the relative reactivities in the EKMA reactivity scales are relative to the same base ROG mixture as employed for the regional reactivity scales, whose composition is given in Table 1. This is somewhat different than the mixture used to represent the anthropogenic VOCs in the model when calculating the EKMA reactivities or determining the NO_x inputs for the MIR scale, which based on the mixture employed in the original calculations of Carter (1994a,b), but is employed in this study for direct comparability with the regional reactivity results.

It is important not to confuse the EKMA MIR, MOIR and EKMA base case reactivity scales discussed in this work with the MIR and other scales developed previously by Carter (1994a, 2000a). The EKMA scales in this work were calculated using the CB4 mechanism as implemented in the CAMx model, while the previous Carter (1994a, 2000a) EKMA scales were derived using versions of the SAPRC mechanism. The CB4-based scales are only considered in this work because the objective is to examine effects of model formulation and not effects of using a different chemical mechanism.

Categorization of Reactivity Characteristics Throughout the Modeling Domain

The results of the DDM calculations of the sensitivities of O_3 to total VOC and NO_x emissions can be used to categorize the modeling domain in terms of general reactivity characteristics. This is useful for relating the results of these regional reactivity calculations to the various NO_x-adjusted reactivity scales developed by Carter (1994a). The various terms used in this report to categorize reactivity characteristics throughout the modeling domain are summarized in Table 3. Note that reactivity categorizations are used only for cells where the daily maximum ozone concentrations are above the cutoff limits of 0.08 ppm or 0.06 ppm for maximum 1-hour or 8-hour averages, respectively. This is because reactivity characteristics are not considered to be relevant in regions where O_3 levels are well below ambient air quality standards.

The terms “MIR”, “MOIR”, and “EBIR” are essentially the same as used by Carter (1994a,b) and above to classify the EKMA scenarios and their associated reactivity scales. (Note that “MIR” has a somewhat different meaning in the context of classifying overall regional reactivity characteristics than it does in the context of the regional MIR metric discussed above, because in the former case it refers to the maximum sensitivity to total VOCs, while in the latter it refers to the sensitivity to anthropogenic emissions or the base ROG. Generally cells with high sensitivity to total VOCs also have high sensitivity to the base ROG, but the cells with the highest sensitivities to each may not always be the same.) The

Table 3. Definition of terms used in this report to define VOC and NO_x sensitivity conditions

Term	Meaning	Definition [a]
MIR	Maximum Incremental Reactivity	Location where the daily maximum O_3 has the highest sensitivity to total VOCs or the base ROG, depending on context [b].
MOIR	Maximum O_3 Incremental Reactivity	Locations where NO_x emissions are most favorable for O_3 formation, all else being equal, i.e., cells where any change in NO_x emissions causes the daily maximum O_3 to decrease. Note that this implies that the sensitivity of the daily maximum O_3 to NO_x is zero in such locations.
Max. O_3	Maximum O_3 Concentration	Location that has the highest daily maximum O_3 concentration. Used for determining maximum O_3 regional reactivity metric. Not same as MOIR.
EBIR	Equal Benefit Incremental Reactivity	Locations where the sensitivity of the daily maximum O_3 to total VOCs and NO_x are equal and positive.
ZBIR	Zero Benefit Incremental Reactivity	Locations where the daily maximum O_3 has zero sensitivity to total VOCs.
NIR	Negative Incremental Reactivity	Locations where the daily maximum O_3 has negative sensitivity to total VOCs.

[a] Locations where the daily maximum 1-hour or 8-hour O_3 is below the cutoff limit or where O_3 has zero sensitivity to either VOCs or NO_x are excluded.

[b] Sensitivity to total VOCs is used in the context of categorizing reactivity characteristics throughout the modeling domain. Sensitivity to the base ROG is used in the context of deriving the regional MIR reactivity metric.

terms “ZBIR” and “NIR” are added to refer to locations with zero or negative sensitivity to VOC emissions, which as indicated below have a non-negligible extent in this regional modeling domain. Note that MIR to EBIR refer to conditions where VOC control is more effective than NO_x control in reducing ozone, which is where VOC reactivity scales are most relevant from a regulatory standpoint. VOC reactivity may have some relevance in EBIR to ZBIR conditions, though by definition NO_x control is more effective in reducing O_3 in those regions. VOC reactivity has no relevance in ZBIR to NIR conditions.

Large Scale Substitution Calculations

Although the DDM calculations discussed above consisted of the major effort in this project, a total of four large-scale substitution calculations were also conducted for this project. Their primary purpose was to assess the effects of large substitutions of current emissions with low-reactivity or borderline exempt compounds, with ethane being used as a surrogate to represent such compounds. The calculations included substitution of all anthropogenic emissions with ethane, either on a mass or mole basis (with carbon number being used as a surrogate for mass), and “null test” substitution calculations, where ethane replaced anthropogenic VOCs at a ratio that should give the same overall ozone reactivity, according to an appropriate metric derived from the DDM calculations. For comparison purposes, calculations were conducted with all anthropogenic VOCs removed. This serves as a basis for determining the ozone formation potential of the ethane replacement, and also represents effects of substitution of current anthropogenic emissions with zero reactivity replacements. A more detailed discussion of the purpose and utilities of these calculations is given in conjunction with the discussion of the results, below.

The large scale substitution calculations that were conducted are summarized in Table 4. Each of these involved changes only to anthropogenic emissions, with anthropogenic VOC emissions either removed or reduced, and varying amounts of ethane added. Footnotes to the table indicate how the ethane substitution factors were derived, where applicable. No changes made to emissions of NO_x or biogenic VOCs, and all other inputs were the same as employed in the base case simulation used in the DDM calculations discussed above. In the cases where ethane was substituted for a portion or all of the anthropogenic emissions, the spatial and temporal distribution of the ethane emissions added were the same as that for the base case anthropogenic VOC emissions that were removed. The results are analyzed by comparing changes caused by the substitution in the daily maximum 1-hour or 8-hour average ozone concentrations in the cells in the substitution or removal calculations.

Table 4. Summary of large scale substitution calculations conducted for this project.

Description	Fraction of Anthropogenic VOCs Removed	Ethane Added Relative to Total Base Case Anthropogenic VOCs (Carbon Basis) [a]
Anthropogenic VOCs Removed	100%	0%
100% Ethane Substitution – Carbon Basis	100%	100%
100% Ethane Substitution – Mole Basis	100%	50% [b]
100% Ethane Substitution – Equal Reactivity Basis	100%	510% [c]
50% Ethane Substitution – Equal Reactivity Basis	50%	255% [c]

[a] The amounts of carbons of ethane model species to add were computed based on total number of carbons in the Carbon Bond model species used in the emissions to represent the anthropogenic VOCs. The carbon numbers for the Carbon Bond model species are given in Table 1.

[b] The weighed average number of carbons per mole of the non-methane VOCs in the EPA emissions mixture used to derive the base ROG composition is 4.03. Based on this, substituting the base ROG mixture with ethane on a molar basis should results in reducing the number of carbons emitted by approximately 50%.

[c] A substitution factor of 5.1 on a carbon basis is based on the average least squares substitution error relative reactivity of 0.19 for ethane on a carbon basis, as derived for the 12 K domain. See discussion in the Results section

RESULTS AND DISCUSSION

Ozone Levels and Reactivity Characteristics of the Episode Days

Figure 6 through Figure 9 show maps of geographical extents of high daily 1-hour maximum ozone concentrations throughout the three nested modeling domains considered in this study, with one set of maps for each episode day. Figure 10 shows similar plots for the 8-hour average maximum ozone concentrations for the 36K domain. In each case, the left hand plots show maps of the O_3 concentrations and the right hand figure shows maps of VOC sensitive regions, defined as discussed in the "Categorization of Reactivity Characteristics" section, above. Numerical summaries of the reactivity characteristics for the various episode days for the various domains are given on Table 5 through Table 7.

The results indicate differences in the episode days, particularly July 12 where the peak O_3 levels were in the South, compared to the other days, when the O_3 tended to be in the North. The results also indicate differences in the extent of cells where the 8-hour O_3 exceeded the cutoff levels were greater than was the case for the 1-hour O_3, despite the fact that the ratio of the cutoff level to the air quality standard level was higher for the 8-hour average. This is consistent with the fact that the current 8-hour standard is considered to be more difficult to obtain than the 1-hour standard.

Figure 11 shows plots of sensitivities of daily maximum 1-hour or 8-hour average ozone levels to changes in total NO_x and VOC emissions for the 36K domain and for selected episode-days in the 4K domain. Each point indicates the sensitivities for a single cell for a given episode day. Note that according to the episode reactivity classifications discussed above, cells with NO_x sensitivities of zero (i.e., cells along the "y" axis) represent MOIR conditions, and cells with negative NO_x sensitivities represent MOIR to MIR or higher NO_x conditions. The dotted line on the plots show the conditions where O_3 formation is equally sensitive to VOC as NO_x controls, referred to as EBIR conditions. Points to the left of this line represent conditions where O_3 is either more sensitive to VOC controls than NO_x controls or where NO_x controls make ozone worse, while points to the right of or below this line represent NO_x sensitive conditions where NO_x control is more effective in reducing ozone. Note that there is a tendency for VOC sensitivity to increase with decreasing NO_x sensitivity, which is consistent with the fact that in general O_3 sensitivities to VOCs tend to increases, while O_3 sensitivity to NO_x tends to decrease, as NO_x levels are increased. The fact that the points do not all fall on the same line indicates that other variable conditions in the domain also affect these O_3 sensitivity factors. Figure 11 shows that similar patterns are seen for the various domains and episode days, though the distributions in the various sensitivity regions vary somewhat, as discussed below.

The percentages of the total number of high O_3 cells in the various domains and episode days that fall into the various VOC and NO_x sensitivity conditions are given on Table 5 through Table 7. (Figure 11 indicates the percentages for all cells – which are somewhat different than those shown on the tables because they include cells with O_3 less than the cutoff levels indicated on the tables.) There is relatively little variation from day to day in distributions of cells in various sensitivity conditions in the 36K and 12K domains, with the maximum 1-hour average O_3 being VOC sensitive (i.e., MIR to EBIR) in ~25% of the cells, and the maximum 8-hour average O_3 being VOC sensitive in ~20% of the cells. There is considerably more variation from day to day in the 4K domain, with the daily maximum 1-hour average O_3 being VOC sensitive in more than half the cells on July 12 and 13, but with the other two days in this domain have sensitivity distributions more representative of the larger domains.

The fact that the numbers of NO_x-sensitive (EBIR to NIR) cells tend to be greater than the number of VOC-sensitive cells, especially in the larger domains, indicates the importance of NO_x control

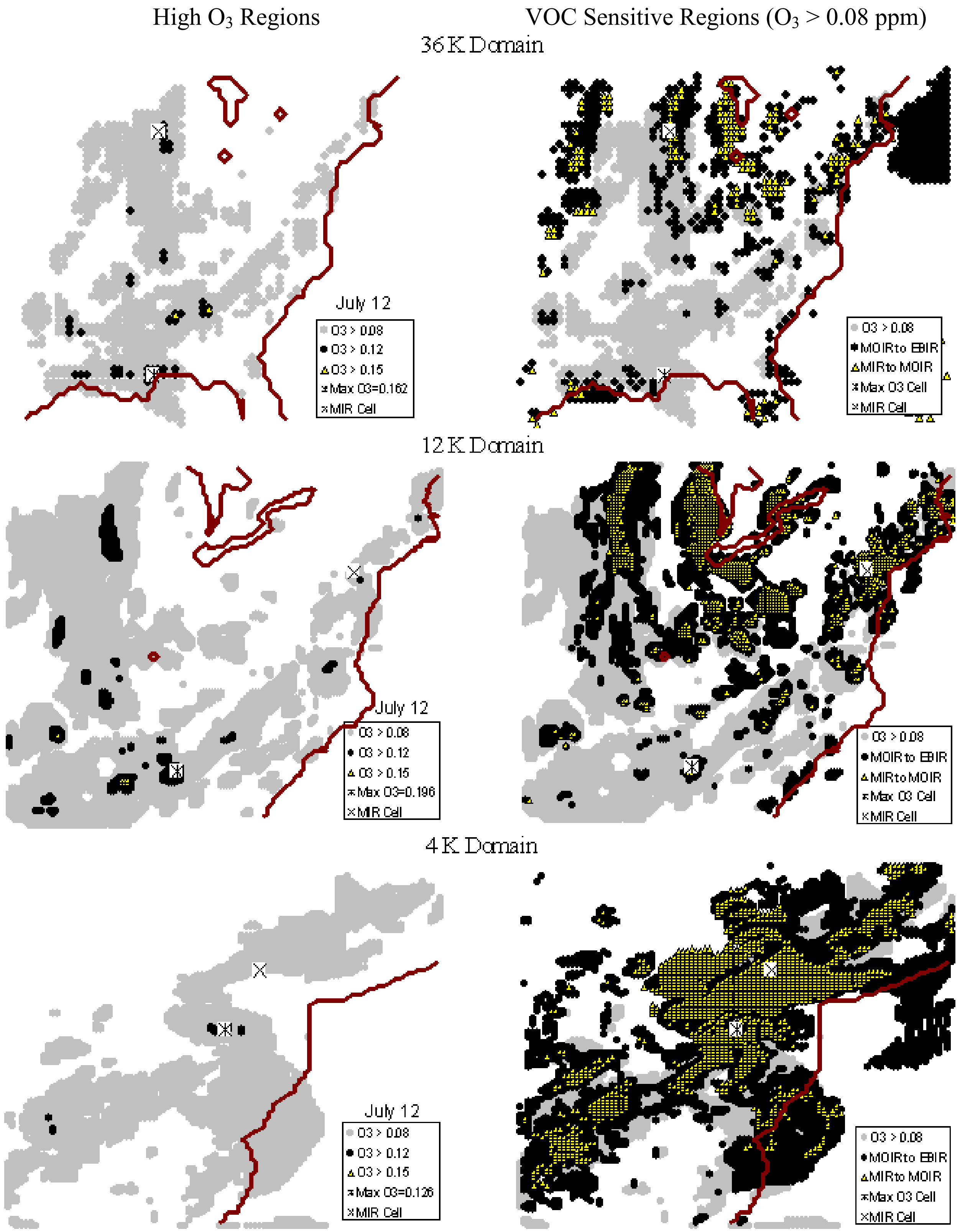

Figure 6. Maps of geographical extent of high 1-hour average ozone and VOC sensitive areas for the July 12 episode day.

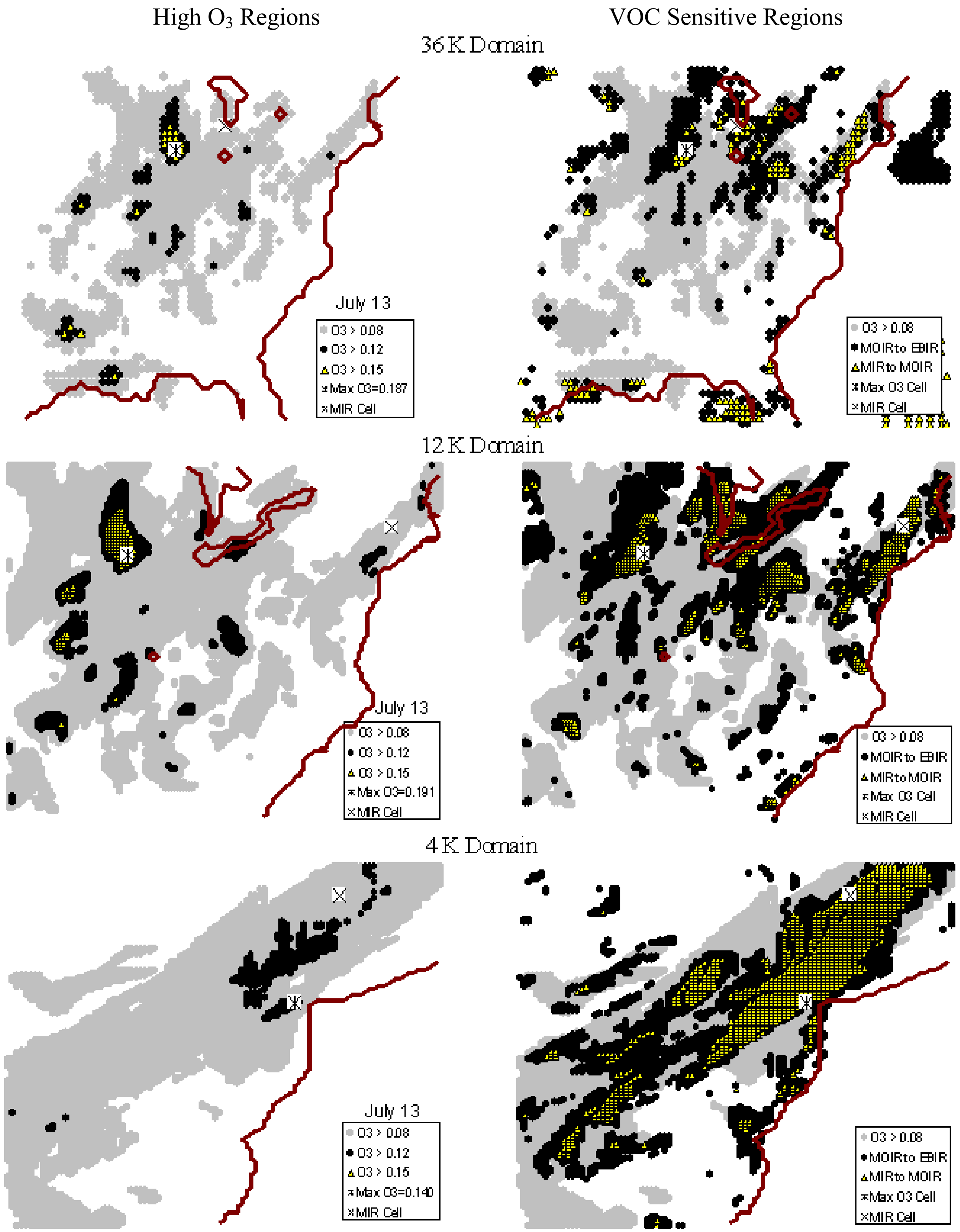

Figure 7. Maps of geographical extent of high 1-hour average ozone and VOC sensitive areas for the July 13 episode day.

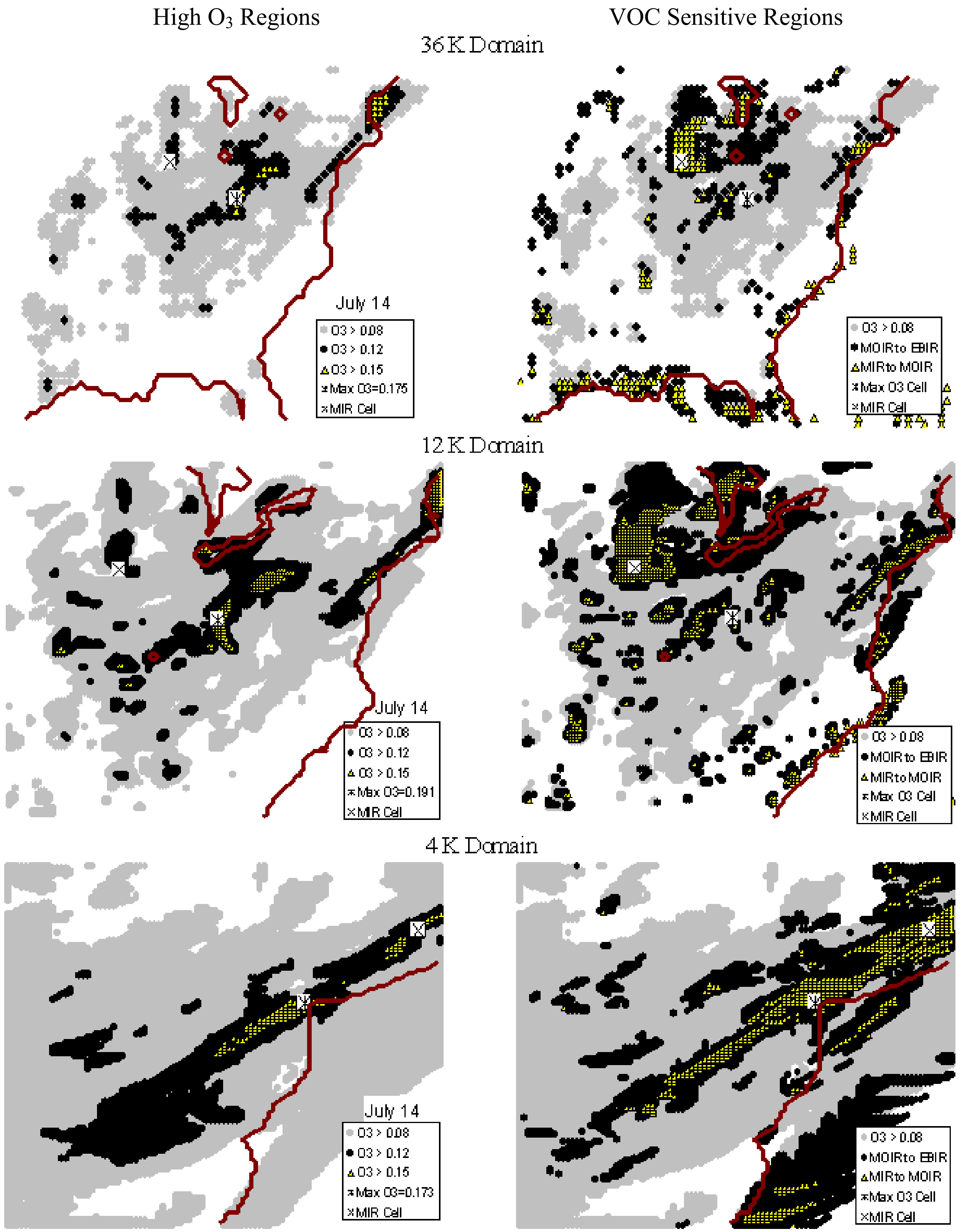

Figure 8. Maps of geographical extent of high 1-hour average ozone and VOC sensitive areas for the July 14 episode day.

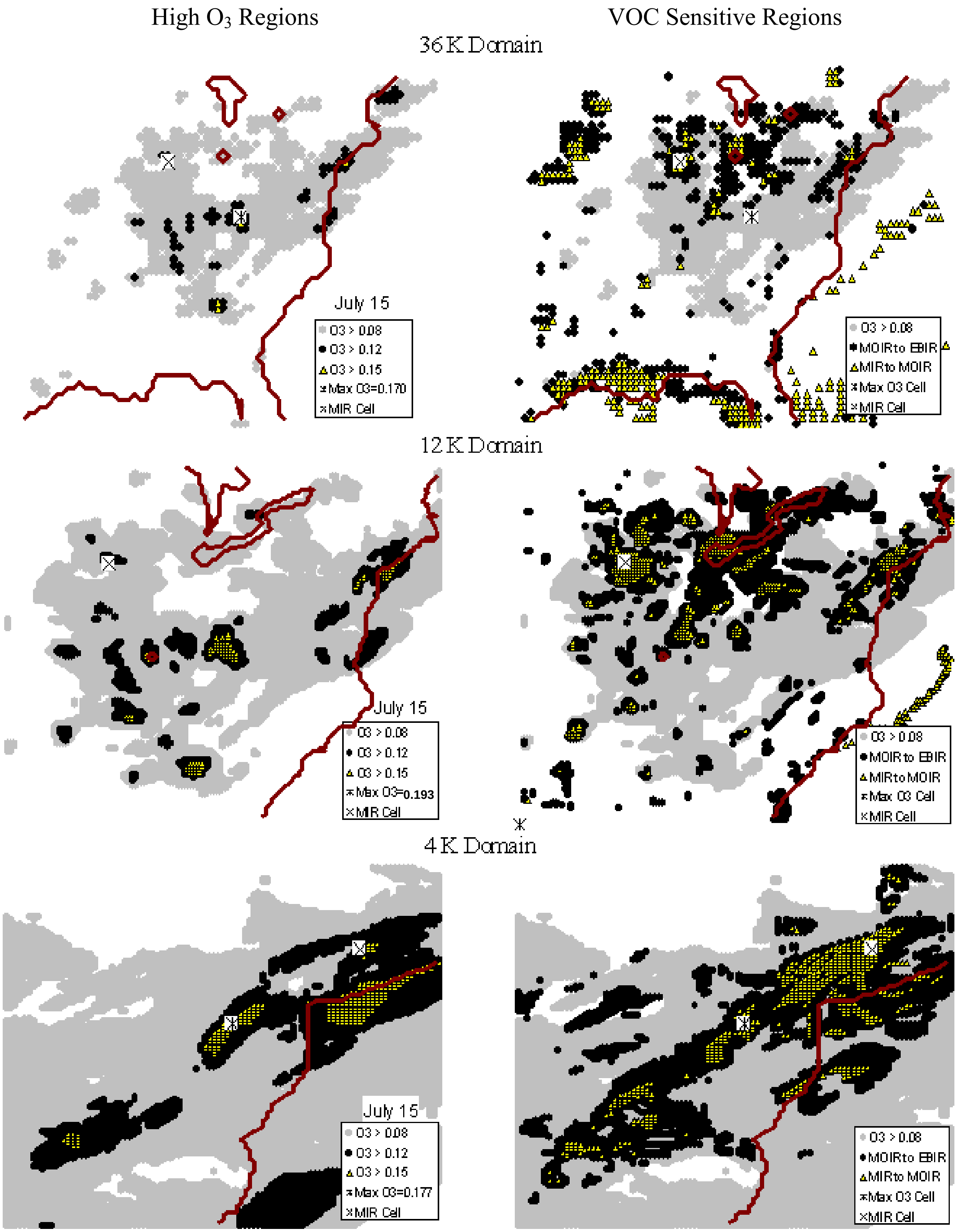

Figure 9. Maps of geographical extent of high 1-hour average ozone and VOC sensitive areas for the July 15 episode day.

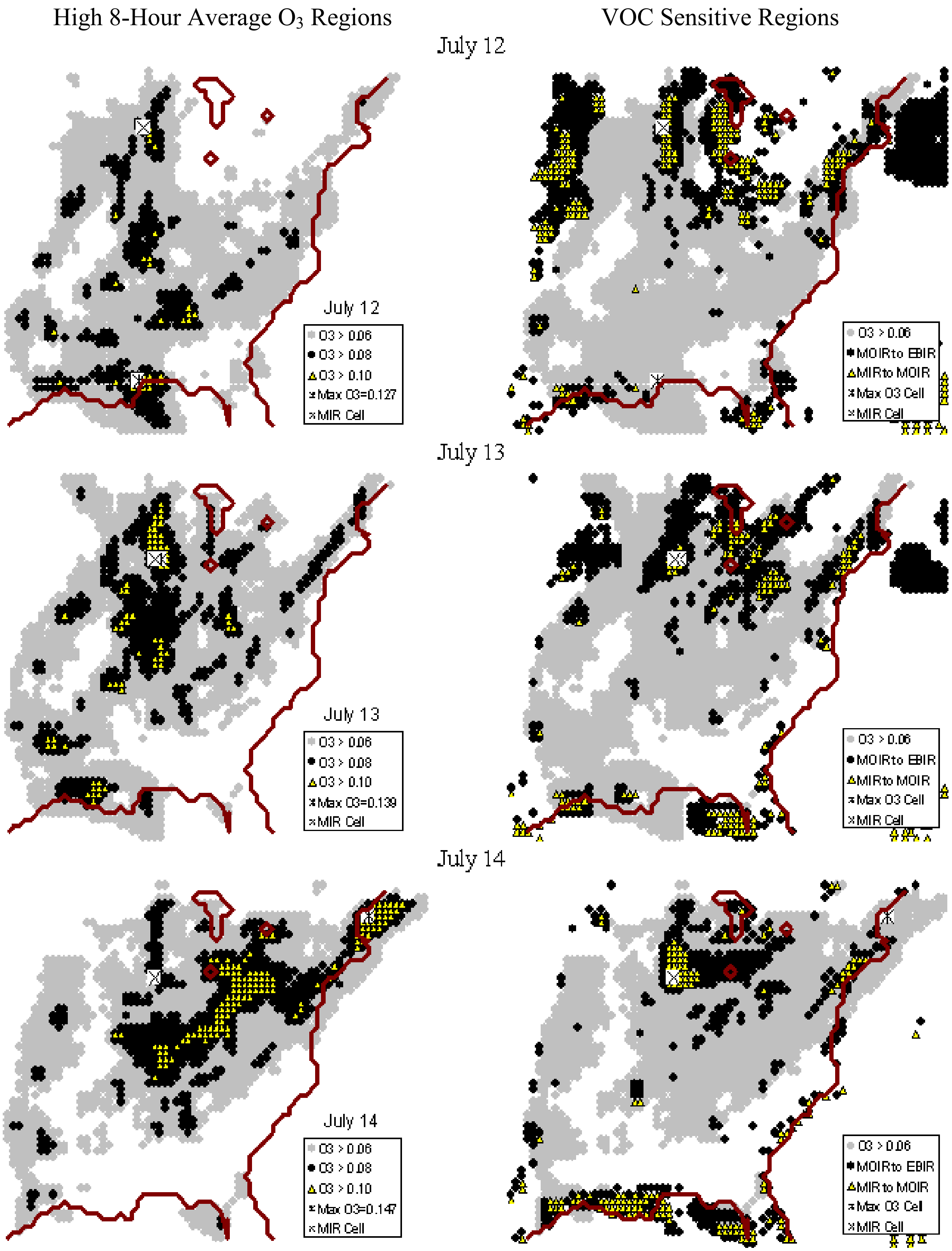

Figure 10. Maps of geographical extent of high 8-hour average ozone and VOC sensitive areas for the July 12-14 episode days.

Table 5. Summary of overall reactivity characteristics of the episode days for the 36K domain.

Episode Day	12-Jul	13-Jul	14-Jul	15-Jul	Overall
Overall Domain-Wide Ozone Maxima (ppb)					
1-Hour Average	162	187	175	170	187
8-Hour Average	127	139	147	-	147
Fraction of Cells Exceeding Given O_3 Levels					
1-hour average > 80 ppb	22%	25%	25%	19%	23%
1-hour average > 120 ppb	1%	2%	4%	2%	2%
8-hour average > 60 ppb	37%	38%	37%	-	37%
8-hour average > 80 ppb	7%	10%	12%	-	10%
Fraction of O_3 > 80 ppb Cells in Various NOx Conditions (1 Hr Avg. O_3 Quantification)					
MIR to MOIR	4%	6%	7%	4%	5%
MOIR to EBIR	19%	21%	18%	18%	19%
EBIR to ZBIR	72%	70%	72%	77%	72%
ZBIR to NIR	5%	3%	3%	1%	3%
Fraction of O_3 > 60 ppb Cells in Various NOx Conditions (8 Hr Avg. O_3 Quantification)					
MIR to MOIR	4%	5%	4%	-	4%
MOIR to EBIR	13%	18%	16%	-	16%
EBIR to ZBIR	79%	72%	76%	-	75%
ZBIR to NIR	5%	5%	5%	-	5%
O_3 Sensitivity to total VOC (ppm O_3 per fractional change in total VOC emissions) (1-Hour maximum O_3 quantification)					
Maximum	0.09	0.15	0.17	0.19	0.19
Minimum	-0.01	-0.02	-0.01	-0.01	-0.02
MIR Cell	0.09	0.11	0.17	0.19	
Maximum O_3 Cell	0.05	0.12	0.07	0.06	
O_3 Sensitivity to Base ROG (ppm O_3 per fractional change in anthro. VOC emissions) (1-hour maximum O3 quantification)					
Maximum (MIR Cell)	0.040	0.055	0.075	0.085	
Maximum O_3 Cell	0.008	0.034	0.005	0.004	
O_3 Sensitivity to total NO_x (ppm O_3 per fractional change in total NOx emissions) (1-Hour maximum O_3 quantification)					
Maximum	0.07	0.07	0.09	0.07	0.09
Minimum	-0.07	-0.10	-0.15	-0.18	-0.18
MIR Cell	-0.06	-0.07	-0.15	-0.18	
Maximum O_3 Cell	0.05	-0.01	0.03	0.04	

Table 6. Summary of overall reactivity characteristics of the episode days for the 12K domain.

Episode Day	12-Jul	13-Jul	14-Jul	15-Jul	Overall
Overall Domain-Wide Ozone Maxima (ppb)					
1-Hour Average	196	191	191	193	196
8-Hour Average	135	146	148	-	148
Fraction of Cells Exceeding Given O_3 Levels					
1-hour average > 80 ppb	33%	42%	45%	37%	29%
1-hour average > 120 ppb	1%	4%	8%	4%	5%
8-hour average > 60 ppb	53%	57%	59%	-	56%
8-hour average > 80 ppb	10%	19%	23%	-	18%
Fraction of O_3 > 80 ppb Cells in Various NOx Conditions (1 Hr Avg. O_3 Quantification)					
MIR to MOIR	6%	7%	6%	5%	6%
MOIR to EBIR	22%	25%	21%	19%	22%
EBIR to ZBIR	71%	68%	72%	75%	71%
ZBIR to NIR	2%	1%	1%	1%	1%
Fraction of O_3 > 60 ppb Cells in Various NOx Conditions (8 Hr Avg. O_3 Quantification)					
MIR to MOIR	5%	6%	4%	-	5%
MOIR to EBIR	14%	21%	16%	-	17%
EBIR to ZBIR	80%	72%	77%	-	76%
ZBIR to NIR	1%	1%	3%	-	2%
O_3 Sensitivity to total VOC (ppm O_3 per fractional change in total VOC emissions) (1-Hour maximum O_3 quantification)					
Maximum	0.13	0.19	0.21	0.24	0.24
Minimum	-0.01	-0.01	-0.01	-0.01	-0.01
MIR Cell	0.10	0.12	0.21	0.24	
Maximum O_3 Cell	0.07	0.11	0.08	0.11	
O_3 Sensitivity to Base ROG (ppm O_3 per fractional change in anthro. VOC emissions) (1-hour maximum O3 quantification)					
Maximum (MIR Cell)	0.051	0.061	0.088	0.120	
Maximum O_3 Cell	0.013	0.029	0.006	0.029	
O_3 Sensitivity to total NO_x (ppm O_3 per fractional change in total NOx emissions) (1-Hour maximum O_3 quantification)					
Maximum	0.07	0.07	0.09	0.08	0.09
Minimum	-0.09	-0.13	-0.18	-0.21	-0.21
MIR Cell	-0.08	-0.07	-0.18	-0.21	
Maximum O_3 Cell	0.05	0.00	0.03	0.01	

Table 7. Summary of overall reactivity characteristics of the episode days for the 4K domain.

Episode Day	12-Jul	13-Jul	14-Jul	15-Jul	Overall
Overall Domain-Wide Ozone Maxima (ppb)					
1-Hour Average	126	140	173	177	177
8-Hour Average	99	100	135	-	135
Fraction of Cells Exceeding Given O_3 Levels					
1-hour average > 80 ppb	27%	37%	72%	76%	53%
1-hour average > 120 ppb	0%	2%	12%	15%	7%
8-hour average > 60 ppb	54%	54%	86%	-	65%
8-hour average > 80 ppb	2%	14%	39%	-	18%
Fraction of O_3 > 80 ppb Cells in Various NOx Conditions (1 Hr Avg. O_3 Quantification)					
MIR to MOIR	24%	24%	6%	5%	11%
MOIR to EBIR	44%	28%	23%	22%	26%
EBIR to ZBIR	32%	48%	71%	72%	63%
ZBIR to NIR	0%	0%	0%	0%	0%
Fraction of O_3 > 60 ppb Cells in Various NOx Conditions (8 Hr Avg. O_3 Quantification)					
MIR to MOIR	13%	15%	5%	-	10%
MOIR to EBIR	28%	22%	15%	-	21%
EBIR to ZBIR	59%	63%	80%	-	69%
ZBIR to NIR	0%	0%	0%	-	0%
O_3 Sensitivity to total VOC (ppm O_3 per fractional change in total VOC emissions) (1-Hour maximum O_3 quantification)					
Maximum	0.14	0.14	0.18	0.17	0.18
Minimum	0.00	0.00	0.00	0.00	0.00
MIR Cell	0.13	0.13	0.18	0.17	
Maximum O_3 Cell	0.12	0.08	0.08	0.08	
O_3 Sensitivity to Base ROG (ppm O_3 per fractional change in anthro. VOC emissions) (1-hour maximum O3 quantification)					
Maximum (MIR Cell)	0.056	0.070	0.078	0.097	
Maximum O_3 Cell	0.045	0.024	0.020	0.019	
O_3 Sensitivity to total NO_x (ppm O_3 per fractional change in total NOx emissions) (1-Hour maximum O_3 quantification)					
Maximum	0.05	0.05	0.06	0.06	0.06
Minimum	-0.10	-0.11	-0.13	-0.13	-0.13
MIR Cell	-0.10	-0.10	-0.13	-0.13	
Maximum O_3 Cell	-0.06	-0.01	0.02	0.02	

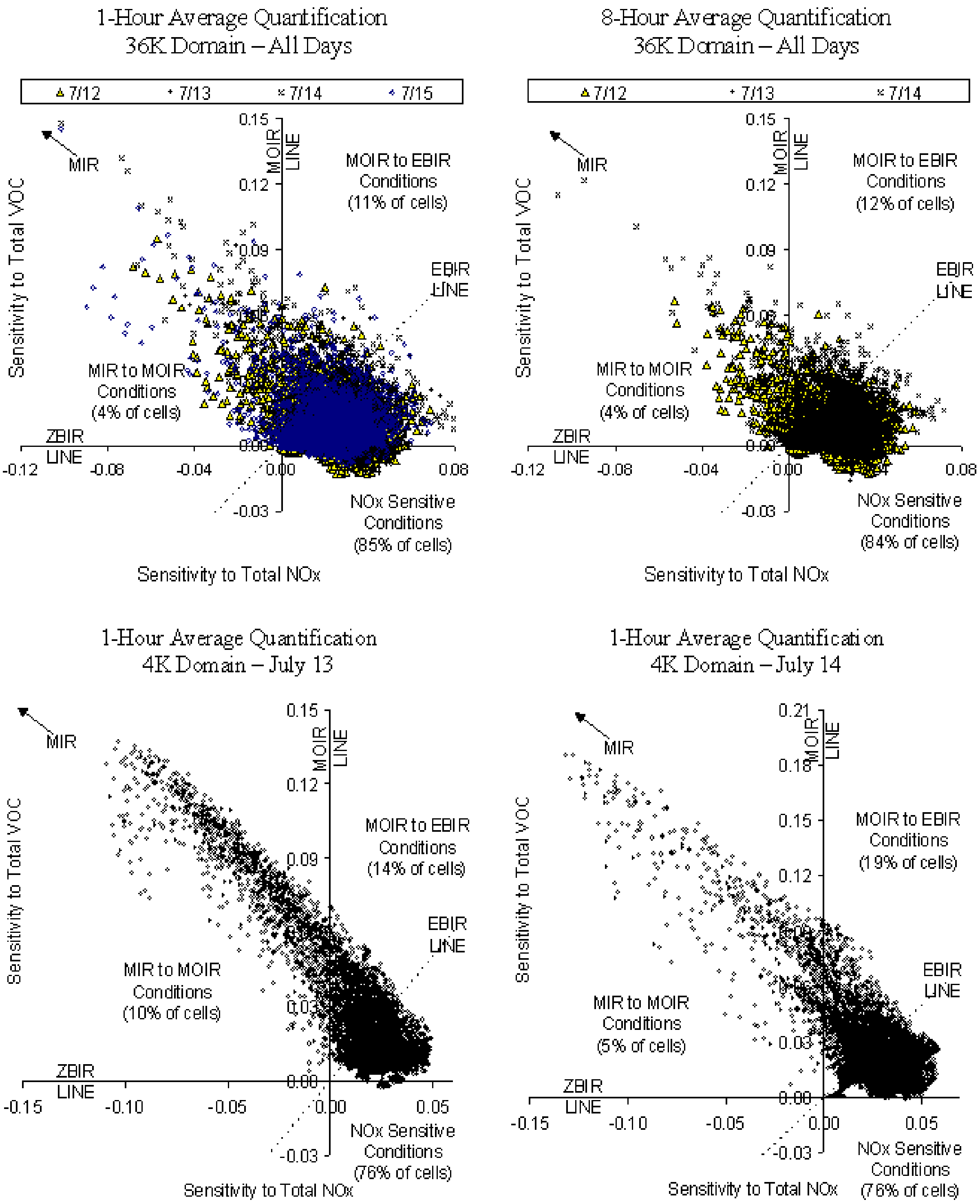

1-Hour Average Quantification
36K Domain – All Days

8-Hour Average Quantification
36K Domain – All Days

1-Hour Average Quantification
4K Domain – July 13

1-Hour Average Quantification
4K Domain – July 14

Figure 11. Plots of sensitivities of daily maximum 1-hour or 8-hour average O_3 to changes in total NO_x and VOC emissions for all cells in representative domains and episode days. The dotted lines show the conditions where O_3 formation is equally sensitive to VOC and NO_x controls.

In affecting O_3 formation on a regional scale. However, O_3 formation is at least as sensitive to VOCs as NO_x in a significant fraction of the cells, particularly in the urban areas. The number of VOC-sensitive high O_3 cells is somewhat less when considering 8-hour averages, but not significantly so.

Ozone Sensitivities to VOC Emissions Categories

In addition to calculating the ozone sensitivities to total VOCs and the base ROG mixture, sensitivities were also directly calculated for total anthropogenic VOCs and the various types of anthropogenic VOC emissions. Sensitivities to total VOCs and anthropogenic VOCs will not be the same because of the role of biogenic VOC emissions, and sensitivities to the base ROG mixture will not necessarily be the same as sensitivity to anthropogenic VOCs because of the different ways they are calculated. This is discussed further below.

Base ROG vs. Anthropogenic VOC Sensitivities

As indicated above, the base ROG sensitivities are calculated from the sensitivities of the individual model species, weighed according to their distribution in a standard VOC mixture designed to represent anthropogenic VOC emissions. If this base ROG mixture has the same distribution of model species as those used to represent anthropogenic emissions in this calculation, and if the distribution of emitted model species from anthropogenic sources does not vary significantly with time and space, then the sensitivity to the base ROG should be the same as the sensitivity to anthropogenic VOCs. However, the base ROG composition used in this work was derived from a different emissions database than employed in this CAMx simulation, and in general the composition of anthropogenic emissions will vary somewhat throughout the domain, depending on the distribution of sources in the various regions. Therefore, they may not necessarily be the same thing.

Figure 12 shows plots of O_3 sensitivities to the base ROG against those for anthropogenic VOCs for all cells in the 36K domain for the 4 episode days. The results for the finer grid domains are similar. Also shown on the figure are the 1:1 lines that show where all points should lie if the two were exactly

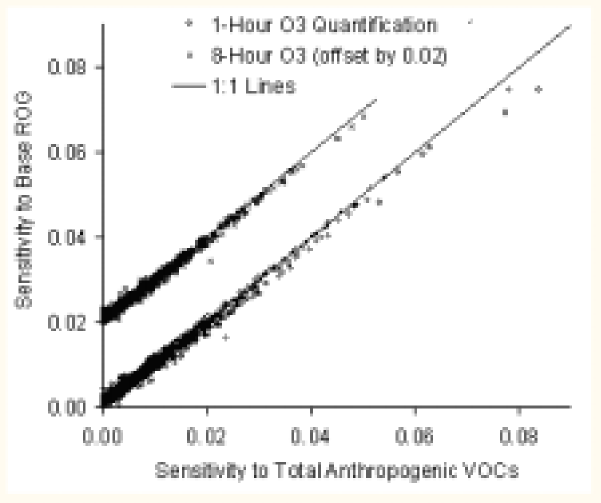

Figure 12. Plots of sensitivities of daily maximum 1-hour or 8-hour average ozone to the base ROG against sensitivities to total anthropogenic VOCs for all the episode days in the 36K domain.

equal in all cases. It can be seen that the correlation is excellent, with essentially all points being very close to the 1:1 lines. The base ROG sensitivities tend to be slightly lower than those for the total anthropogenic VOCs, with the slopes for the best-fit lines for the 36K domain being 97% and 95% for the sensitivities for 1-hour and 8-hour O_3, respectively. This is probably due to the base ROG composition used in this work being slightly less reactive than a base ROG composition derived from the modeling database used in this particular CAMx simulation. However, this bias is small compared to the variability of reactivities of the different VOC classes as discussed below. In general, the base ROG sensitivities are sufficiently close to the directly calculated total anthropogenic VOC sensitivities that they can be considered to be essentially the same for the purpose of this discussion.

Anthropogenic vs. Total VOC Sensitivities

As indicated above, the sensitivities to anthropogenic VOCs is not the same as sensitivities to total VOCs because of the significant role of biogenic VOCs in this modeling domain. Figure 13 shows the percentages of anthropogenic to total VOC sensitivities, plotted against the total VOC sensitivities, for the various domains for two selected episode days with different reactivity characteristics. The data shown are for the daily 1-hour average ozone quantification; the data for the 8-hour average quantification are similar. It can be seen that relative importance of anthropogenic VOCs compared to total anthropogenic + biogenic is highly variable throughout the domains, though the variability tends to be slightly less in the 4K, as might be expected due to the smaller size of that domain.

Figure 14 shows maps of regions of relatively high sensitivity of O_3 to anthropogenic VOC emissions on the various episode days. It can be seen that there is significant variability from day to day on which regions are most sensitive to anthropogenic VOCs, due to differences in meteorology. It is interesting to note that it is not always the urban areas that are the most sensitive to anthropogenic VOCs, presumably due to transport of urban VOCs to other regions.

Relative Contributions of Anthropogenic Source Types

In conjunction with the DDM calculations to determine the sensitivities of O_3 to the total anthropogenic VOC emissions, sensitivities were also calculated for the three major anthropogenic VOC source types, specifically mobile, area, and point sources. Plots of the sensitivities of the daily maximum 1-hour or 8-hour average O_3 to the three source types against sensitivities to total anthropogenic VOCs for the cells in the 36K domain for all four episode days are shown in Figure 15. Overall, the area, mobile, and point sources contribute approximately 50%, 30%, and 20% of the total O_3 sensitivity to anthropogenic VOCs over the 36K domain, with sensitivities for the daily maximum 8-hour and 1-hour averages being very similar. There is some variability from cell to cell in the relative sensitivities to the various source types, though the variability is relatively small for area and mobile sources. The variability is much greater for the point sources, with some regions having almost no sensitivity to point sources, and others with the sensitivity approaching 70% of that of total anthropogenic VOCs. This is as expected, given the relatively localized nature of point compared to mobile and stationary sources.

Ozone Sensitivities of Model Species

Figure 16 through Figure 19 show plots of the ozone sensitivities (incremental reactivities) of the PAR, formaldehyde, ethane, and TOL model species against the incremental of the base ROG mixture for all cells and episode days in the 36K domain, and for the cells in the 4K domain for the July 12 and 13 episode days. These are representative of the results for the other model species, as shown on Figure 20, which shows plots of daily maximum 1-hour O_3 sensitivities for the other model species in the 36K domain. The relatively small number of points where the incremental reactivities of the base ROG are

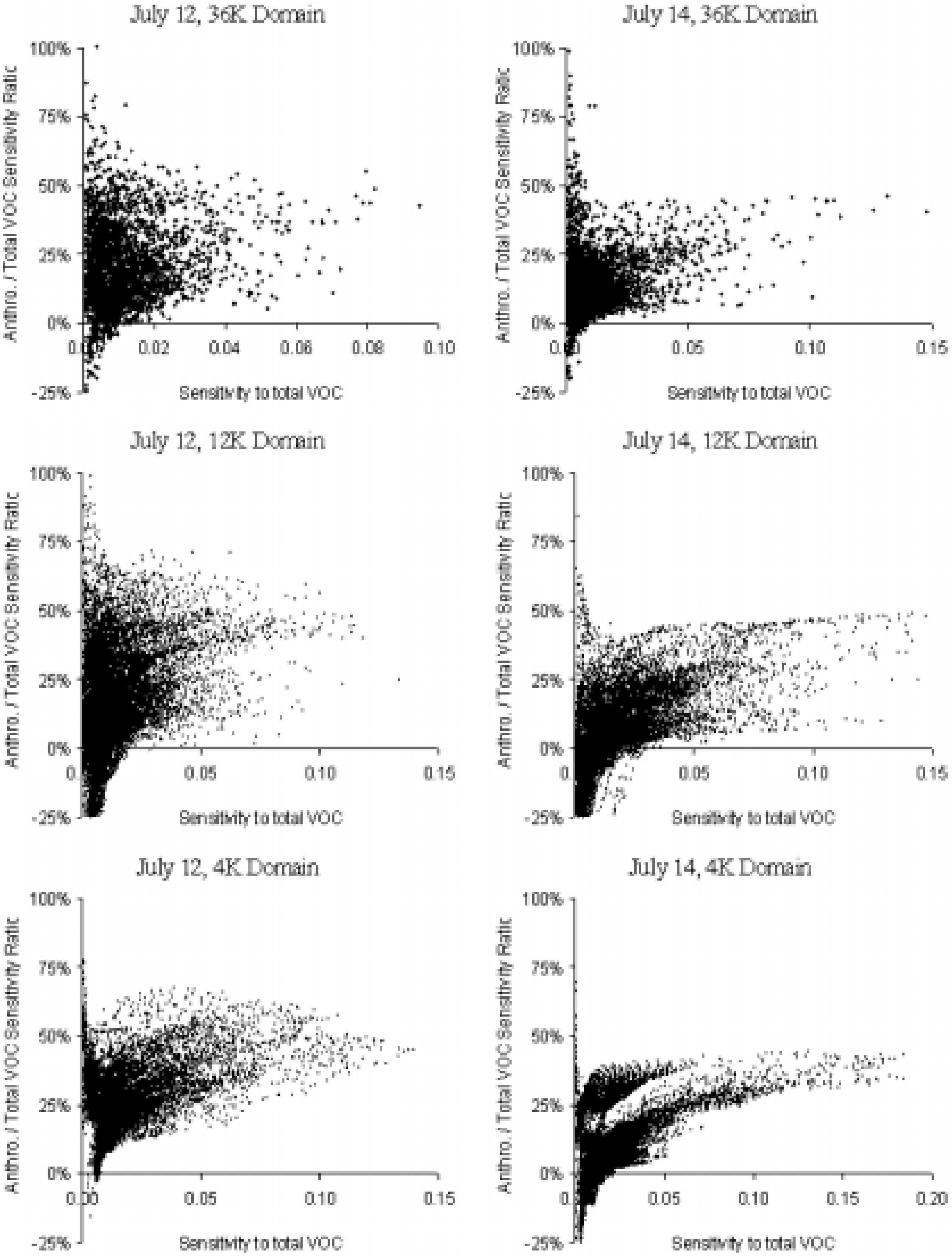

Figure 13. Plots of anthropogenic / total VOC sensitivities against total VOC sensitivities for the 1-hour daily average ozone in the various domains for July 12 and July 14.

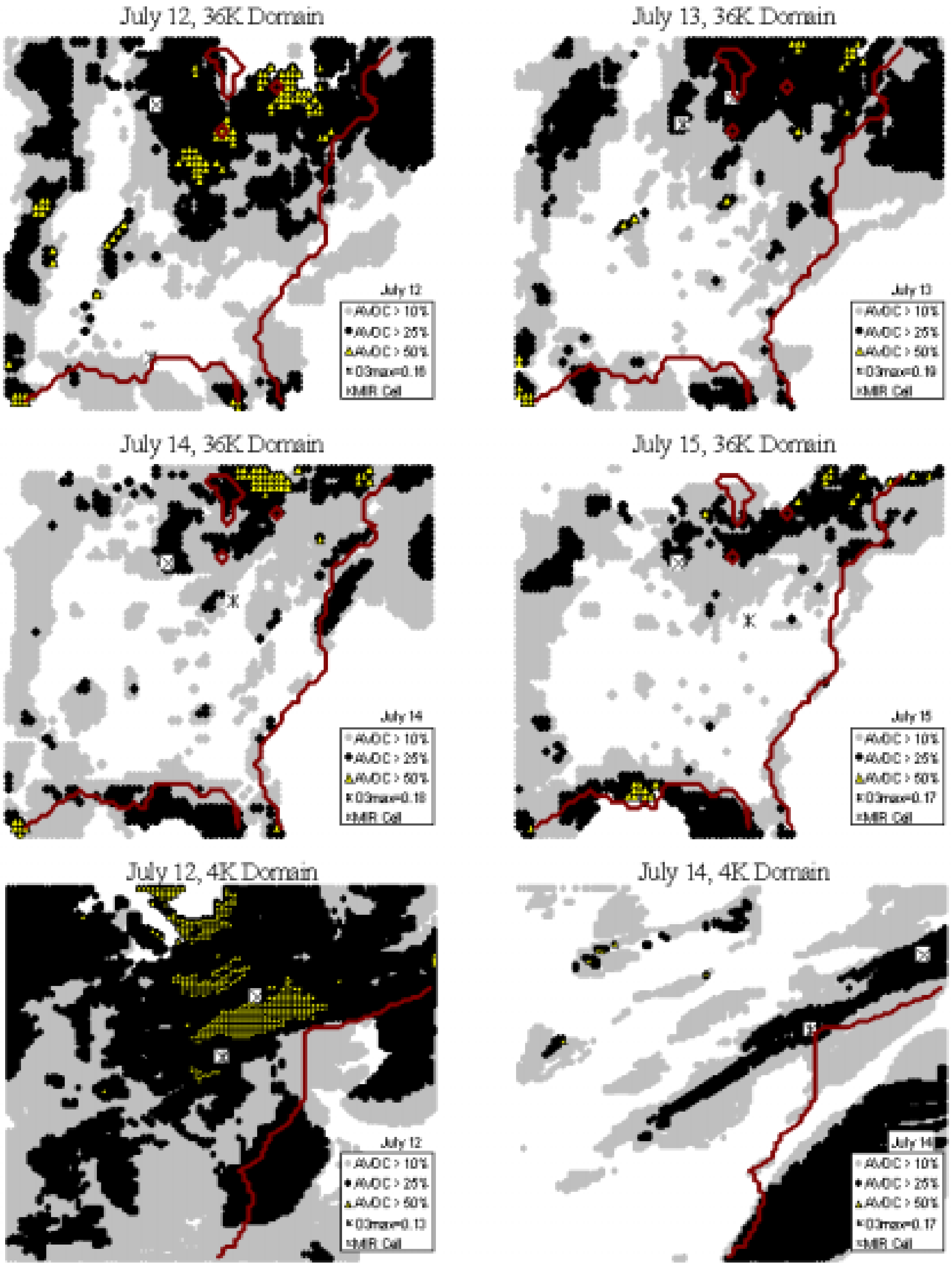

Figure 14. Maps of regions with relatively high sensitivities of daily maximum 1-hour average O_3 to anthropogenic VOC emissions for selected episode days and domains. Only cells where total VOC sensitivity is greater than 1 ppb O_3 per 100% change in total VOC emissions are shown. Percentages on the legend refer to percentages of sensitivities of anthropogenic to total VOC emissions.

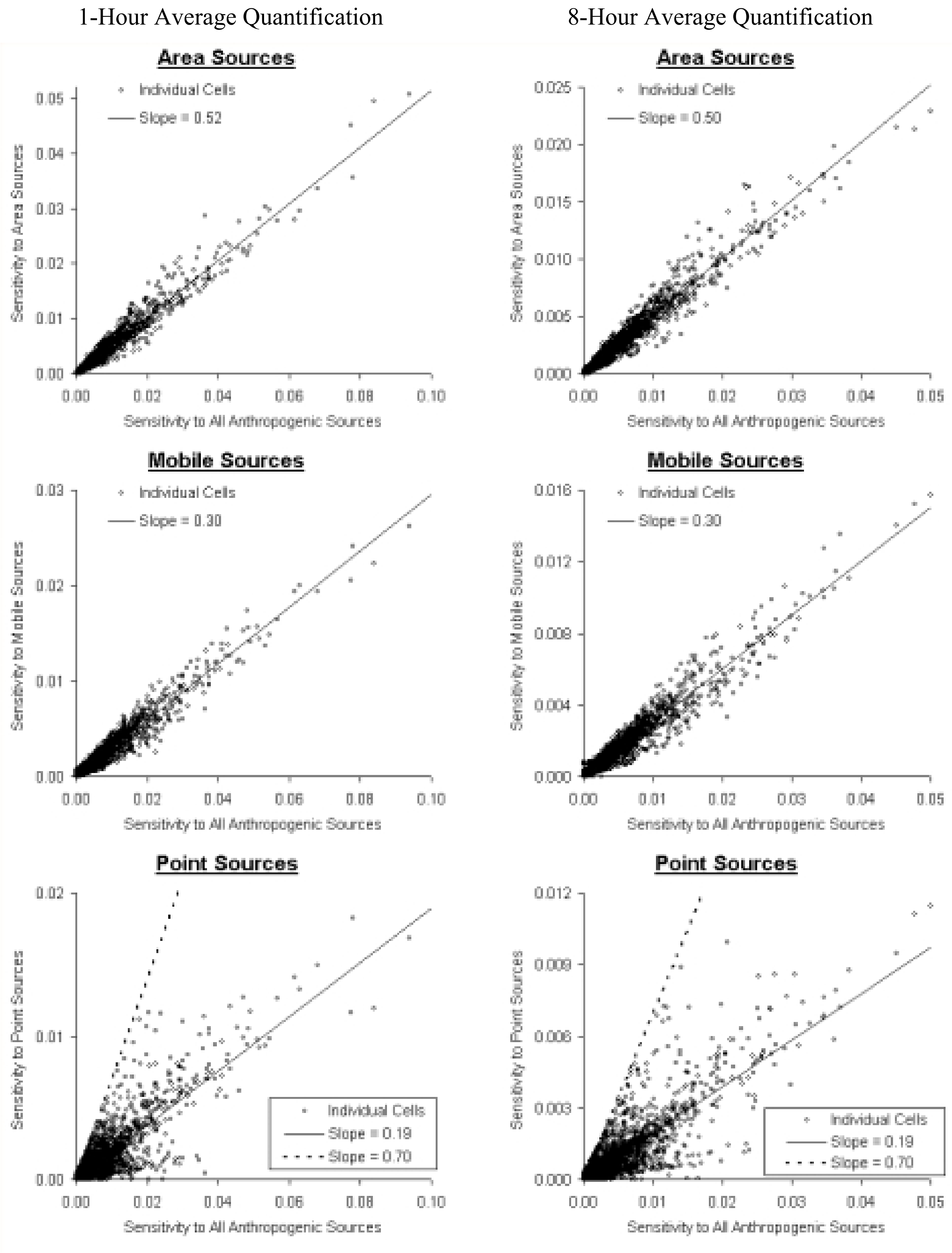

Figure 15. Plots of sensitivities 1-hour or 8-hour average O_3 of various types of anthropogenic VOC sources against sensitivities to total anthropogenic VOCs.

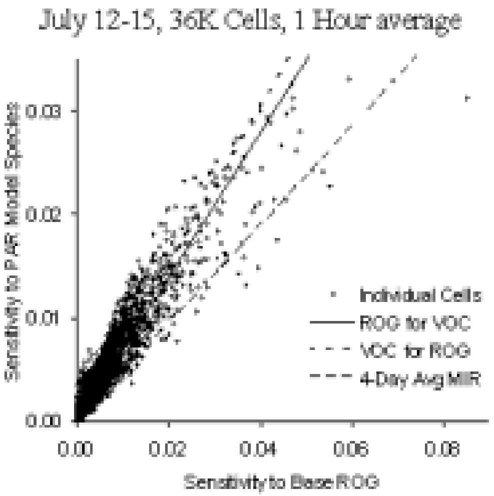
July 12-15, 36K Cells, 1 Hour average

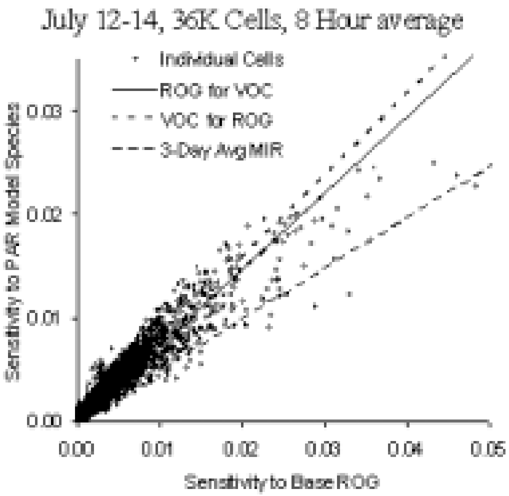
July 12-14, 36K Cells, 8 Hour average

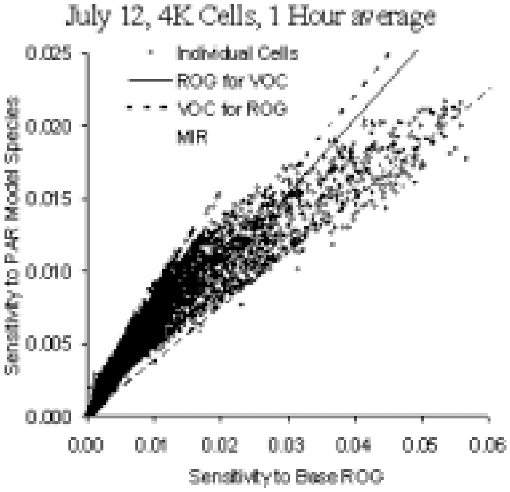
July 12, 4K Cells, 1 Hour average

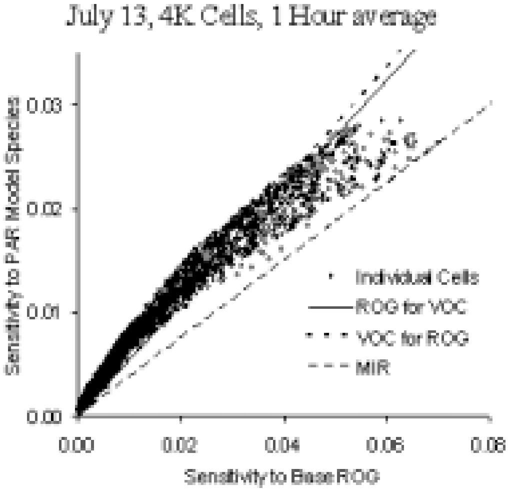
July 13, 4K Cells, 1 Hour average

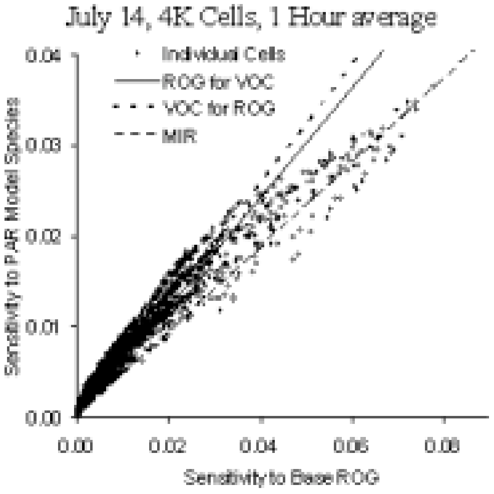
July 14, 4K Cells, 1 Hour average

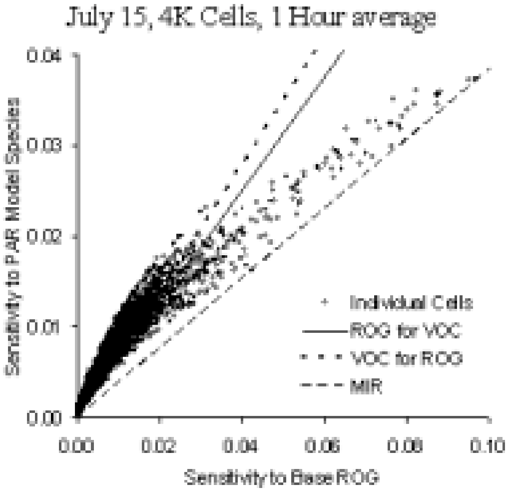
July 15, 4K Cells, 1 Hour average

Figure 16. Plots of sensitivities of ozone formation to the PAR model species against sensitivities to the base ROG mixture for the coarse grid and fine grid cells.

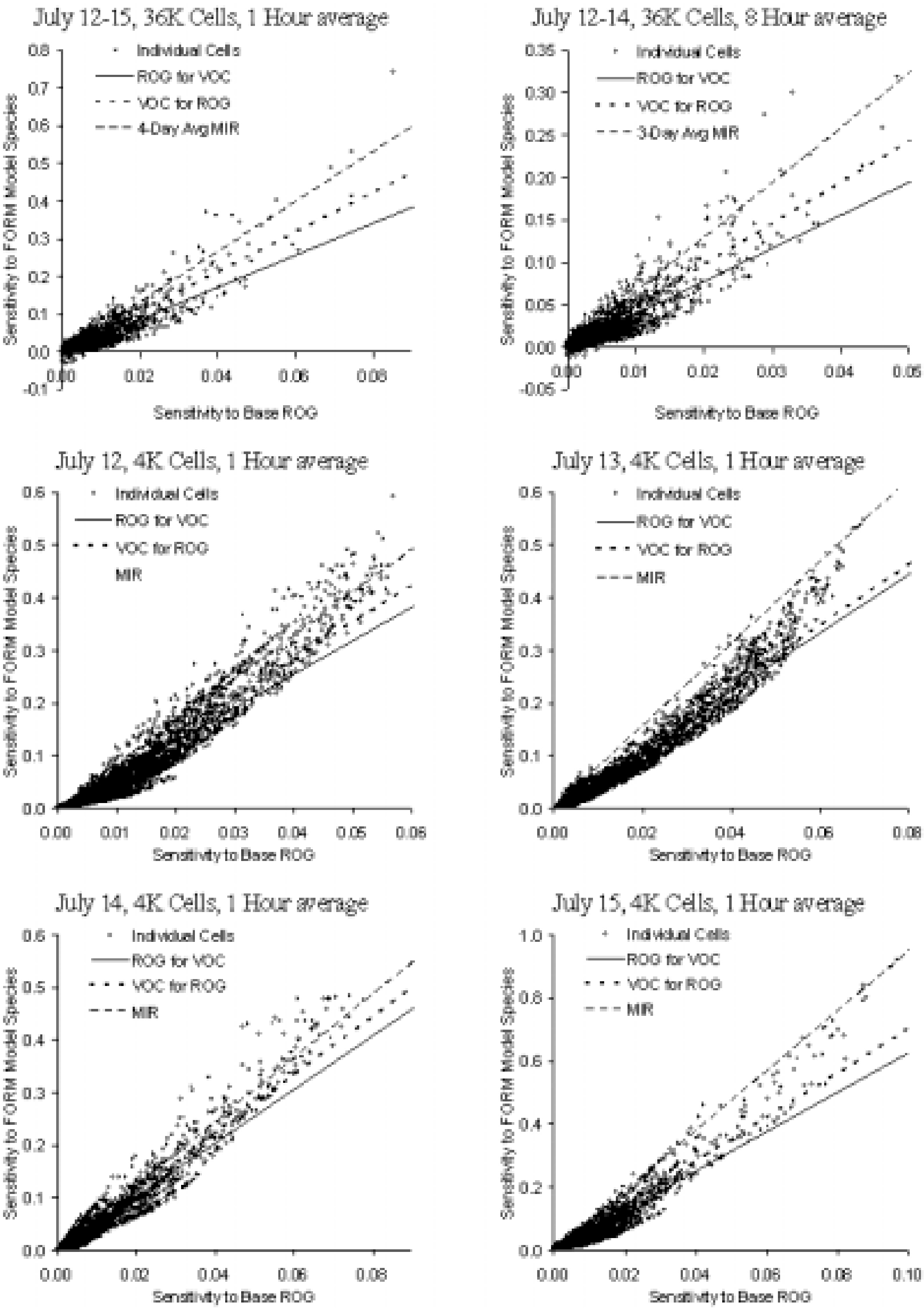
July 12-15, 36K Cells, 1 Hour average

July 12-14, 36K Cells, 8 Hour average

July 12, 4K Cells, 1 Hour average

July 13, 4K Cells, 1 Hour average

July 14, 4K Cells, 1 Hour average

July 15, 4K Cells, 1 Hour average

Figure 17. Plots of sensitivities of ozone formation to formaldehyde against sensitivities to the base ROG mixture for the coarse grid and fine grid cells.

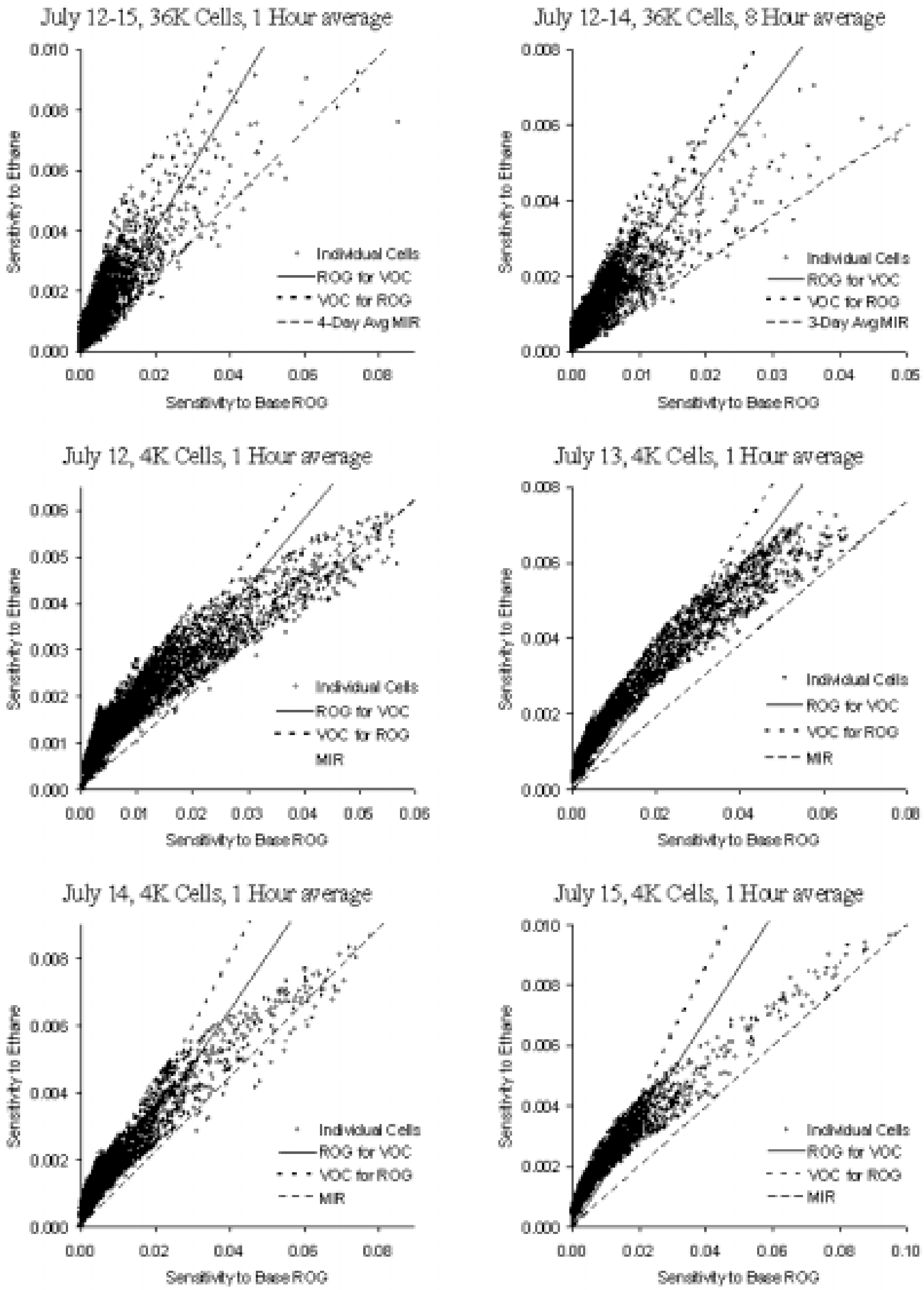

Figure 18. Plots of sensitivities of ozone formation to ethane against sensitivities to the base ROG mixture for the coarse grid and fine grid cells.

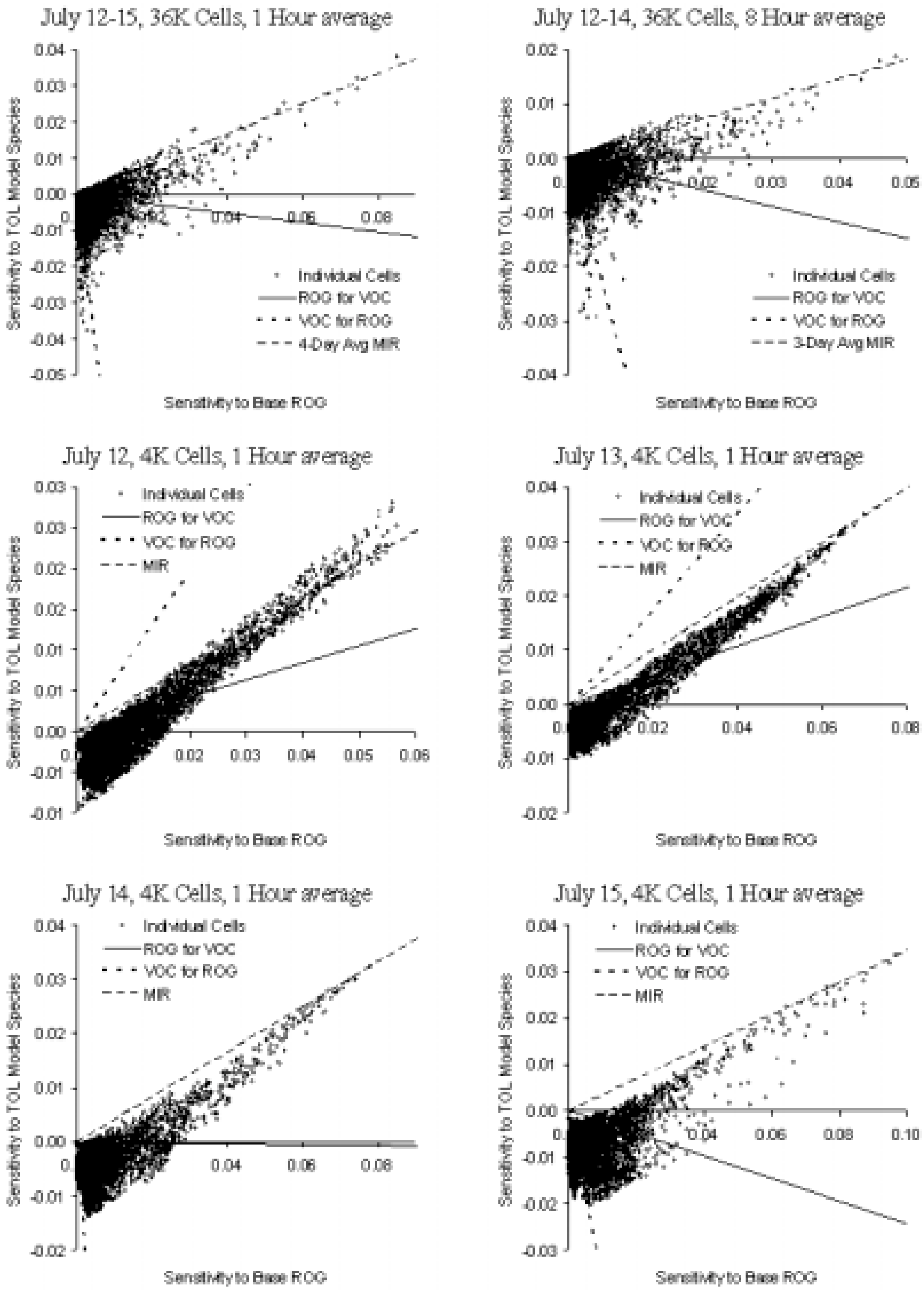

Figure 19. Plots of sensitivities of ozone formation to the TOL model species against sensitivities to the base ROG mixture for the coarse grid and fine grid cells.

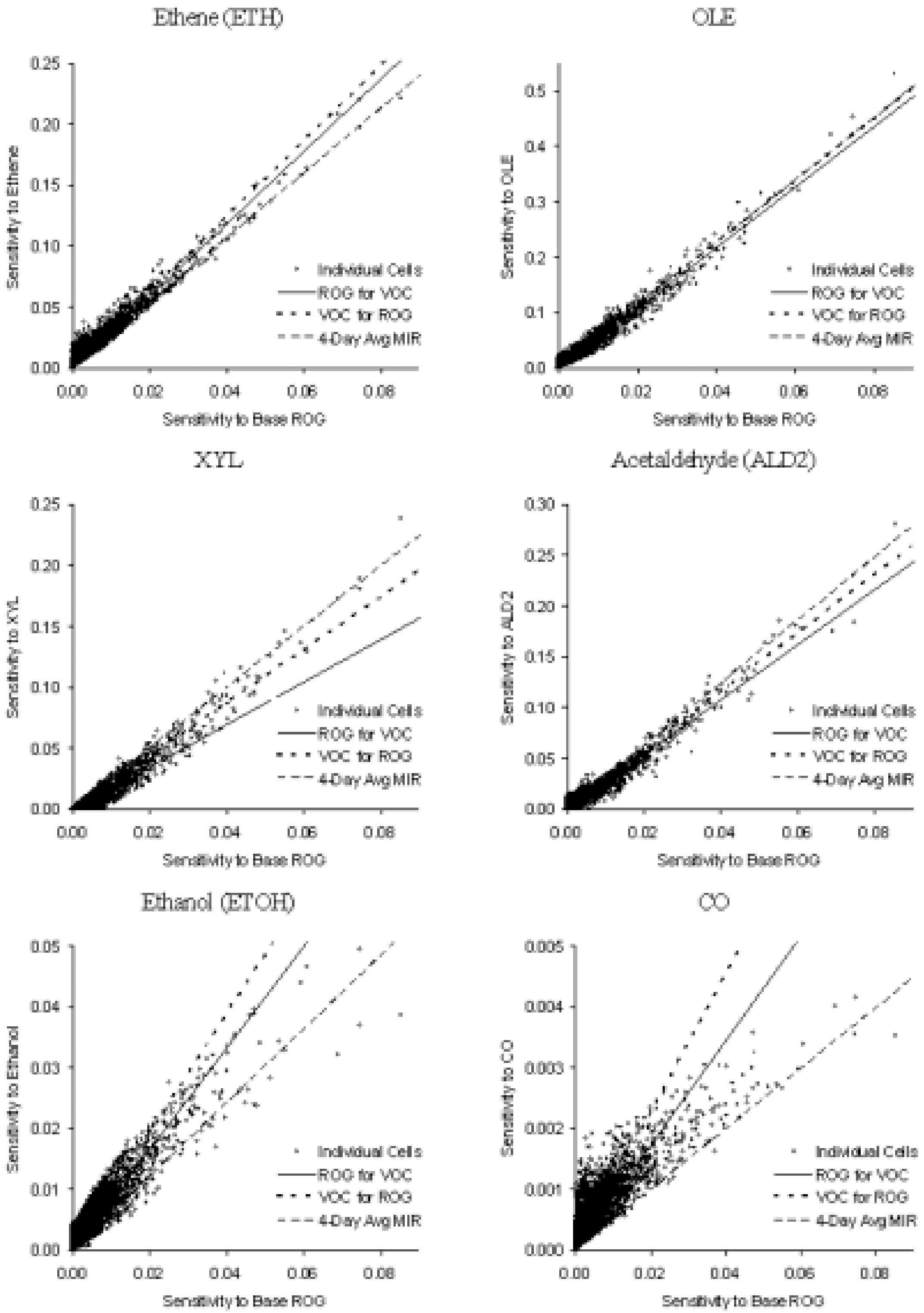

Figure 20. Plots of sensitivities of daily maximum 1-hour ozone formation to the ethane, OLE, XYL, ALD2, ethanol, and CO model species for the 36K grid cells

negative are not shown – in all cases the distribution of points are very similar to those with zero base ROG reactivity. The solid and dotted lines on the plots show the least squares fit lines, forced through zero, for the data for all four days. The slopes of these lines give the minimum substitution error reactivities for the domains and episode days shown. The solid lines show the fits for the ROG for VOC substitution (referred to as MSE 1 in the tabulations), while the dotted lines show the fits for the VOC to ROG substitution (MSE 2). The slopes of the dashed lines indicate average regional MIR relative reactivities for the episode days. These are averages of the slopes of lines (not shown on the plots) from origin to the point between the farthest to the right on each plot (i.e., the point with the highest base case ROG reactivity) for each episode day.

It can be seen that for most model species the incremental reactivities correlate reasonably well to the incremental reactivities of the base ROG throughout most of the modeling domain, except for those cells where the sensitivity to anthropogenic VOCs is very low. The main exception is the TOL model species, which is discussed below. The species with the best correlation to the base ROG are ETH, OLE, ALD2 and XYL, and those with the most scatter (besides TOL) are formaldehyde, CO, and ethane. There is no large difference in the degree of scatter of the data for the 8-hour compared to the 1-hour quantification data, though the scatter may be very slightly less in the case of the 8-hour data, especially for XYL. There is some day-to-day variability in the distributions of sensitivities for the 4K domain, with the data for the July 12 and July 13 shown on the figures being representative of this variability. This is discussed further below.

The high degree of scatter for the TOL model species is due to its extreme sensitivity to NO_x conditions, caused by unique characteristics in its mechanism as discussed above. In particular, it tends to have moderately high positive reactivity under higher NO_x conditions because of its radical initiating characteristics, but very negative reactivities in moderate or low NO_x conditions because its mechanism has strong NO_x sinks. As discussed above the CB4 TOL model species may not be a good representation for toluene itself, and other mechanisms do not show such large scatter for relative reactivities of this compound (e.g., Hakami et al, 2002). However, the qualitative reactivity characteristics of the TOL species are probably similar to compounds such as styrenes, phenols, or alkyl bromides, whose reactivities tend to exhibit this type of strong dependence on NO_x conditions (Carter, 2000a, Carter et al, 1997b). The reactivity characteristics of toluene may be better represented by the XYL model species, except with lower magnitudes because of its lower rate constant (Carter, 2000a).

The relative reactivities of the formaldehyde, CO, ethane and (to a lesser extent) the PAR model species are quite variable in the various cells, though nowhere near the extent that is the case for the TOL species. In the case of formaldehyde, this is probably due to variations throughout the domain in sensitivities to radical initiators, which tend to be more important in high NO_x conditions than when NO_x is limited. The variation is less than for TOL because although the formaldehyde relative reactivity tends to decline in lower NO_x conditions, it does not generally become negative. In the case of CO, ethane, and (to a lesser extent) PAR, the variability may reflect different sensitivities throughout the domain to relatively slowly reacting species. The ozone impact of slowly reacting species is expected to dependent on details of transport conditions. For example, if such species are transported out of the source area only to NO_x limited regions where little additional O_3 formation can occur it will have a relative lower impact than would the case if they were transported over other source areas, where fresh NO_x emissions would permit its reactions to form additional O_3.

Based on these considerations, one would expect reactivities of slowly reacting species to correlate better to each other than to the base ROG, since the dependences of their impact on conditions should be similar. This is shown on Figure 21, which gives plots of the reactivities of ethane and CO vs. PAR. It can be seen that the scatter is significantly less in the case of ethane, and somewhat less in the case of CO. The lesser improvement in correlation in the case of CO is probably due to at least in part to

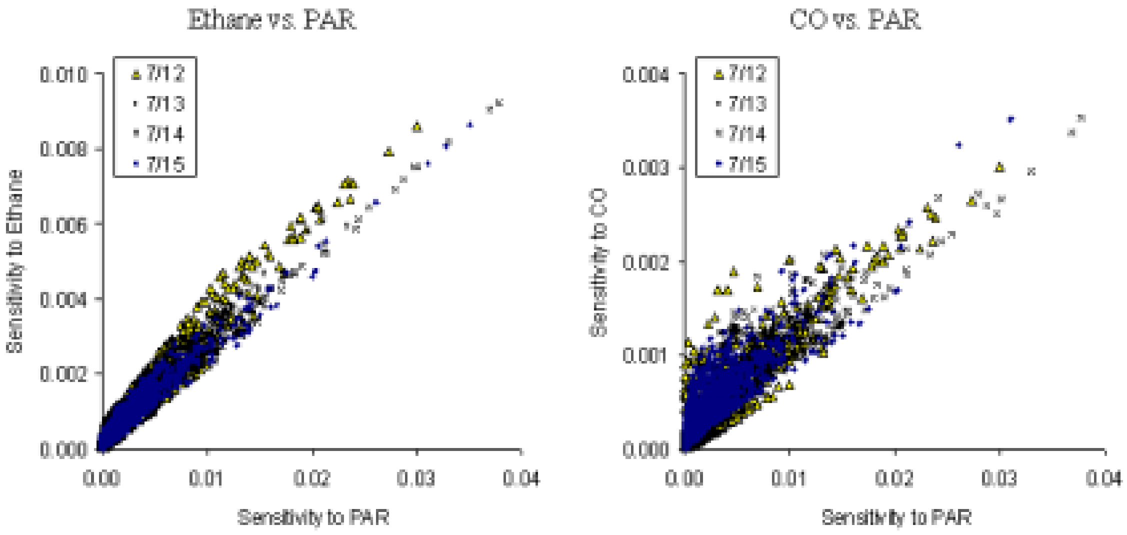

Figure 21. Plots of incremental reactivities of ethane and CO against those of the PAR model species. Reactivities are shown for the 1-hour maximum O_3 quantification and are on a carbon basis.

the fact that this has the lowest rate constant, but could also be due to other differences in its mechanism compared to other model species, such as lack of radical sources and NO_x sinks.

Regional Relative Reactivity Scales

Comparison of Regional Metrics

As discussed above, relative reactivities reflect ratios of incremental reactivities of the model species against those of the base ROG mixture, and since these ratios vary with location within the modeling domain several different approaches can be used to derive relative reactivity scales reflecting the distributions of sensitivities during a given episode day for a given modeling domain. Tables in Appendix B give the relative reactivities for each episode day, ozone quantification method, and metric for deriving regional reactivity numbers for each of the model species. EKMA relative reactivities derived using corresponding metrics are also shown for comparison. Averages of selected regional reactivity results and selected comparable EKMA reactivities are shown on Table 8, and these data are compared graphically on Figure 22 through Figure 24. These indicate how the different types of models, metrics, and ozone quantification methods differ in terms of their relative reactivity values for the various model species considered in this work.

In order to show comparisons of different reactivity scales for the full range of model species, Figure 25 through Figure 35 show plots giving comparisons of selected pairs of relative reactivity metrics. The larger plots on the left show the full range of species, and the smaller plots to the right have expanded ranges to aid comparisons for the lower reactivity species. Each point on the plots consists of relative reactivities of a single compound for a single episode day, with the “x” and “y” values being the relative reactivities in the two scales being compared. Different symbols are used to indicate different compounds in the low, medium, and high reactivity range, and circles, triangles, or diamonds around the symbols are used to indicate data from the 4K, 12K, or 36K domains, respectively. The diagonal lines on

Table 8. Summary of selected reactivity metrics for the Carbon Bond species whose ozone sensitivities were calculated

VOC type or Model Species	Relative Reactivities (Carbon Basis) – Averages and standard deviations for the episode days (Maximum 1-hour average quantification and 36K domain unless noted otherwise)										
	Avg O3 (8 Hr)	Avg O3	Avg O3 (4K)	EKMA Avg O3	Avg O3 >Std	Reg'l Max O3	Min Sub Err #1	Min Sub Err #2	Avg MIR-MOIR	Reg'l MIR	EKMA MIR
PAR Species	0.87 6%	0.87 4%	0.75 18%	0.60	0.89 7%	1.07 21%	0.69 8%	0.76 6%	0.62 6%	0.51 34%	0.40
Ethene	3.57 4%	3.66 6%	3.54 5%	3.05	3.60 8%	3.22 29%	2.97 2%	3.11 2%	2.81 2%	2.67 5%	2.64
OLE Species	6.55 3%	6.50 5%	6.17 5%	5.91	5.84 9%	4.57 30%	5.45 6%	5.67 5%	5.36 5%	5.51 13%	5.50
TOL Species	-1.73 17%	-1.63 15%	-0.82 74%	-0.63	-1.11 30%	-0.99 64%	-0.13 21%	-9.28 39%	0.24 12%	0.40 19%	0.57
Xylenes	0.64 37%	0.62 31%	1.25 45%	1.79	0.86 33%	0.57 120%	1.75 8%	2.19 9%	2.09 5%	2.42 17%	2.68
Formal-dehyde	3.19 4%	3.32 17%	4.36 9%	5.01	3.86 26%	2.34 58%	4.33 22%	5.27 18%	4.81 13%	6.29 35%	6.47
Acetal-dehyde	3.53 2%	3.28 6%	2.76 8%	3.83	2.48 13%	2.03 28%	2.70 4%	2.90 2%	2.63 3%	3.05 13%	3.45
Ethanol	1.38 3%	1.26 7%	0.98 6%	1.12	0.91 12%	1.08 41%	0.83 13%	0.96 11%	0.73 9%	0.64 25%	0.76
Ethane	0.36 4%	0.34 2%	0.26 17%	0.16	0.27 15%	0.33 42%	0.21 13%	0.26 9%	0.17 9%	0.13 42%	0.09
CO	0.15 7%	0.15 8%	0.12 15%	0.07	0.13 12%	0.15 28%	0.09 8%	0.11 5%	0.07 6%	0.05 28%	0.03

the plots are the 1:1 lines where all the points would fall if the relative reactivities in the two scales were equal, with the distances between the various points and these lines indicating the extent to which the two scales give comparable results. These comparisons are discussed further below.

Although there are differences between the various relative reactivity measures as discussed below, in most cases the differences between the metrics are less than the differences between the model species. The least variability in reactivity results are obtained for the olefin model species (ethene and OLE) and the greatest variability is obtained for TOL (as expected) and to a lesser extent formaldehyde and xylenes. There is also some differences I the various types of metrics for the slowly reacting species CO, ethane and (to a lesser extent) PAR. The sources of these differences are discussed below.

In general, the reactivity metrics derived from impacts over the entire domain or over large subsets of the domains tend to give less variable results than metrics based on impacts in a single selected cell, such as the regional MIR or maximum O_3 metrics. The regional maximum ozone metric is

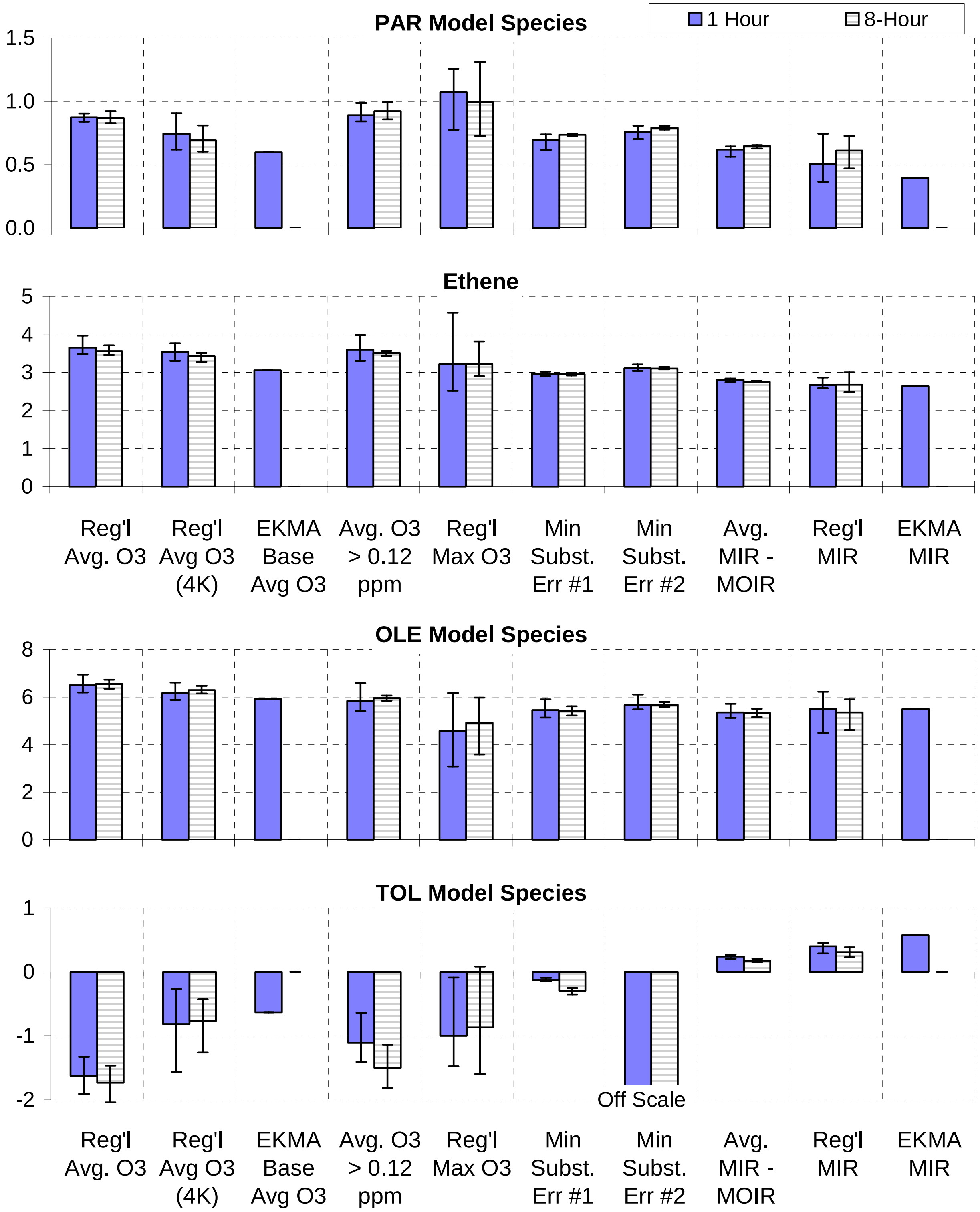

Figure 22. Comparison of selected reactivity metrics for the PAR, OLE, and TOL model species and ethene. Regional metrics are for the 36K domain unless indicated otherwise, and averages and ranges are shown.

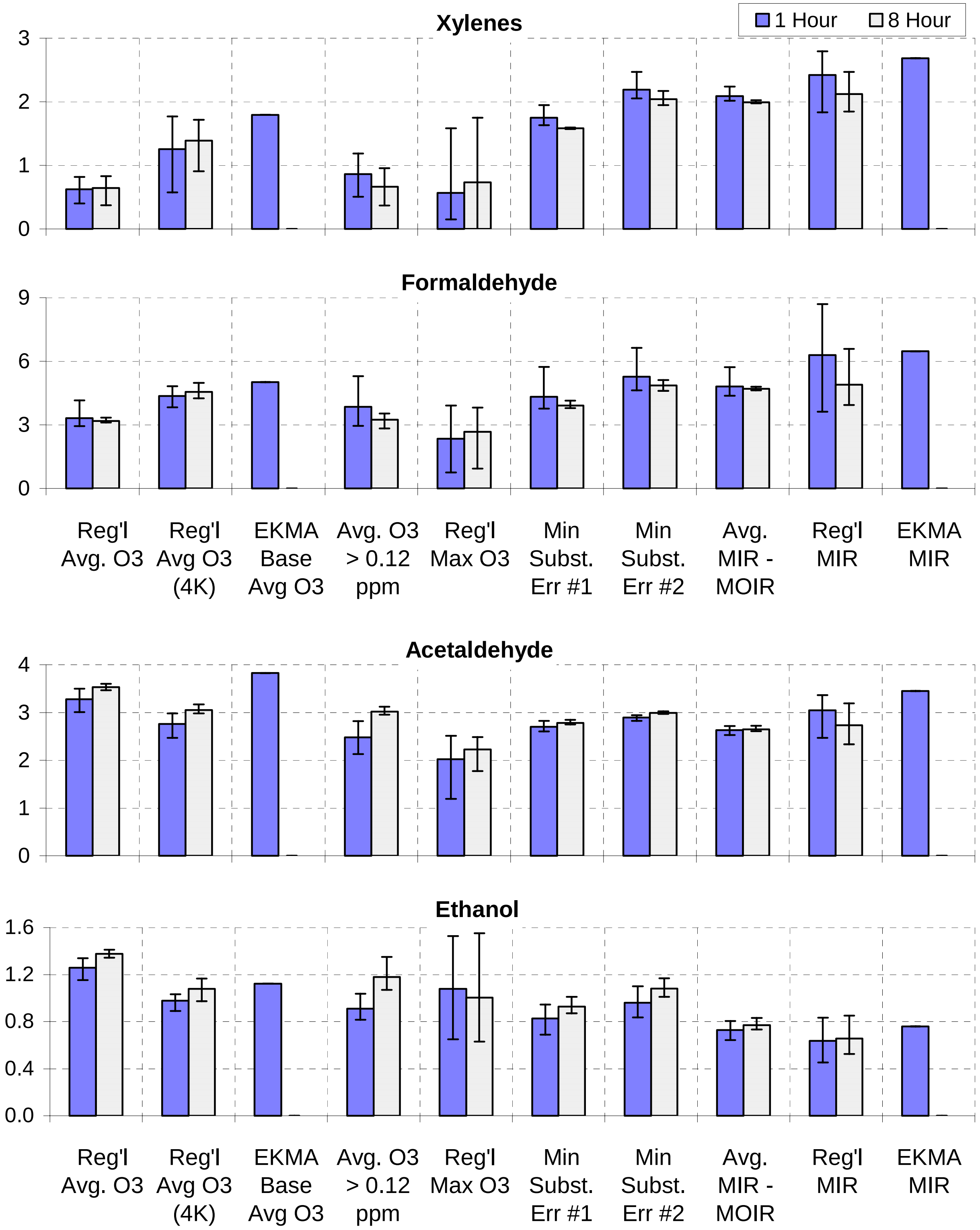

Figure 23. Comparison of selected reactivity metrics for the xylenes, formaldehyde, acetaldehyde, and ethanol. Regional metrics are for the 36K domain unless indicated otherwise, and averages and ranges are shown.

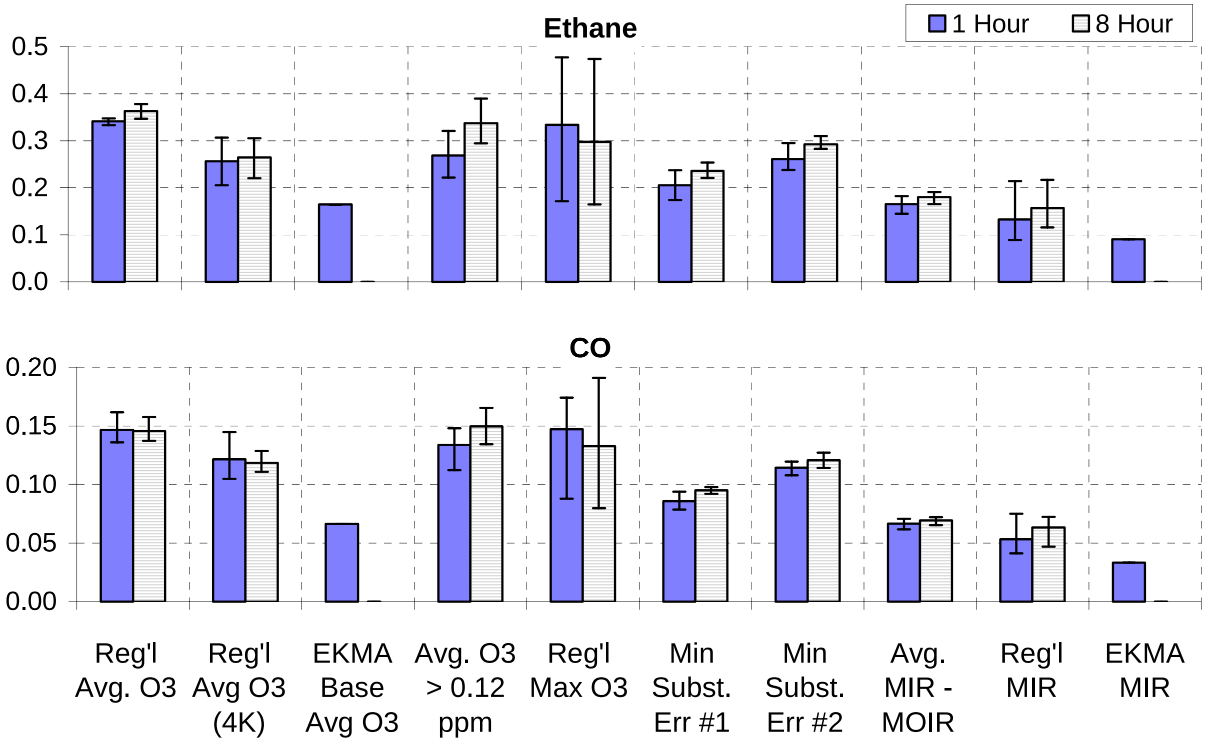

Figure 24. Comparison of selected reactivity metrics for ethane and CO. Regional metrics are for the 36K domain unless indicated otherwise, and averages and ranges are shown.

particularly variable because of relatively large variability of conditions in the cells with the highest O_3 levels on the various episode days and domains. For example, Table 5 indicates that in three of the four episode days the highest 1-hour ozone cell in the 36K domain had quite high positive NO_x sensitivities, indicating very NO_x limited conditions, while for the other day (July 13) the highest 1-hour O_3 cell had a slightly negative NO_x sensitivity, indicating MIR to MOIR conditions. Clearly, a combination of factors must be involved in causing a particular cell to have the highest O_3 level, with multi-day transport probably playing a significant role in most cases. In some cases the highest O_3 cell was found to be very insensitive to anthropogenic VOCs, yielding relative reactivity values that are ratios of very small numbers and therefore not particularly well defined. Because of this, the regional average ozone over the standard metric, which tends to give less variable results because it reflects impacts on larger numbers of cells, provides a much better alternative to the regional maximum ozone metric if the interest is determining the relative effects of VOCs on high ozone regions. This is discussed further in the "Effect of Varying the O_3 Cutoff" section, below.

Figure 25 shows a comparison of the relative reactivities in the regional maximum ozone metric against those derived using the regional ozone over the standard method. Although there is considerable scatter because of the significant variability of the regional maximum ozone metric, it can be seen that there are no systematic biases. This is indicated by the fact that the differences between the two metrics for any model species is considerably less than the differences between the metrics derived for different episode days or grid domains for the same species and metric.

There is less variability in the regional MIR metric because the cells where ozone has the highest base ROG sensitivity all have comparable chemical conditions, i.e., are all very VOC-sensitive and have negative NO_x sensitivity. However, the variability in reactivity metrics is even less in the comparable

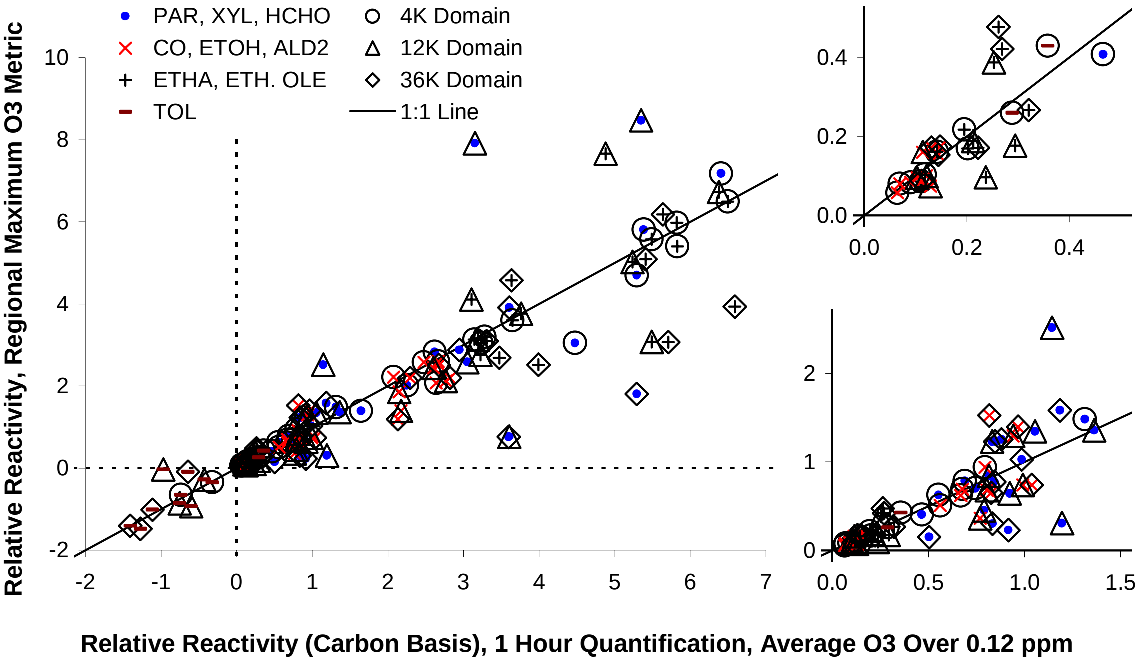

Figure 25. Plots of relative reactivities derived using the regional maximum ozone metric against relative reactivities using the average ozone over the standard metric, for the 1-hour average quantification.

average MIR to MOIR scale, which has an average standard deviation among the episode days in the 36K domain of only ~7%, compared with ~25% for the regional MIR scale. Therefore, the average MIR to MOIR scale presents a somewhat less variable metric if the interest is determining the relative effects of VOCs on ozone formation in the regions where ozone formation is the most sensitive to changes in VOC emissions.

Figure 26 shows a comparison of relative reactivities in the regional MIR metric against those derived using the average MIR-MOIR method. With the possible exception of formaldehyde there is considerably less variability in the data compared to the maximum O_3 or average O_3 over the standard methods, and except for formaldehyde the variability is relatively small. Because of this smaller variability among episode days, some consistent differences can be seen between the two metrics for certain model species. In particular, the relative reactivities in the regional MIR metric are somewhat higher (in most cases) for formaldehyde and the TOL model species and somewhat lower for the slower reacting species. These differences can be attributed to the contribution of cells whose characteristics are closer to MOIR than MIR in the average MIR-MOIR metric. The lower NO_x levels in the MOIR cells would result in lower reactivities for the highly NO_x sensitive TOL species and somewhat less sensitivity to radical initiating species such as formaldehyde, compared to the higher NO_x MIR cells. The lower NO_x also results in somewhat higher overall radical levels, which means that slower reacting species such as ethane undergo relatively more reaction and thus have higher relative reactivity. However, the differences are relatively small compared to the differences between some of the other scales, as discussed below.

As indicated above, there are two ways to derive the minimum substitution error metric, with method #1 being based on a base ROG for VOC substitution, and method #2 being based on substituting the base ROG for the VOC. A comparison of the two scales is shown on Figure 27, with the data for the TOL model species not shown because the most of the values for method #2 tend to be off scale. It can be

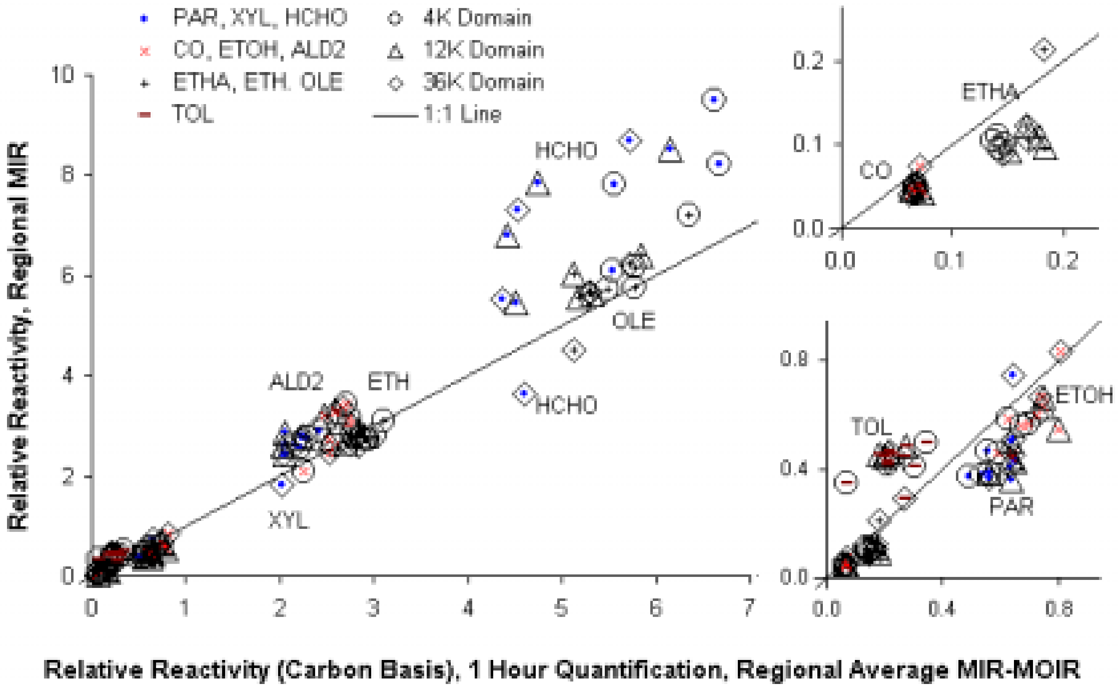

Figure 26. Plots of relative reactivities derived using the regional MIR metric against relative reactivities using the average MIR-MOIR metric, for the 1-hour average quantification.

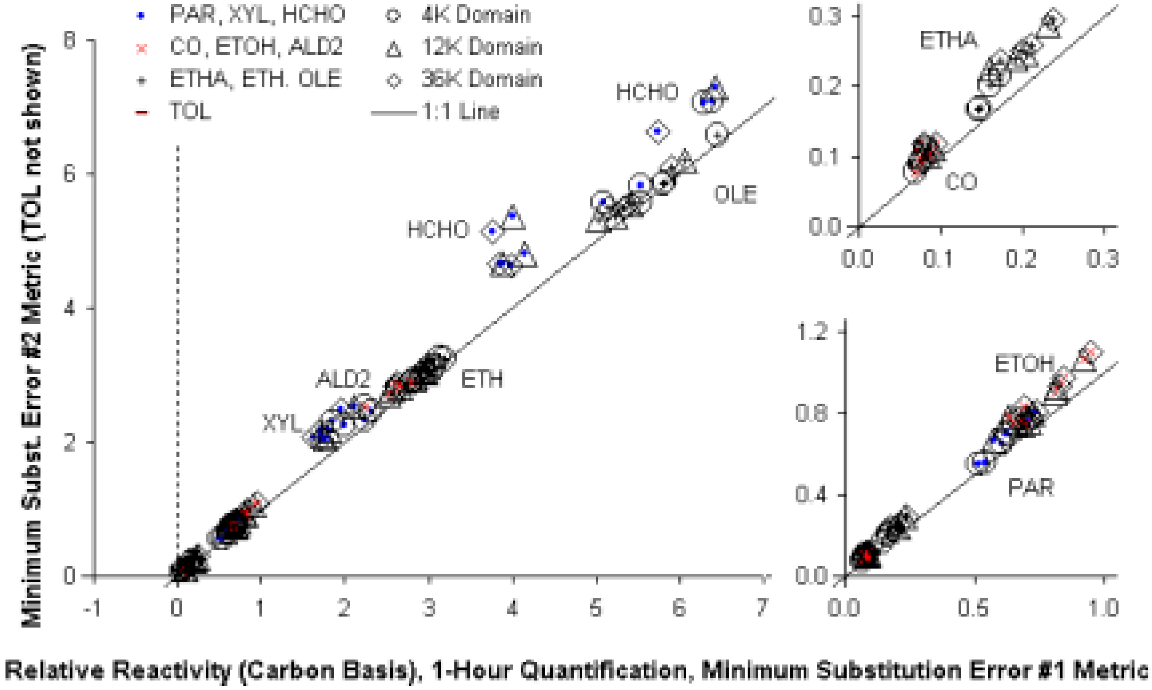

Figure 27. Plots of minimum substitution error relative reactivities using method #2 against those using method #1 for the 1-hour average quantification. Data for TOL are not shown.

seen that there is a good correspondence for all species shown, though method #2 tends to give somewhat higher relative reactivities for formaldehyde and the slower reacting species. The results for the two methods should be similar if plots such as those shown on Figure 16 through Figure 20 are reasonably well fit by lines forced through zero, and will diverge when the data are more variable or less well fit by such lines. This is the case for the TOL species and to a much lesser extent formaldehyde. In addition, method #2 does not give numerically stable results if the incremental reactivity of the model species is scattered around zero, as is the case for the TOL model species. Because of this, the TOL reactivities derived using method #2 are extreme in magnitude and variability and probably should be considered to be meaningless (and for that reason are not shown on Figure 27). Because of this, and the fact that the two metrics give similar results for the other species, use of method #1 is considered to be preferable if the interest is deriving a relative reactivity scale based on the minimum substitution error approach.

Comparisons of the minimum substitution error #1 relative reactivities with relative reactivities in other selected metrics are shown on Figure 28 through Figure 30. (The regional maximum O_3 and regional MIR metrics are not shown because as discussed above other metrics that represent generally similar conditions are considered to be preferable.) In most cases the differences between the scales are not large, with most points being reasonably close to the 1:1 line and general trends in terms of orders of magnitude and relative reactivity rankings being preserved. However, as discussed below there are some systematic differences between some of these scales that can be explained in terms of differences in their derivations in terms of weighting of relative importances of difference types of cells.

Figure 28 shows that there are systematic differences between the average ozone and the minimum substitution error metrics for certain types of species. In particular, the average O_3 metric tends to give lower relative reactivities for slowly reacting species such as CO and ethane, higher reactivities for radical initiating species such as formaldehyde and xylenes, and more negative reactivities for the TOL species, compared to the minimum substitution error (#1) metric. These differences can be explained by the fact that the minimum substitution error method gives greater weight to the more VOC-sensitive cells that have higher VOC incremental reactivities, while the average O_3 method gives relatively more weight to the many NO_x-limited cells where incremental reactivities are low and most of the ozone is due to long range transport. One would expect slowly reacting species such as CO and ethane to have relatively higher ozone impacts in areas dominated by long-range transport compared to the near-source areas where NO_x levels, because they have had longer periods in which to react. On the other hand, species with NO_x sinks in their mechanisms, such as TOL and a lesser extent xylenes, and species that are radical initiations, such as formaldehyde and xylenes would have lower (or more negative) relative reactivities in the NO_x-limited regions that are given more weight in the average ozone scale. Therefore, these NO_x-sink or radical source compounds tend to have lower relative reactivities in that scale.

On the other hand, Figure 29 shows that the average MIR-MOIR and the minimum substitution error methods tend to give remarkably similar values for the various episode days for most of the model species. This similarity can be attributed to the fact that both scales weigh impacts in the relatively high NO_x, VOC sensitive areas most highly, even though the specific weighting methods are quite different. The major exception is the TOL species, which has positive reactivities in the average MIR-MOIR metric but negative or near zero relative reactivities in the minimum substitution error (#1) scale. The difference for toluene is due to the fact that the MIR-MOIR scale gives zero weight to the NO_x-limited cells where TOL has highly negative reactivities, while these large magnitude negative reactivities can significantly affect the minimum substitution error derivation. The average MIR-MOIR metric also gives slightly lower reactivities for the slowly reacting species and slightly higher reactivities for formaldehyde, at least in some of the episode days. Other than that, from a practical standpoint both of these can be considered to give very similar scales.

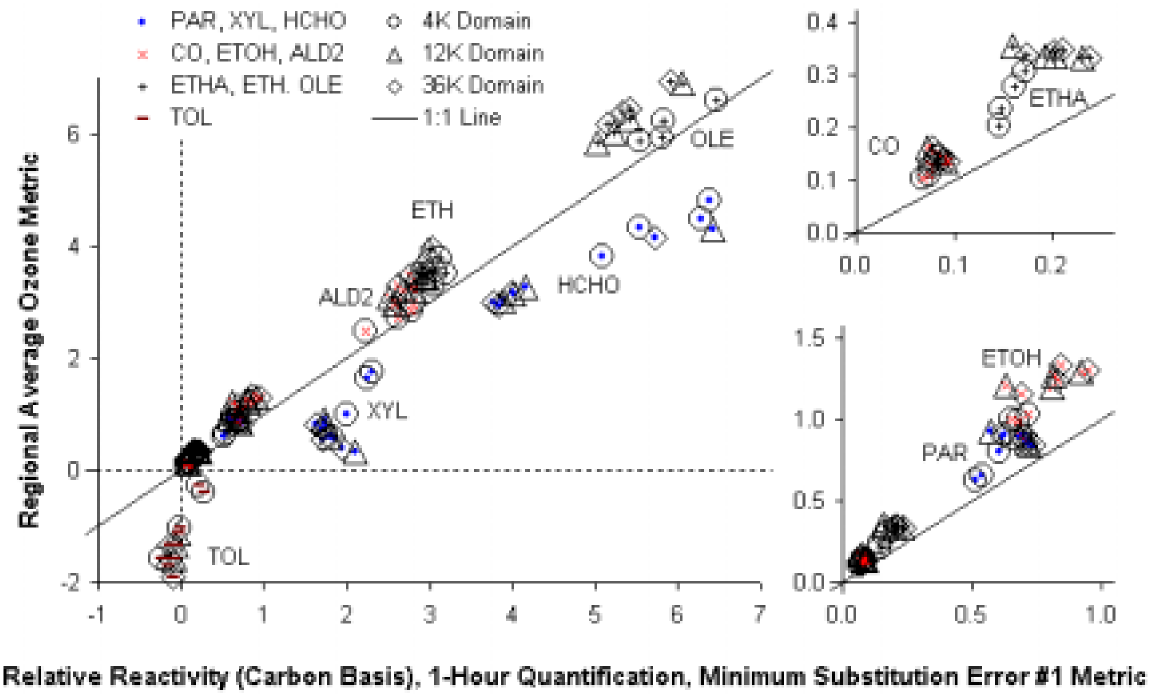

Figure 28. Plots of relative reactivities derived using the regional average ozone metric against relative reactivities using the Minimum Substitution Error #1 method, for the 1-hour average quantification.

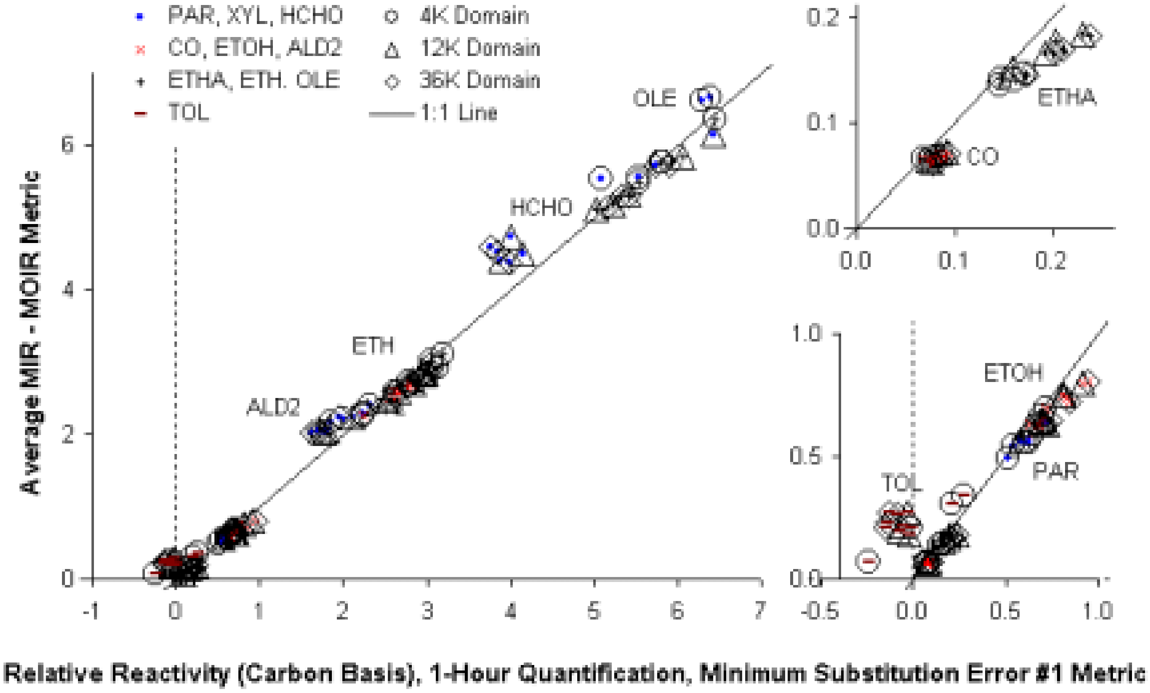

Figure 29. Plots of relative reactivities derived using the average MIR-MOIR metric against relative reactivities using the Minimum Substitution Error #1 method for the 1-hour average quantification.

Figure 30 and Figure 31 show comparisons of the average ozone over the standard metric against the minimum substitution error and average ozone metrics, respectively. The average O_3 over the standard scale appears to be between the average ozone and the minimum substitution error scales in its general characteristics, at least in terms of differences in relative reactivities of the slowly reacting on the one hand, and the radical initiating species on the other. In addition, the variability in relative reactivities with episode day is somewhat less correlated than is the case for the other two scales, presumably due to differences in meteorological conditions leading to the higher ozone levels. Because of this, the differences between this and the other two scales is somewhat less significant compared to the variability with episode day.

In general, the ozone quantification method (1-hour vs. 8-hour averages) does not have a significant effect on the regional relative reactivity metrics that are derived, particularly for the truly global metrics. For example, Figure 32 and Figure 33 show that the relative reactivities in the average ozone and minimum substitution error metrics are essentially the same. (The averages on Table 8 and Figure 22 through Figure 24 may in some cases indicate greater differences because the July 15 episode day is counted in the averages for the 1-hour but not the 8-hour data.) Somewhat greater differences between the 1-hour and 8-hour quantifications are seen for the regional ozone over the standard metric as shown on Figure 34 and the regional maximum ozone metric as shown on Figure 35. The differences for the average ozone over the standard metrics can be attributed to the fact that the spatial domain of cells over the 8-hour is different than those over the 1-hour standard, and the differences for the maximum ozone metric is attributed to the general variability of this metric, as discussed above. (Note that the extreme outliers on Figure 35 are all due to the 8-hour data for the July 14 episode day in the 12K domain, where the peak 8-hour average ozone occurred in an extremely NO_x-sensitive cell with a very low sensitivity to anthropogenic VOCs.) However, in both these cases the differences between the two quantification methods are less than the differences between the various episode days, and no systematic differences or biases between the two quantification methods are seen.

The minimum substitution error and average ozone reactivity metrics in the 12K domain are generally similar to those in the 36K domain, though the differences are greater when comparing the 4K and the 36K domains. A similarity in results for the 12K and 36K domains is expected given that the 12K domain encompasses a relatively large fraction of the 36K domain, especially if the over-water cells are excluded, and probably contain a similar distribution of conditions. However, the 4K domain is much more dominated by urban source areas, and tends to include relatively larger fractions of higher NO_x, more VOC-sensitive cells. For that reason, the slowly reacting species such as CO and ethane tend to have lower reactivities, and the radical initiating species such as XYL and formaldehyde have higher reactivities in the 4K domain compared to the larger domains. The relatively importance of VOC sensitive cells also varies from day to day to a much greater extent than is the case with the larger domains. This is indicated by the fact that on July 12 and 13 almost 25% of the cells had NO_x conditions in the MIR to MOIR range, while on the other two days only ~5% of the cells had NO_x conditions in this range, as which is approximately the same as their relative importance in the large domains.

Effect of O_3 Cutoff Level

One critique of the average ozone metric is that includes the many very low O_3 cells where ozone levels are not of concern from a policy perspective in addition to those cells that are of greater concern. The average ozone over the standard metric addresses this by considering only cells over the air quality standard, and as shown on Figure 31 there are some differences between these metrics. However, ozone impacts in regions that just barely meet the current standards are also of concern, especially if a substitution strategy results in ozone increases in those regions result in O_3 levels that no longer meet the standard. Therefore, it might be appropriate to use an O_3 cutoff level higher than zero but lower than the air quality standard when deriving an average ozone reactivity metric.

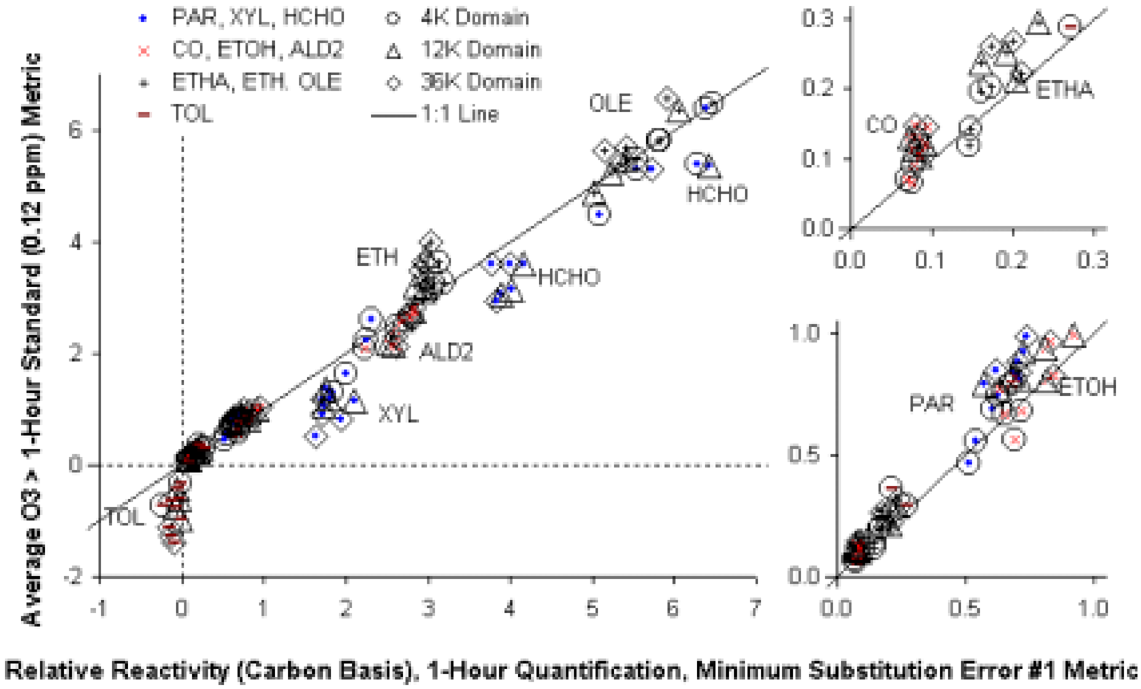

Figure 30. Plots of relative reactivities derived using the average O_3 over the standard metric against relative reactivities using the Minimum Substitution Error #1 method for the 1-hour average quantification

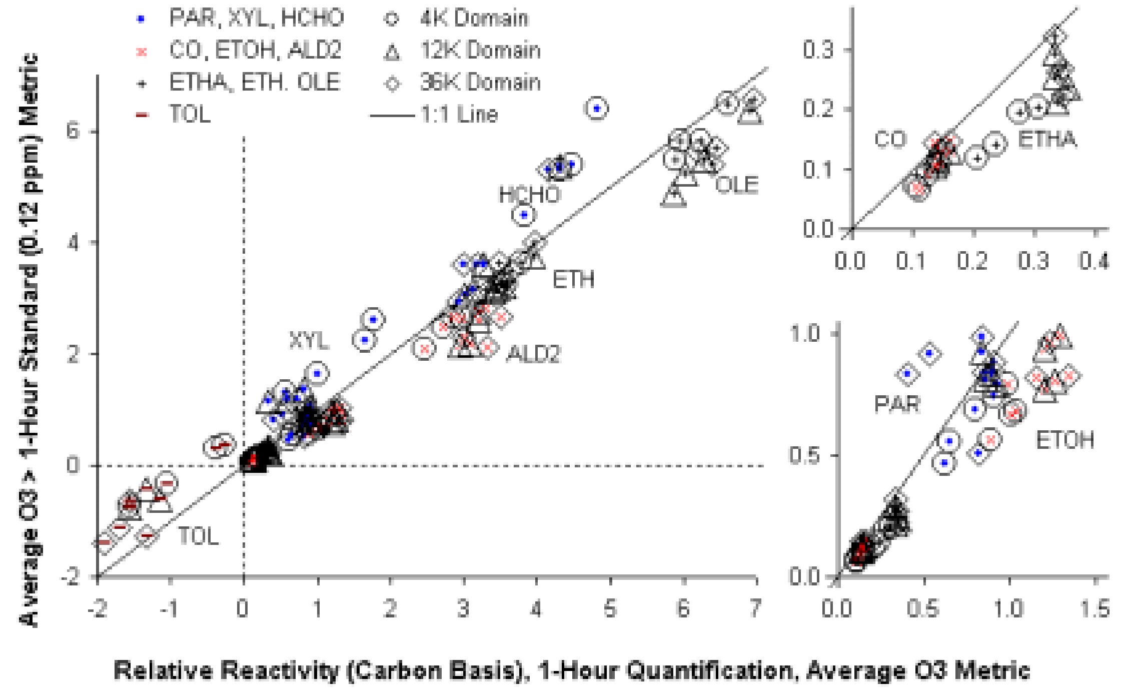

Figure 31. Plots of relative reactivities derived using the average O_3 over the standard metric against relative reactivities using the regional average ozone method, for the 1-hour average quantification.

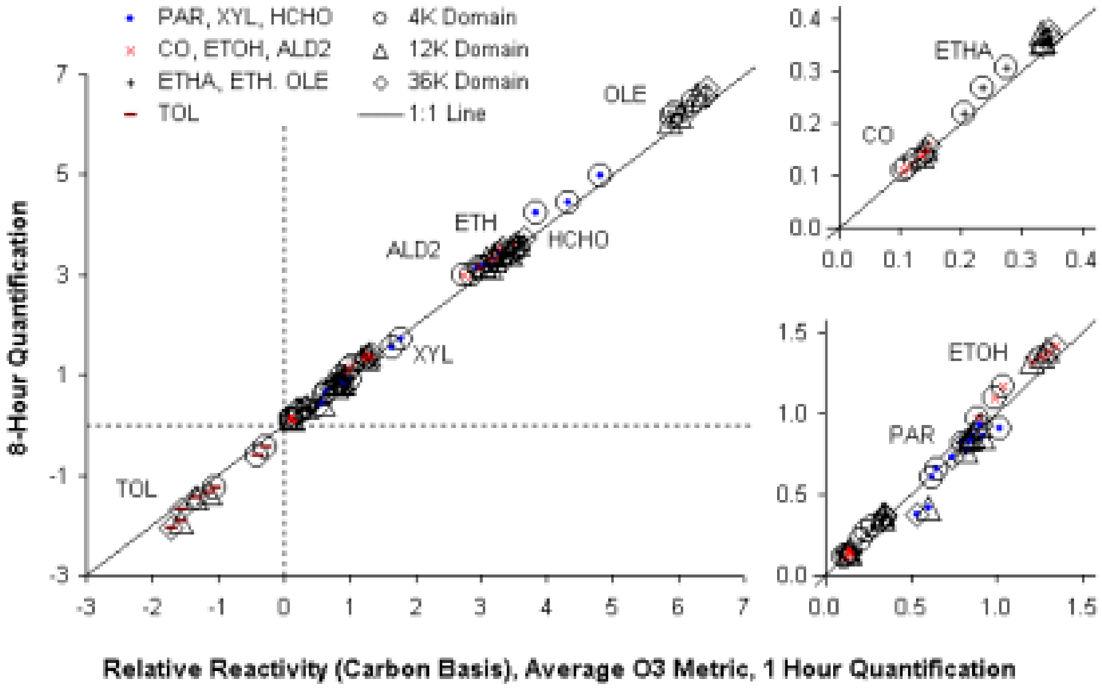

Figure 32. Plots of relative reactivities derived using the maximum 8-hour average O_3 quantification against those derived using maximum 1-hour average quantification for the regional average ozone metric.

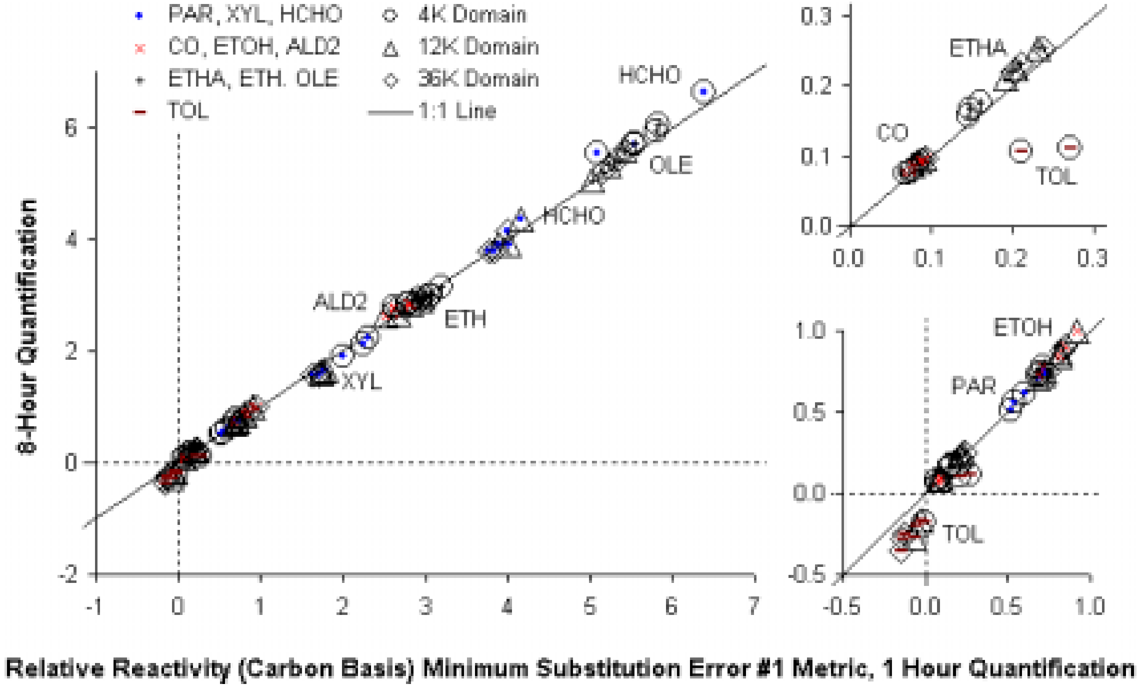

Figure 33. Plots of relative reactivities derived using the maximum 8-hour average O_3 quantification against those derived using maximum 1-hour average quantification for the minimum substitution error #1 metric.

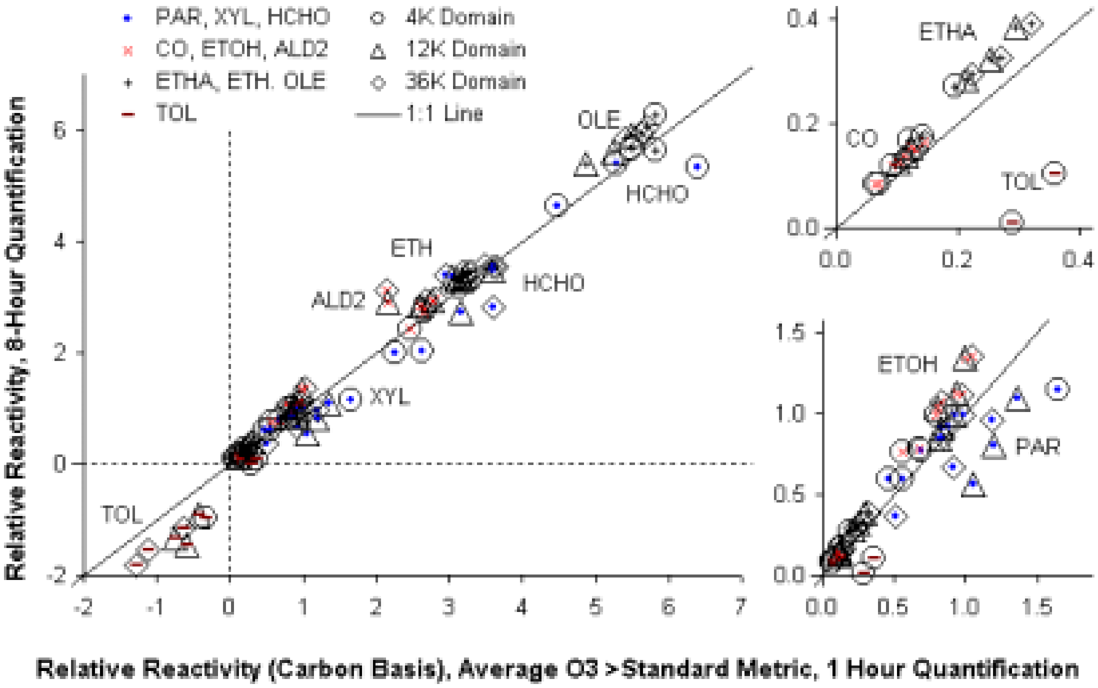

Figure 34. Plots of relative reactivities derived using the maximum 8-hour average O_3 quantification against those derived using maximum 1-hour average quantification for the average ozone over the standard metric.

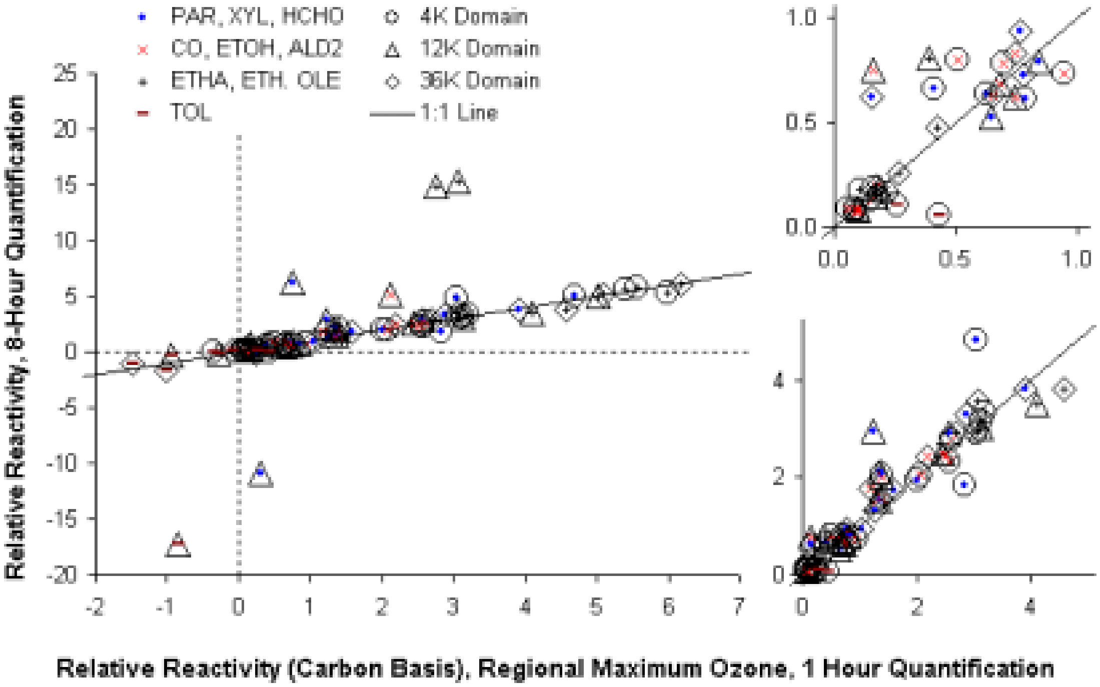

Figure 35. Plots of relative reactivities derived using the maximum 8-hour average O_3 quantification against those derived using maximum 1-hour average quantification for the regional maximum ozone metric.

Figure 36 shows plots of regional average ozone relative reactivities using various cutoff levels for the maximum 1-hour average ozone quantification against the ozone cutoff level for all the model species for each of the 4 episode days in the 36K domain. Note that the values on the far left hand side of the plots are the regional average ozone metrics (i.e., without cutoffs), the values for 0.12 ppm (shown by the solid vertical line) are the average ozone over the standard metrics, and the values on the far right are the regional maximum ozone metrics. It can be seen that for most model species and episode days the use of cutoffs up to about 0.08 ppm does not significantly change the average ozone metric, while using cutoffs above the standard begin to give divergent and variable results. The main exception is acetaldehyde, where the relative reactivities tend to monotonically decline for cutoffs above 0.04 ppm for all four episode days, and ethanol for three of the four episode days. However, in general using cutoff levels significantly below the ozone standard does not greatly affect the average ozone relative reactivity metrics.

Comparison of Regional and EKMA Relative Reactivities

Although the major focus of this project is to derive relative reactivities using the regional model, it is also of interest to determine the extent to which regional model relative reactivities differ from those derived using the 1-day EKMA scenarios employed to derive the reactivity scales of Carter (1994a,b, 2000). The relative reactivities derived using these scenarios but with the same chemical mechanism and comparable metrics as used in this work are included with the regional model relative reactivity tabulations on Table 8 and the tabulations in Appendix B, and in the comparisons of the selected reactivity scales on Figure 22 through Figure 24. Note that the EKMA as well as the regional relative reactivities are all given on a carbon basis, so the units are consistent.

Figure 37 through Figure 39 show comparisons of EKMA with regional relative reactivity scales derived using comparable metrics, with Figure 37 comparing reactivities using the average ozone metric, Figure 38 comparing reactivities using the minimum substitution error method, and Figure 38 comparing average MIR-MOIR reactivities. In the case of the average ozone and minimum substitution error metrics each of the base case EKMA scenarios is treated in the same way as separate cells in the regional scales, and in the case of the MIR-MOIR metrics the EKMA relative reactivities are averages of relative reactivities in the EKMA MIR and EKMA MOIR scales.

For most model species the EKMA results are surprisingly close to the comparable regional relative reactivity metrics given the significant differences in the types of models and scenarios employed. Even for the highly variable TOL species the EKMA reactivities are within the scatter of the data for the comparable regional metrics, as shown on Figure 22 and Figure 37 through Figure 39. For species other than TOL, the average of all the EKMA metrics differ from the averages of all the regional metrics except maximum O_3 by less than 40%, with the difference being less than 25% for about half the species.

However, there are some consistent differences in EKMA vs. regional relative reactivities for certain model species. Perhaps the most significant is the consistent bias for the EKMA scales towards predicting lower relative reactivities for the slower reacting species, specifically CO, ethane, and to a lesser extent PAR. The bias appears to be somewhat less with the average MIR-MOIR and the MIR metrics, with the EKMA MIR values being within the day-to-day scatter of the regional MIR values for most species. A bias in the EKMA model towards underpredicting reactivities in slowly reacting species is expected because the slower reacting compounds have less of a chance to react in the one day EKMA scenarios then they would in multi-day regional model simulations.

There is also a consistent tendency for the relative reactivities for acetaldehyde (ALD2) and (to a lesser extent) ethanol, which forms acetaldehyde as its major product, to be lower in the regional scales compared to the EKMA scales. The reason for this is unclear and may require process analysis to

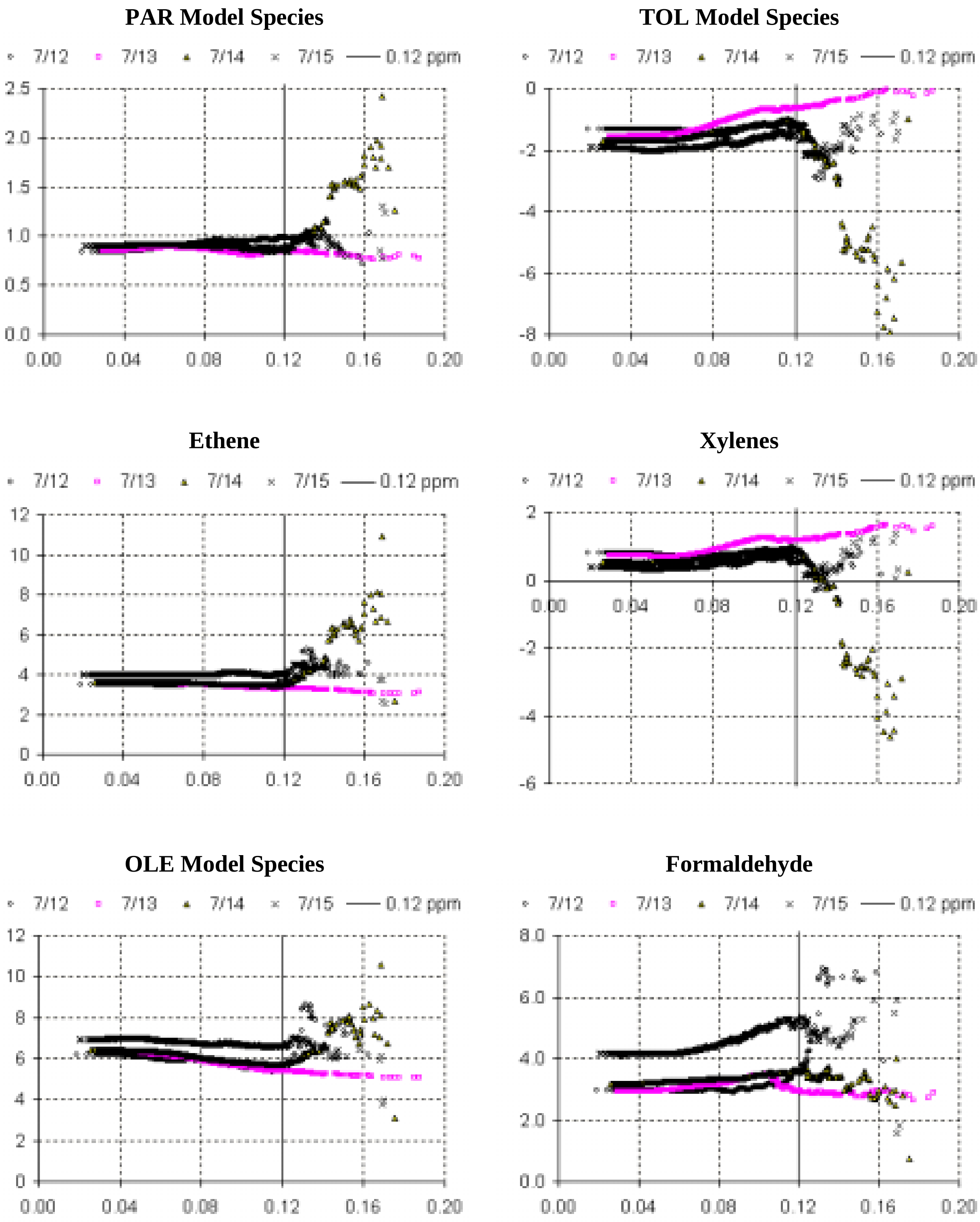

PAR Model Species

TOL Model Species

Ethene

Xylenes

OLE Model Species

Formaldehyde

Regional Average Relative Reactivity (carbon basis) vs. O_3 Cutoff level (ppm)

Figure 36. Plots of regional average relative reactivities against the O_3 cutoff level used for computing the averages. The four sets of points refer to the four episode days.

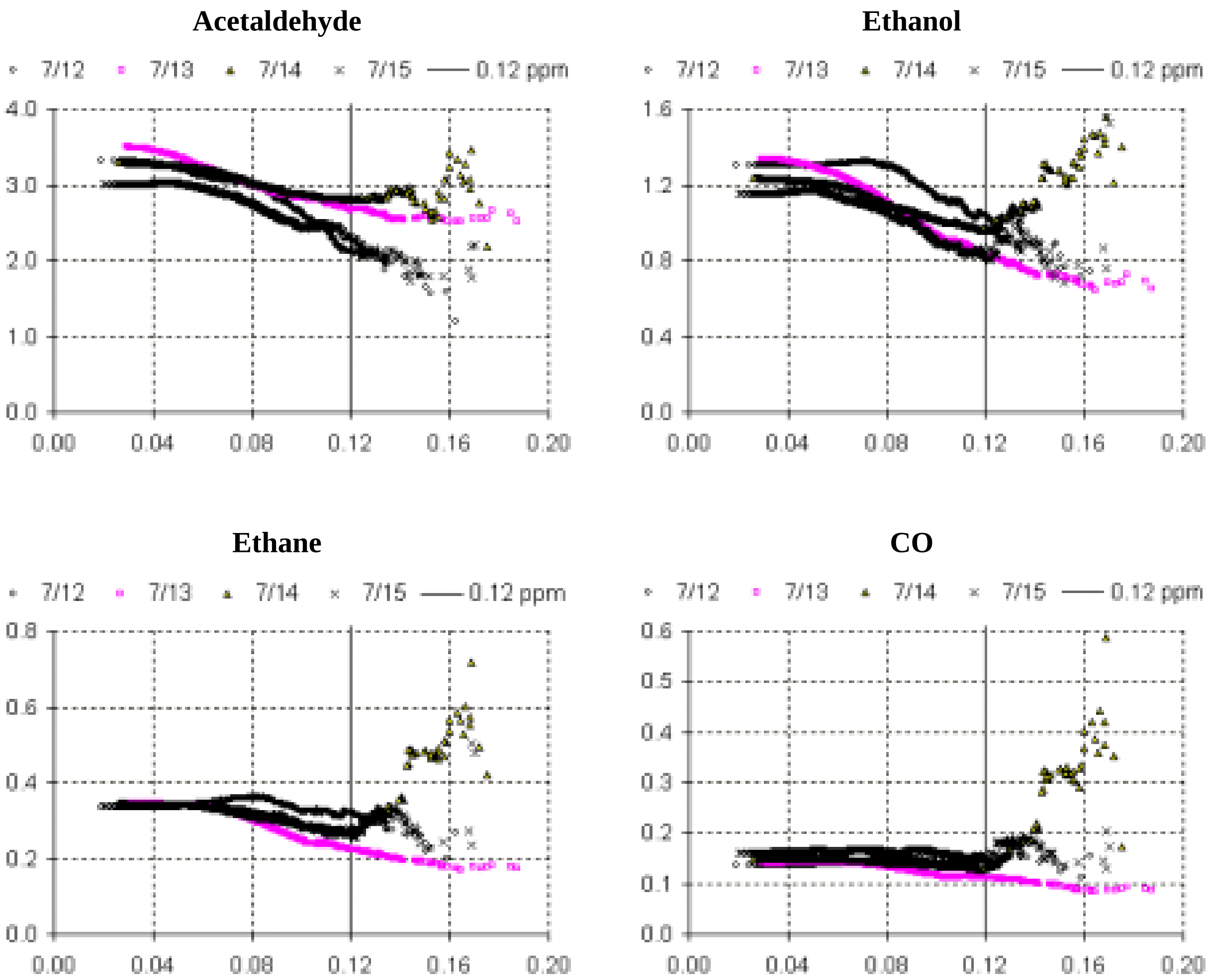

Regional Average Relative Reactivity (carbon basis) vs. O_3 Cutoff level (ppm)

Figure 36 (continued)

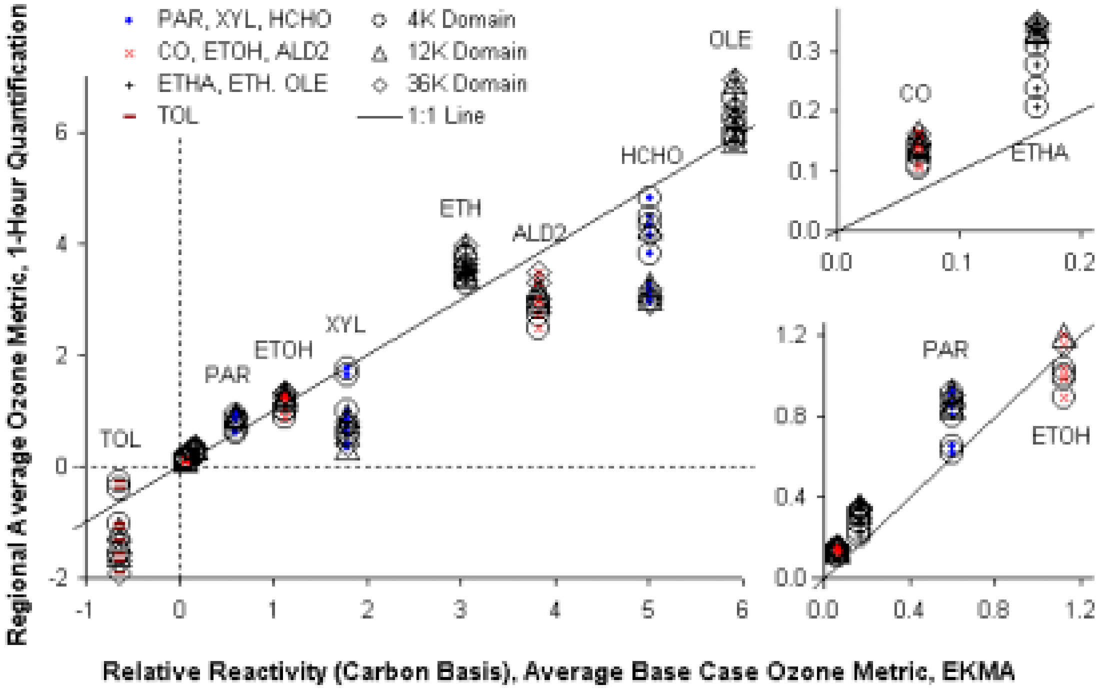

Figure 37. Plots of Regional vs. EKMA relative reactivities derived using the regional or base case average O_3 metric. Regional reactivities are based on the maximum 1-hour average quantification.

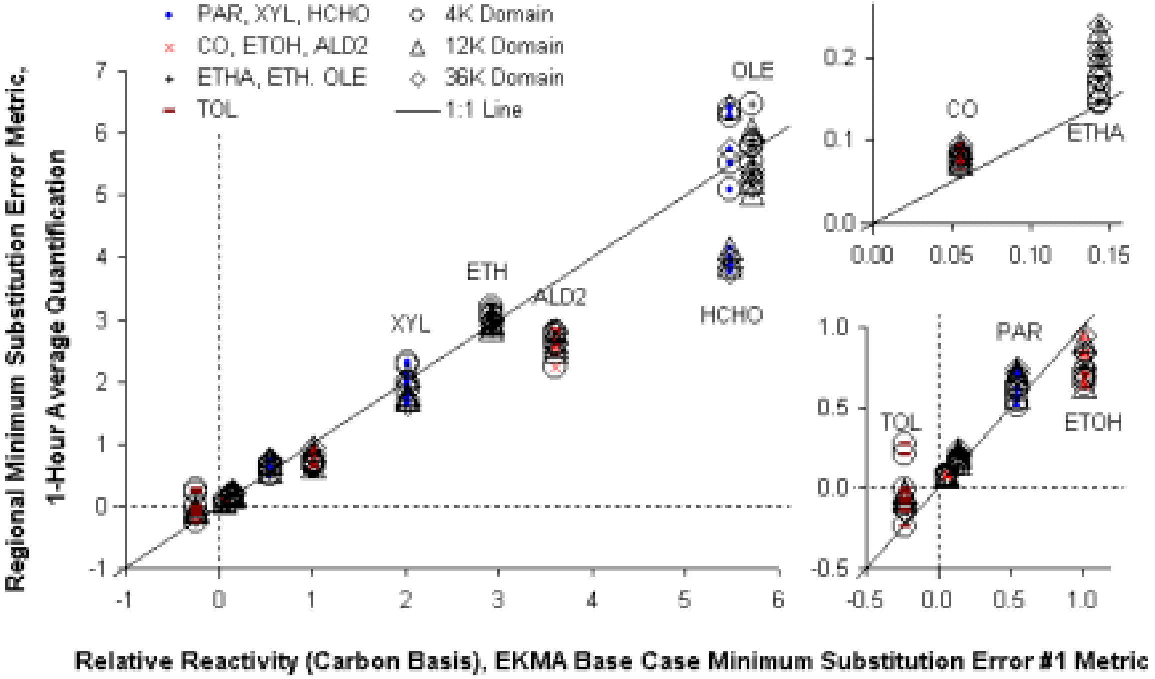

Figure 38. Plots of Regional vs. EKMA relative reactivities derived using the minimum substitution error (#1) metric. Regional reactivities are based on the maximum 1-hour average quantification.

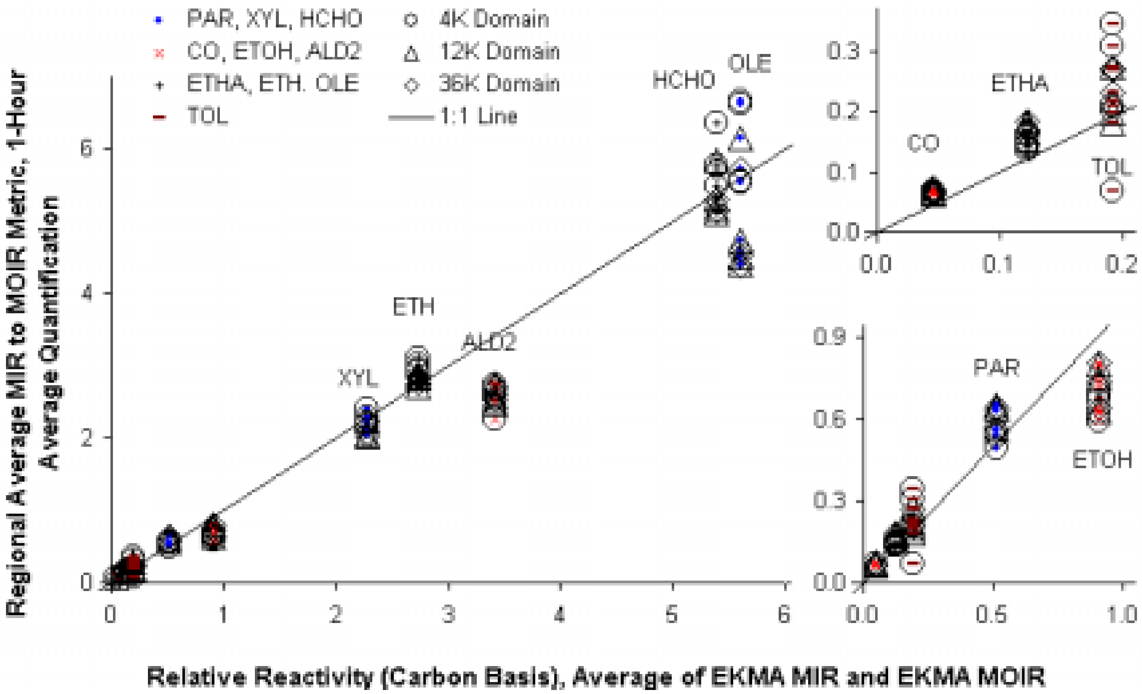

Figure 39. Plots of Regional vs. EKMA relative reactivities derived using the average MIR to MOIR metric. Regional reactivities are based on the maximum 1-hour average quantification.

elucidate. The xylene and TOL model species reactivities in the regional model also tend to be lower (or more negative) than the EKMA values when derived using the average ozone metric, though not when derived using the metrics that are more influenced by VOC-sensitive cells. This may be due to NO_x removal effects of these species being relatively more important in the low-NO_x cells in the regional model than is the case in the lower NO_x EKMA base case scenarios. A different result may be obtained if a different set of low NO_x base case scenarios were employed.

The differences between EKMA and regional model relative reactivities tend to be somewhat less in the 4K domain compared to the larger domains, perhaps because the 4K domain is more dominated by ozone exceedences urban conditions that the EKMA scenarios are designed to represent. This can be seen in Figure 37 through Figure 39, though it is perhaps more clearly shown in Figure 40, which shows plots of ratios of EKMA to average regional reactivities for the various species for the 36K and 3K domains. It can be seen that the regional relative reactivities of the slower reacting species in the 4K domain, and also for xylenes and formaldehyde, are in most closer to the EKMA values than those for the 36K domain. The main exception to this is ethanol, where the differences between EKMA and regional model reactivities are apparently due to other factors. This requires further investigation, which is beyond the scope of this project.

Results of Large-Scale Substitution Calculations

As indicated on Table 4, above, the large scale substitution calculations carried out for this project consisted of removing all anthropogenic VOC emissions and then replacing these with varying amounts of ethane, to represent effects of large scale substitutions of current emissions with slowly reacting, low reactivity compounds. Summaries of the ozone results obtained in these calculations are

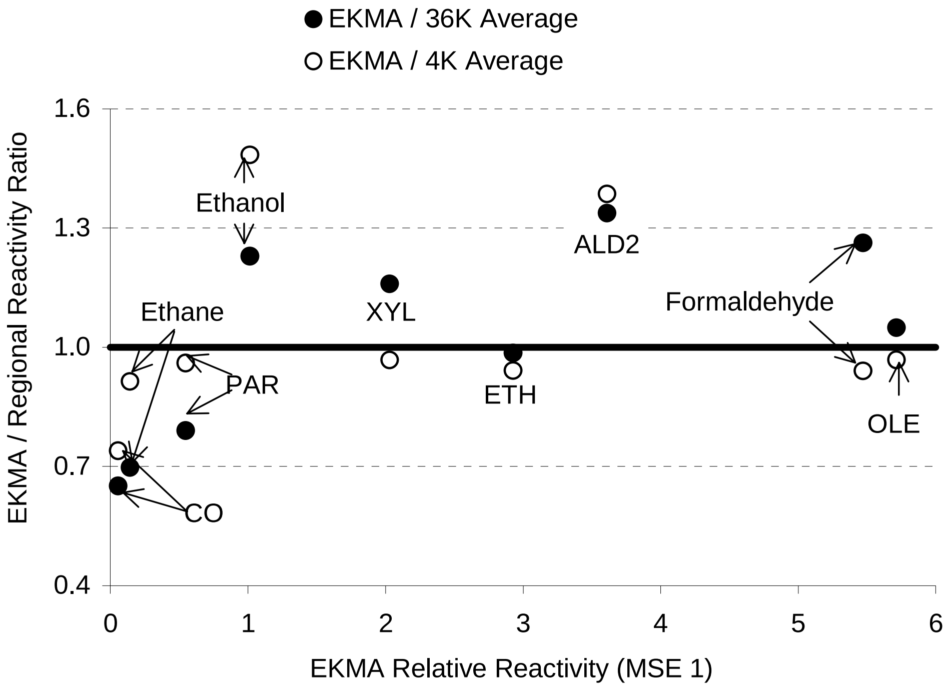

Figure 40. Plots of ratios of EKMA to regional model relative reactivities derived using the minimum substitution error (#1) method. Results for the highly variable TOL model species are not shown.

given on Table 9 through Table 12. Specifically, Table 10 and Table 9 show changes in domain-wide maximum and average daily maximum O_3 concentrations, Table 11 shows maximum changes in daily maximum ozone concentration, and Table 12 shows changes in percentages of cells over the 1-hour or 8-hour standards, for the various episode days and domains. These results are discussed in further detail below.

Effect of Anthropogenic VOC Removal

The anthropogenic VOC (AVOC) removal calculations were carried out for comparison purposes and also serve as the baseline for showing the effects of adding ethane in the substitution calculations. They also can be thought of as substituting anthropogenic VOC emissions with completely inert emissions. As such, the anthropogenic VOC removal calculations should have the greatest difference between the base case calculation, and also indicate the importance of the anthropogenic VOC emissions to ozone formation in the modeling domain.

As discussed above, the DDM calculations of the sensitivities to total and total anthropogenic VOCs indicate that the anthropogenic VOCs have relatively small contributions to ozone formation in most of the modeling domain, because of the significant amounts of reactive biogenic VOCs that are emitted. This is particularly evident in Table 9, where average O_3 changes of only 2-3 ppb are seen in the 36K and 12K domains, though larger changes of up to 6 ppb are seen in the more urban 4K domain. There are relatively small changes compared to the 60-90 ppb domain-wide averages for the base case calculation. The relative effects of removing the anthropogenic VOCs is somewhat larger in terms of domain-wide maximum ozone and maximum ozone changes, as shown on Table 10 and Table 11,

Table 9. Summary of changes in domain-wide averages of daily maximum O_3 concentrations in all the grid cells in the large-scale substitution calculations

Episode and Domain	Base Case Average Daily Max O_3 (ppb)	O_3 Change (ppb)				
		100% AVOC Removed	Ethane Substitution			
			100% By Carbon	100% By Mole	100% by React'y	50% by React'y
1 Hour Averages						
36 K Domain						
July 12	62	-2.0	-1.2	-1.6	1.7	0.8
July 13	64	-1.9	-1.1	-1.5	1.8	0.9
July 14	63	-1.7	-1.0	-1.3	1.7	0.8
July 15	59	-1.4	-0.8	-1.1	1.2	0.6
12K Domain						
July 12	70	-2.9	-1.7	-2.3	2.4	1.2
July 13	75	-2.8	-1.6	-2.2	2.5	1.3
July 14	77	-2.5	-1.4	-2.0	2.4	1.2
July 15	71	-1.8	-1.0	-1.4	2.0	1.0
4K Domain						
July 12	71	-6.0	-4.6	-5.3	0.5	0.2
July 13	75	-4.9	-3.5	-4.2	1.7	0.8
July 14	92	-4.1	-2.63	-3.3	2.5	1.2
July 15	96	-4.0	-2.5	-3.2	3.0	1.5
8 Hour Averages						
36 K Domain						
July 12	55	-2.0	-1.2	-1.6	1.2	0.5
July 13	56	-1.8	-0.8	-1.4	1.3	0.6
July 14	55	-1.5	-0.6	-1.2	1.2	0.5
12K Domain						
July 12	61	-2.8	-1.8	-2.3	1.7	0.7
July 13	63	-2.7	-1.7	-2.2	1.7	0.6
July 14	64	-2.3	-1.4	-1.8	1.6	0.6
4K Domain						
July 12	60	-4.4	-3.2	-3.8	0.7	0.4
July 13	63	-3.7	-2.5	-3.1	1.7	0.9
July 14	75	-3.0	-1.9	-2.4	2.2	1.1

Table 10. Summary of changes in domain-wide maximum O_3 concentrations in the large-scale substitution calculations

Episode and Domain	Base Case Regional Max O_3 (ppb)	Change in Maximum O3 (ppb)				
		100% AVOC Removed	Ethane Substitution			
			100% By Carbon	100% By Mole	100% by React'y	50% by React'y
		1 Hour Averages				
36 K Domain						
July 12	162	11	8	10	3	2
July 13	187	25	24	25	-7	-3
July 14	175	2	-1	0	9	3
July 15	170	4	2	3	6	3
12K Domain						
July 12	196	17	14	15	-2	-1
July 13	191	24	19	21	-4	-1
July 14	191	6	4	5	6	3
July 15	193	11	8	9	4	1
4K Domain						
July 12	126	22	19	20	-7	-6
July 13	140	23	20	22	-6	-3
July 14	173	27	21	24	2	1
July 15	177	24	19	22	-3	-2
		8 Hour Averages				
36 K Domain						
July 12	127	8	7	7	1	-0
July 13	139	20	18	18	-4	-2
July 14	147	7	3	5	6	1
12K Domain						
July 12	135	13	10	12	-2	-1
July 13	146	16	13	14	-5	-3
July 14	148	2	-1	0	11	6
4K Domain						
July 12	99	14	12	13	-2	-1
July 13	100	9	7	8	1	1
July 14	135	22	19	20	-2	1

Table 11. Summary of maximum changes in daily maximum O_3 concentrations in the various grid cells in the large-scale substitution calculations.

Episode and Domain	Base Max O3 (ppb)	Maximum Change in O3 (ppb)						
		100% AVOC Removed	Ethane Substitution					
			100% By Carbon	100% By Mole	100% by Reactivity (Increase)	100% by Reactivity (Decrease)	50% by Reactivity (Increase)	50% by Reactivity (Decrease)
1 Hour Averages								
36 K Domain								
July 12	162	-36	-32	-33	13	-19	7	-10
July 13	187	-60	-52	-56	10	-20	5	-10
July 14	175	-69	-61	-65	12	-30	6	-15
July 15	170	-74	-68	-71	9	-39	5	-20
12K Domain								
July 12	196	-51	-46	-48	13	-26	7	-14
July 13	191	-66	-57	-61	12	-26	6	-13
July 14	191	-74	-67	-71	13	-36	7	-19
July 15	193	-86	-81	-83	10	-59	5	-36
4K Domain								
July 12	126	-53	-48	-51	6	-28	3	-15
July 13	140	-49	-43	-46	5	-21	3	-15
July 14	173	-58	-53	-56	7	-31	4	-16
July 15	177	-84	-76	-80	8	-47	4	-24
8 Hour Averages								
36 K Domain								
July 12	127	-31	-25	-28	11	-12	7	-7
July 13	139	-42	-32	-40	8	-17	6	-10
July 14	147	-42	-34	-40	11	-19	7	-11
12K Domain								
July 12	135	-34	-28	-30	12	-16	7	-9
July 13	146	-46	-40	-43	8	-20	7	-13
July 14	148	-46	-42	-44	11	-26	7	-17
4K Domain								
July 12	99	-31	-28	-29	4	-17	2	-10
July 13	100	-36	-32	-34	8	-15	7	-8
July 14	135	-38	-34	-36	6	-17	6	-11

respectively but the effects are still relatively small. Table 12 shows that removing the anthropogenic VOCs also does not cause large reductions in the fractions of cells over the standard, except for some episode days in the 4K domain, where the effects on the exceedences of the 1-hour standard are significantly greater than the effects on the 8-hour exceedences.

Figure 41 shows maps of maximum 1-hour average ozone changes resulting first from removing the AVOCs over the 36K domain, and Figure 42 shows maps of the changes in maximum 1-hour average ozone resulting when they are removed. Figure 41 shows that there are still areas where the daily maximum 1-hour O_3 exceeds the standards even if there are no anthropogenic VOC emissions, due to the reactions of the NO_x and biogenic VOCs. As with the base case calculation, the spatial patterns of the O_3 in the no AVOC calculations vary from day to day because of the different meteorological conditions. The O_3 changes shown in Figure 42 indicate the areas that are sensitive to AVOC emissions, where they can be compared with distributions of AVOC sensitivities derived from the DDM calculations, as shown on Figure 14. It can be seen that the regions of AVOC sensitivity derived using the two methods agree reasonably well, as might be expected, though they are not exactly the same.

If O_3 formation from anthropogenic VOCs were a linear process, the DDM calculations should provide a prediction of the effect of total AVOC removal. As indicated above the units of the DDM calculations are ozone changes caused by a 100% change in the input whose sensitivity is being calculated, which is the same as the change caused by removing that input entirely. However, O_3 formation from VOCs and NO_x is in fact a nonlinear process, and the performance of the linear approximations in predicting large perturbations to the system should become increasingly worse as the magnitude of the perturbation increases. Since removing all anthropogenic VOCs represents the largest perturbation that can be made in a VOC-only control strategy, the performance of the linear approximation is of particular interest in this case.

The ability of the linear approximation to predict the effects of AVOC removal is shown on Figure 43, which shows plots of the O_3 change predicted by the direct calculation against that predicted by the DDM sensitivity of AVOCs. The left hand plot shows that the DDM calculation gives a fair prediction of the effect of total AVOC removal in the 36K domain, but there is some scatter. Although this performance of the linear approximation may seem surprising at first, as discussed above the anthropogenic VOCs generally have less of a contribution to O3 formation over the entire domain then biogenics. The right hand plot shows that DDM is much less successful in predicting effects of total AVOC removal in the 4K domain. The worse performance of the linear approximation in this case is expected because of the relatively greater importance of anthropogenic VOCs in this more urban domain.

Ethane Substitution Calculations

The ethane substitution calculations carried out for this project consisted of adding back ethane to replace the removed anthropogenic VOCs by varying amounts relative to the amount of anthropogenic VOCs removed. As indicated on Table 4, above, these consisted of, in order of amount of ethane added, no ethane added, ethane added on an approximately equal mole basis, ethane added on an equal carbon basis, and ethane added on an approximately equal reactivity basis. The equal carbon basis is based on the total number of carbons in the carbon bond model species used to represent the anthropogenic VOCs that are removed (as given on Table 1, above), and the molar and the reactivity-based factors are derived from this and the relative numbers of moles or ozone impact per carbon. The weighed average number of carbons per mole of the compounds in the base ROG mixture is approximately 4, so the molar substitution factor of 0.5 on a carbon basis was used. The optimum reactivity substitution factor would depend on the episode day, domain, and metric used, and for these calculations we (somewhat arbitrarily) chose to use the average of the minimum substitution error (#1) relative reactivities for the 36K domain, which predicts that ethane forms a factor of 5.1 less ozone on a carbon basis than the base ROG mixture.

Table 12. Summary of percentages of cells over the air quality standards for the base case and large scale substitution calculations.

Episode and Domain	Cells Over Standard (%)					
	Base Case	100% AVOC Removed	Ethane Substitution			
			100% By Carbon	100% By Mole	100% by React'y	50% by React'y
Maximum 1-Hour Average O_3 > 120 ppb						
36 K Domain						
July 12	1.0	0.7	0.7	0.7	1.3	1.1
July 13	2.0	1.5	1.6	1.6	2.4	2.2
July 14	3.6	2.2	2.6	2.3	4.7	4.2
July 15	1.7	1.2	1.5	1.3	2.2	1.8
12K Domain						
July 12	1.4	0.7	0.8	0.8	2.1	1.7
July 13	3.8	2.5	2.9	2.7	4.7	4.2
July 14	7.7	4.5	5.5	4.9	9.6	8.5
July 15	3.9	2.7	3.1	2.9	4.7	4.2
4K Domain						
July 12	0.11	none	none	none	none	0.01
July 13	2.1	none	none	none	0.6	1.2
July 14	11.7	5.9	7.8	6.8	14.8	13.1
July 15	15.3	8.4	10.4	9.4	17.9	16.4
Maximum 8-Hour Average O_3 > 80 ppb						
36 K Domain						
July 12	7	5	6	5	9	7
July 13	10	7	9	8	12	11
July 14	12	9	11	10	14	13
12K Domain						
July 12	10	7	8	8	14	11
July 13	19	13	14	14	22	20
July 14	23	18	20	19	26	24
4K Domain						
July 12	2.2	0.2	0.4	0.3	2.0	1.8
July 13	14	4	5	4	14	14
July 14	39	34	36	35	45	42

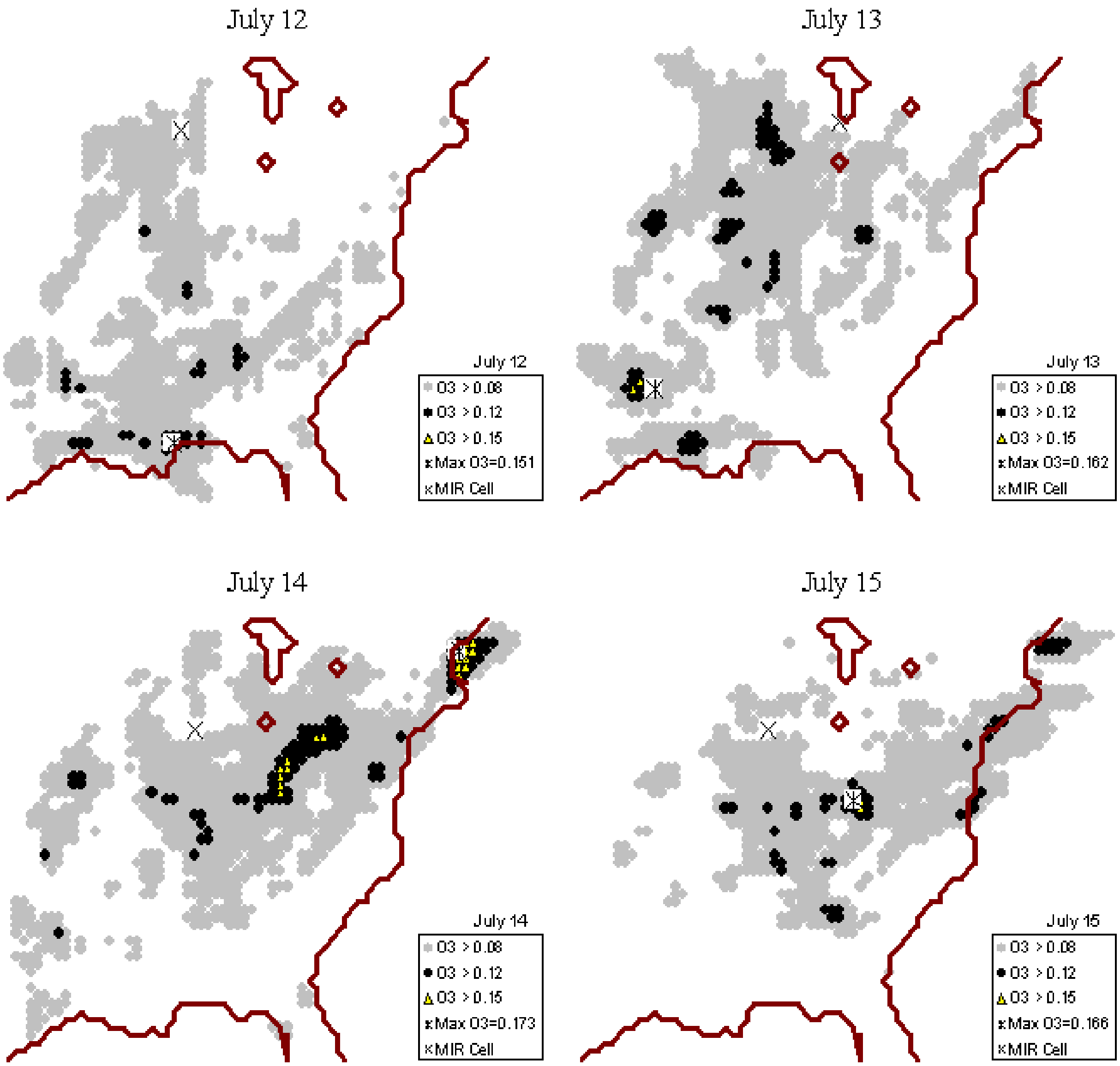

Figure 41. Maps of maximum 1-hour average ozone concentrations for the calculations where all anthropogenic VOCs are removed for each of the episode days in the 36K domain.

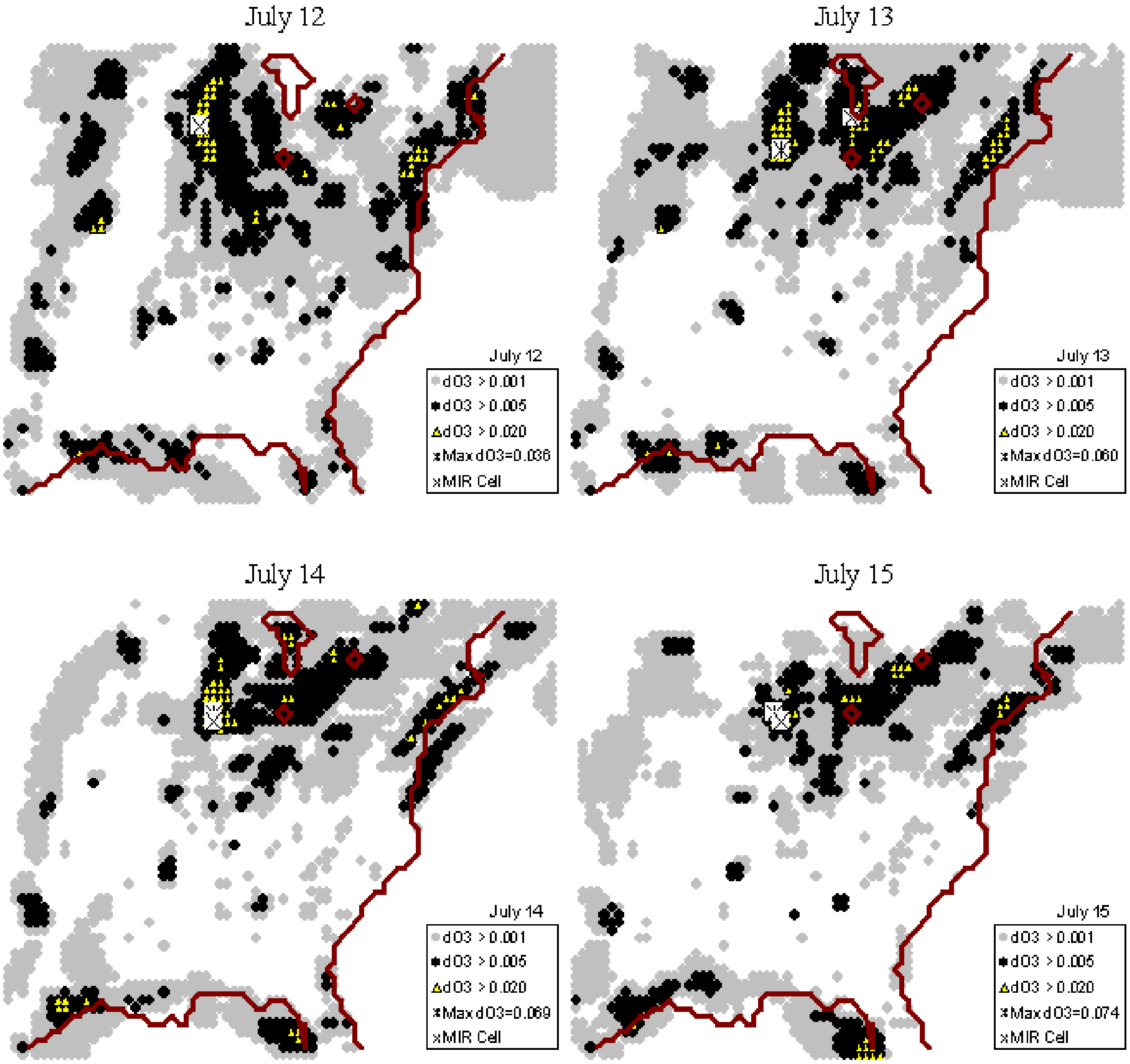

Figure 42. Maps of change in maximum 1-hour average concentrations (in ppm) caused by removing all anthropogenic VOC emissions for each of the episode days in the 36K domain.

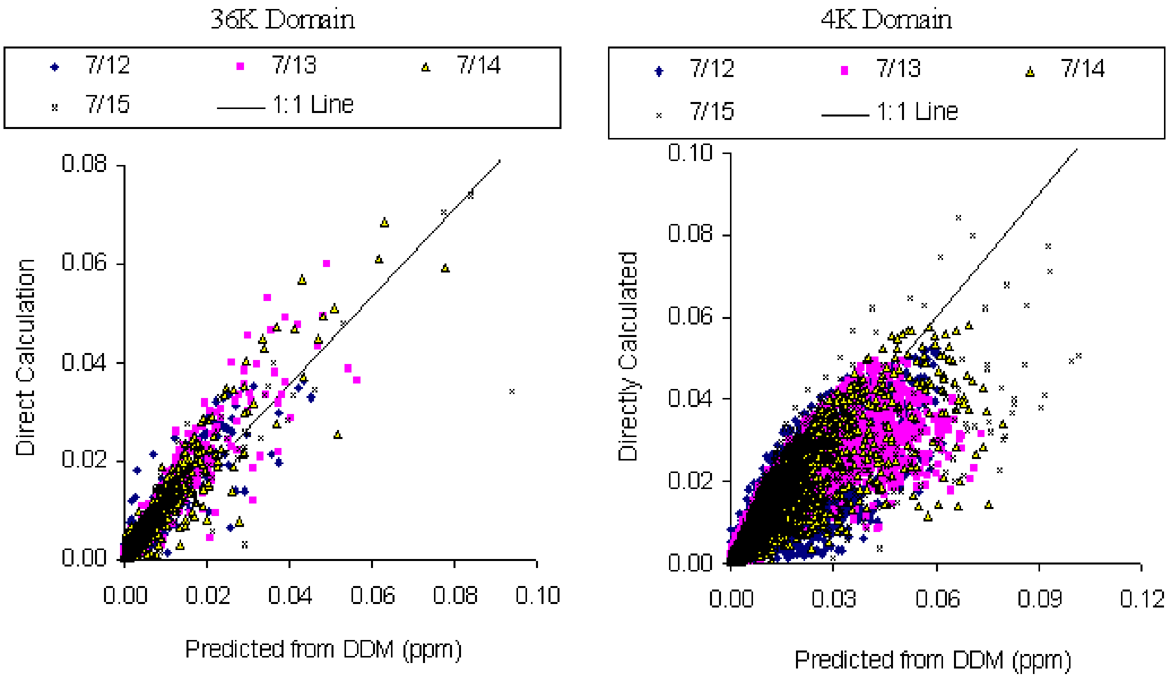

Figure 43. Plots of calculated changes in daily maximum 1-hour ozone concentrations caused by removing all anthropogenic VOC emissions that were directly calculated against the predictions of the effects of AVOC removal from the DDM sensitivities for the 36K and 4K domains.

Therefore, adding back 5.1 moles carbon of ethane for each mole carbon of AVOC removed should give the same ozone according to this reactivity metric.

In order to assess the effects of partial substitutions of ethane for the AVOC, a second null-test calculation was conducted where half the AVOC carbons were replaced by 5.1 carbons of ethane. This represents a slightly less unrealistic scenario than replacing 100% of the AVOC emissions. If the effects of the ethane substitution were approximately liner, the ozone changes in this calculation should be approximately half that in the 100% substitution calculation, and if there are significant non-linearities then qualitative differences in ozone changes in these two calculations should be observed.

The effects of the ethane substitution calculations in terms of average and maximum ozone, maximum ozone change, and cells over the 1- and 8-hour standards are shown on Table 9 through Table 12. Because ethane has a much lower ozone impact than the mixture of anthropogenic VOCs on both a carbon and a molar basis, the results of the carbon- and mole-based substitution calculations result are similar to the results of the calculations where the anthropogenic VOCs are removed. All these calculations give similar spatial distributions of ozone levels and ozone changes relative to the base case calculation. However, since ethane has a nonzero (and generally positive) reactivity, the ozone in these substitution calculations are higher than the AVOCs-removed calculations, though the differences are not large. The differences between the AVOC-removed and the ethane addition calculations are obviously much larger in the reactivity-based substitution calculation, since the amount of ethane added are factors of ~5 or ~10 greater than the carbon or mole-based substitutions, respectively.

If the effects of the ethane additions were linear, the ozone changes in the ethane substitution calculations compared to the AVOC-removed calculation should be proportional to the ethane substitution factor, which as indicated above ranged from 0.5 to 5.1. Figure 44 shows plots of the ozone changes in the mole- and reactivity-based substitutions against the changes in the carbon based substitution, where the results should differ by factors of 0.5 or 5.1, respectively, if the system were linear. It can be seen that the linear approximation works quite well in predicting the ozone changes in the in the 36K domain in the calculations where the substitution factor varies from 0.5 to 1, which is not unexpected since as indicated above these mole and carbon based substitutions resulted in relatively small changes in O_3 compared to the AVOC-removed calculations. The changes are larger in the 4K domain because this is more influenced by anthropogenic VOC emissions, and thus the linear approximation does not work quite as well. The linear approximation also does not work as well when the factor varies from 1 up to 5.1, which is also expected since the change is relatively large. However, the correspondence is reasonably good given the magnitude of the change. The performance of the linear approximation in this case is comparable to the performance of the DDM results in predicting the effects of AVOC removal for the different domains, as shown in Figure 43 above. This comparability is expected because the magnitudes of the changes are about the same in each case.

If the substitution factor in the null test calculation were a perfect representation of the reactivity of ethane compared to the mixture of AVOCs in all location, the ozone formed in this calculation should be exactly the same as in the base case simulation. However, since as discussed above the relative reactivity of ethane varies with location and episode days, there will be differences in ozone formations in the two scenarios, with more ozone being formed in some locations and less in others. The extent to which this is the case provide a measure of how ozone will respond differently in substitutions to low reactivity compounds like ethane compared to equivalent mass-based reductions according to the reactivity metric used.

The summary data on Table 9 through Table 12 indicate how the various measures of ozone formation change in the null test calculations, and Figure 45 shows maps of the regions where ozone changes by more than 2 or 5 ppb and the locations where the greatest ozone changes occur. Figure 45 shows that there are extensive regions where the ozone increases or decreases in the ethane null test calculation by 5 ppb or more, but that these regions vary from day to day. Indeed, as shown on the maps for the two representative episode days in the 4K domain shown in Figure 42, large regions that had ozone decreases on July 12 had ozone increases on July 14. In general, the extent of the areas where the ethane substitution causes an increase in ozone are significantly larger than the ozone is reduced, with results in the ethane null substitution giving higher domain-wide average ozone levels than in the base case calculation, as indicated on Table 9. On the other hand, the magnitudes of the ozone reductions caused by the substitution tend to be greater than the magnitudes of the increases, as indicated by the maximum ozone change data shown on Table 11. Since the minimum substitution error metric that was used as the basis for these null test calculations is designed to minimize the sum of squares of this ozone change, a relatively small number of cells with relatively large ozone reductions can balance out a larger number of cells with smaller ozone increases.

Figure 46 shows plots of the ozone change in the null test calculation against various reactivity characteristics for the cells in the 36K domain. It can be seen that there is essentially no correlation between the base case ozone level and the ozone change in the ethane null substitution calculation, which means that the impacts of the substitution cannot be determined by ozone level alone. There is rather poor correlation between the ozone change and the total VOC sensitivity, except for the most highly VOC-sensitive cells, where the greatest O_3 reduction is seen in the ethane substitution calculation. The ozone change in the null calculation correlates somewhat better with the total anthropogenic VOC sensitivity, with regions with the greatest AVOC sensitivity (i.e., MIR-like locations) again being the areas where the greatest reduction on O_3 occurred in the substitution. However, the best correlation is with the total NO_x

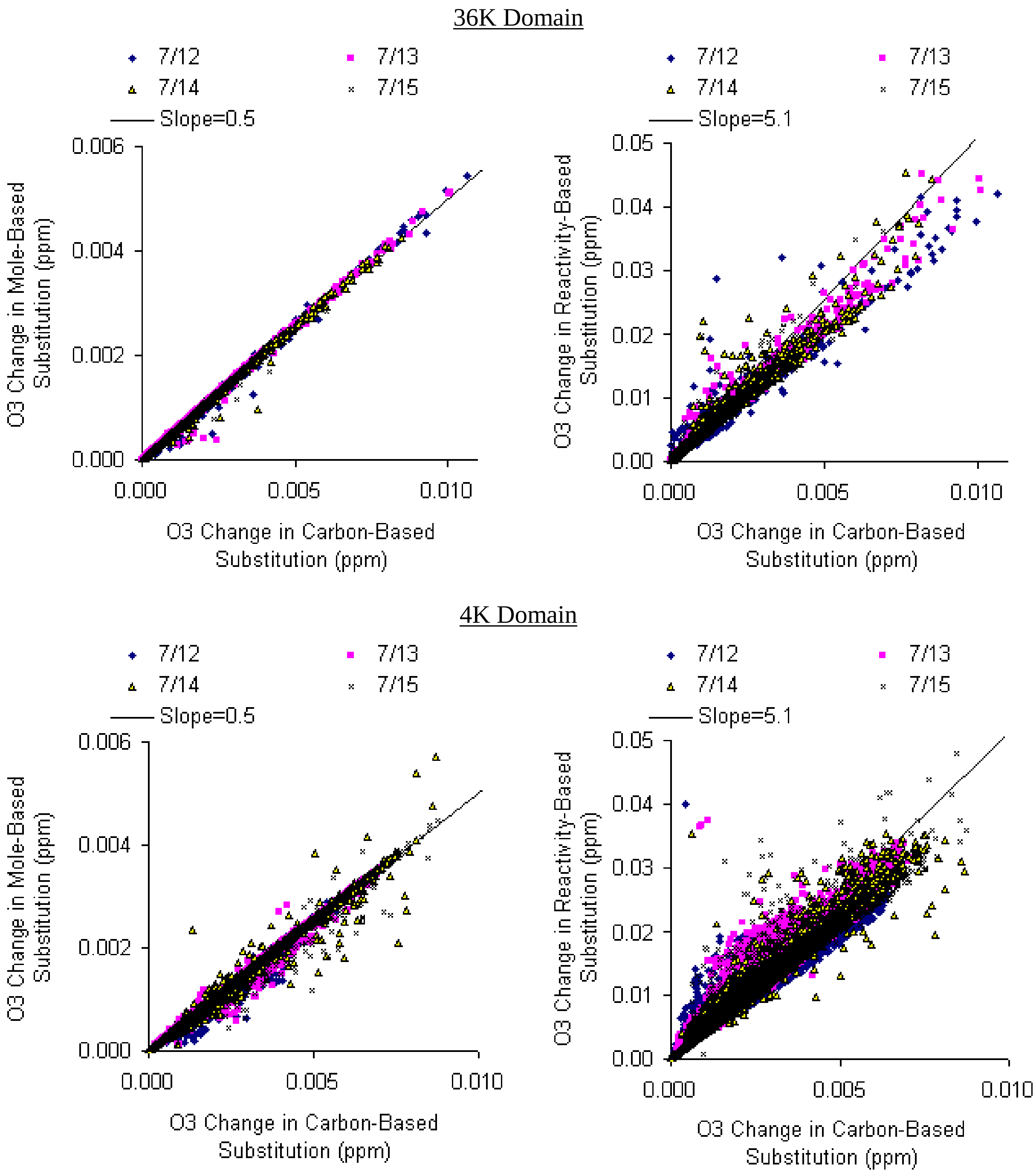

Figure 44. Comparisons of ozone changes relative to the AVOC-removed calculation in each of the cells in the 36K and 4K domains for selected pairs of ethane substitution calculations with differing substitution factors. Lines indicate relative changes predicted by the ratios of substitution factors and the linear approximation.

July 12, 36K Domain

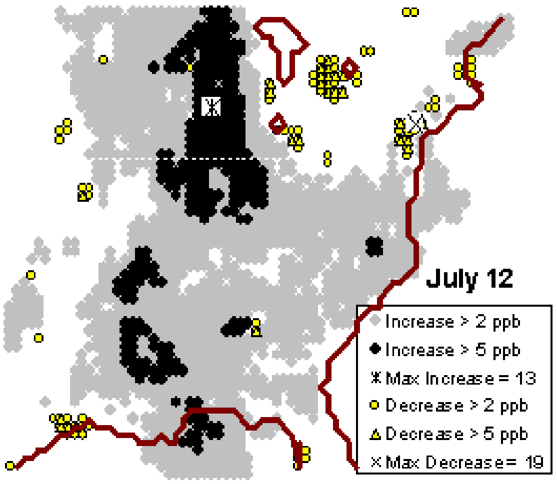

July 13, 36K Domain

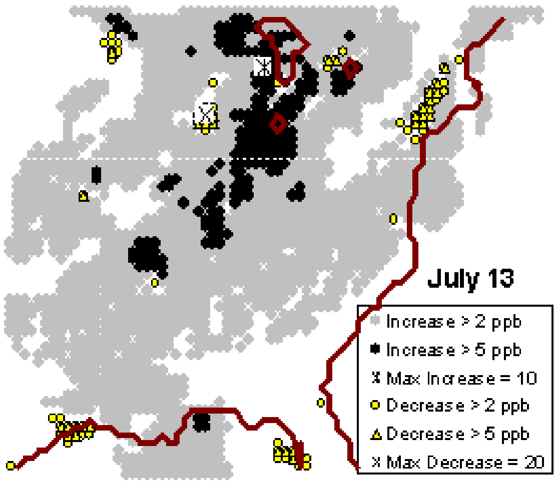

July 14, 36K Domain

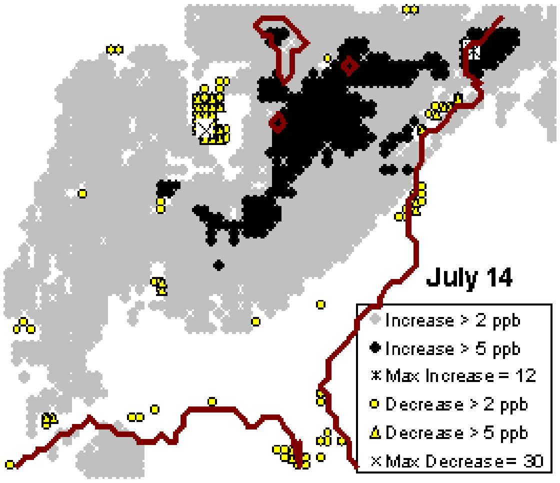

July 15, 36K Domain

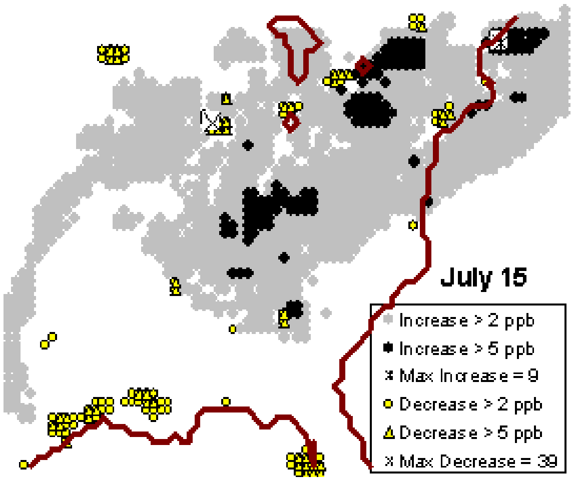

July 12, 4K Domain

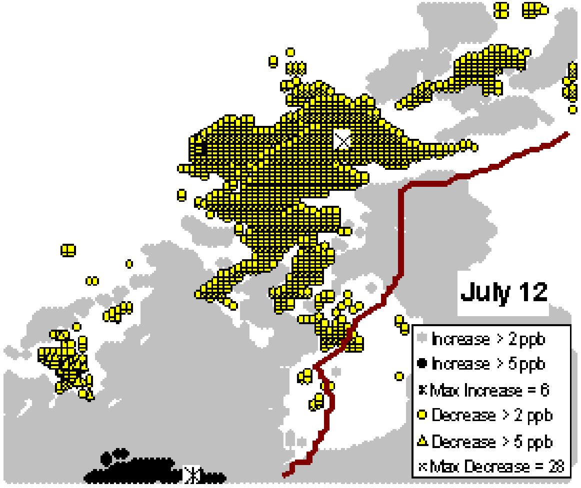

July 14, 4K Domain

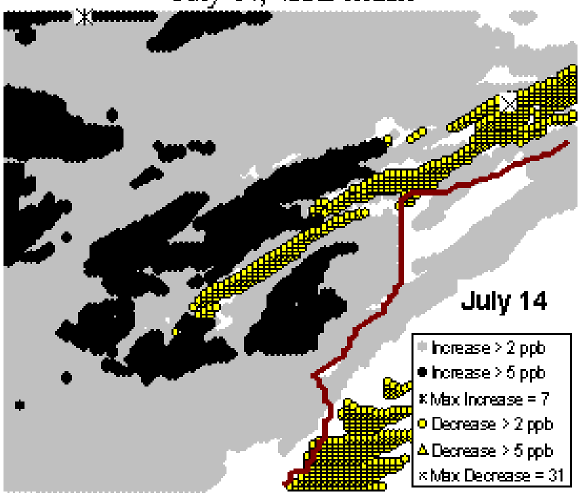

Figure 45. Maps of changes in daily maximum 1-hour average ozone concentrations in the 100% ethane null test substitution calculation relative to the base case calculation.

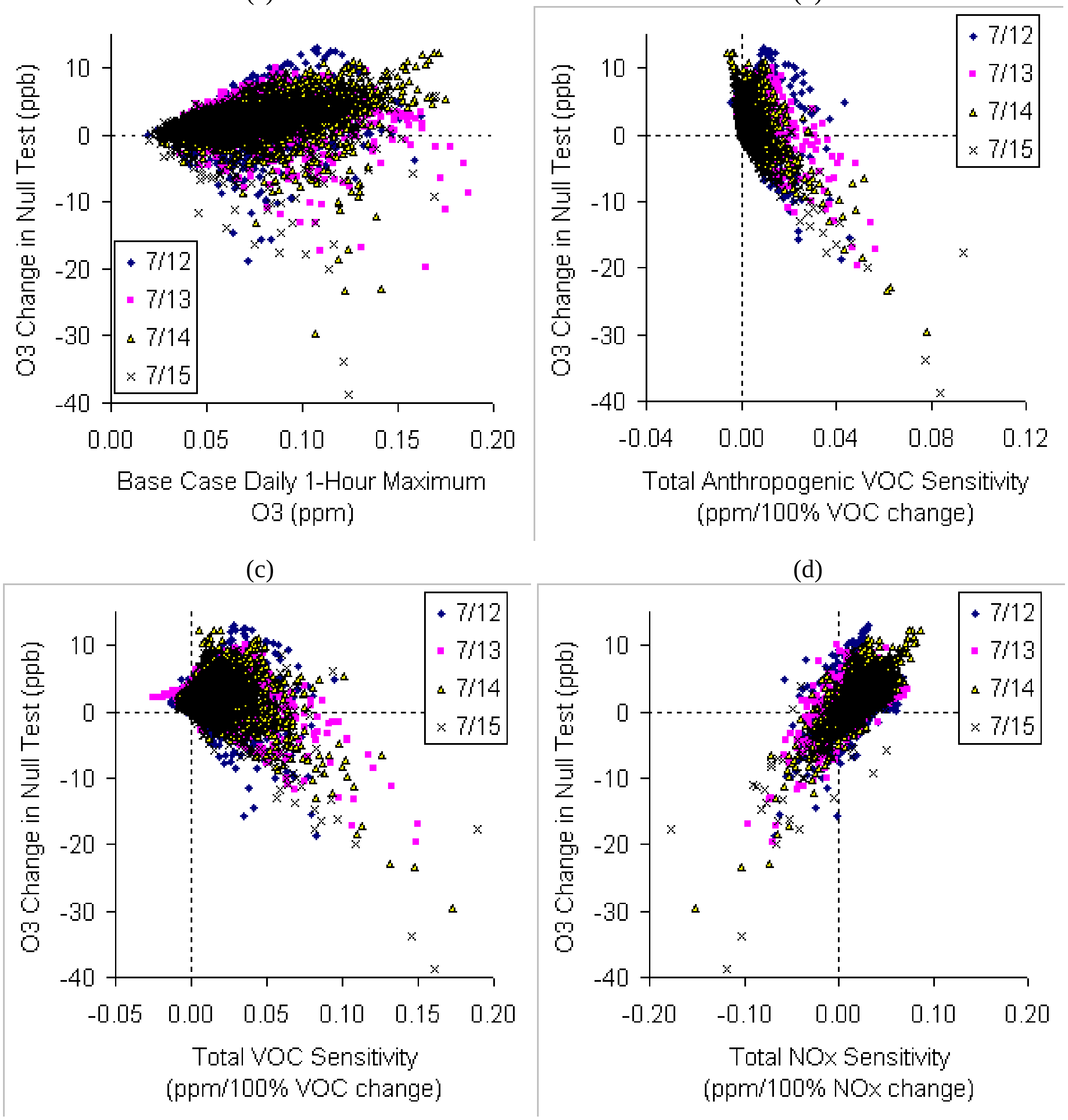

(a) (b) (c) (d)

Figure 46. Plots of the changes in the daily maximum 1-hour average ozone in the 100% ethane substitution null test calculation relative to the base case 1-hour maximum ozone concentration, (b) the anthropogenic VOC sensitivity, (c) the total VOC sensitivity, and (d) the total NO_x sensitivity.

sensitivity, with the many highly NO_x-sensitive cells tending to be those where O_3 increase in the ethane substitution, and the cells with negative NO_x sensitivity tending to be those where the substitution causes ozone to decrease.

The correlation between ozone change in the null test calculation and the AVOC or NO_x sensitivities is consistent with the changes in the relative reactivities of ethane with the various types of regional relative reactivity metrics as discussed above. Generally the metrics that give the greatest weight to cells with higher AVOC sensitivities or cells with negative NO_x sensitivities (e.g., the regional MIR-MOIR metric) tend to have lower relative reactivities for slowly reacting species such as ethane than metrics, compared to the metrics, such as regional average ozone, that weigh the cells more equally. Regions where the relative reactivity of ethane is lower than that used to derive the substitution factor in the null test calculation will have lower ozone in the null test calculation, and vise-versa.

If the ozone formation process were linear, then the ozone change in the ethane substitution calculations could be obtained from

$$O_3 \text{ Change in Cell} = Fs \cdot \left[F_R \cdot IR_{cell}(\text{Ethane}) - IR_{cell}(\text{Base ROG})\right] \qquad (X)$$

where F_R is the ethane substitution factor that was used, and F_S is the fraction that was substituted (100% or 50% in this case), and the IR's are the incremental reactivities obtained in the DDM calculations. The ability of this linear approximation to predict the directly calculated null test ozone changes is shown in Figure 47, which shows plots of the directly calculated against the DDM-predicted (using Equation X) ozone changes in the 50% and the 100% substitution calculations. It can be seen that although the agreement is not perfect, overall the directly calculated null test results agree quite well with the estimates using the incremental reactivities from the DDM calculations. This suggests that these incremental reactivity data can be used to give reasonably good estimates of results of null test calculations using other substitutions or substitution factors, should that be desired.

Diagrams showing DDM predictions and direct calculations of various global ozone metrics for 100% ethane substitution calculations with varying ethane substitution factors are shown on Figure 48 through Figure 50. The filled circles show the directly calculated results for the mole, carbon, and reactivity-based substitutions and the solid horizontal lines show the differences between the base case and the no AVOC direct calculations. The horizontal dashed lines on Figure 48 and Figure 49 show the difference between the base case and the no AVOC case as predicted by the DDM calculations of the AVOC sensitivities. The dotted lines and the open symbols show the DDM predictions of the effects of the substitutions for various substitution factors relative to the no AVOC case, estimated using

$$[O_3]_{cell}(\text{Substitution case}) = [O_3]_{cell}(\text{No AVOC case}) - F_R \cdot IR_{cell}(\text{Ethane}) \qquad (XI)$$

where F_R is the ethane substitution factor. (This is used rather than Equation X to give the same results for the no AVOC case, which is used to define the zero points in Figure 48 and Figure 49. Using Equation X would give data that are offset by the differences between the horizontal dashed and horizontal solid lines on those figures.) Figure 48 and Figure 49 show changes in regional average and regional maximum 1-hour maximum ozone concentrations relative to the no-AVOC calculation, and Figure 50 shows calculated percentages of cells over the 8-hour ozone standard of 0.08 ppm.

The large open circles and squares show the DDM predictions of the ethane substitution factors corresponding to the relative reactivities of ethane derived using the regional average ozone or the minimum substitution error (#1) metric for the particular episode day that is plotted. The variation of the substitution factors corresponding to these points reflects the variation in the relative reactivities by these

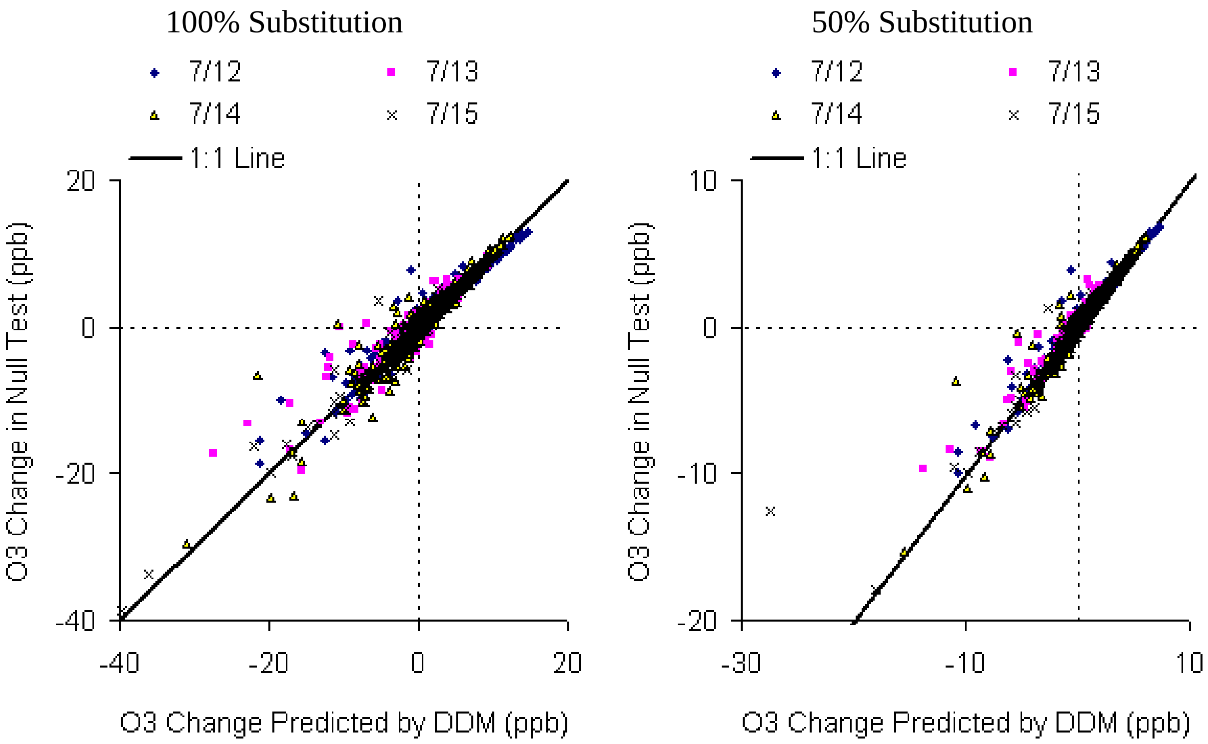

Figure 47. Plots of the changes in daily maximum 1-hour average ozone in the ethane substitution ethane null test calculations relative to the base case simulations against the ozone change predicted by the DDM sensitivities.

metrics with episode day and domain, as discussed previously. If these reactivity factors gave "perfect" null test results for the particular ozone metric they would give the same predicted ozone change for the corresponding ethane substitution as the base case relative to the no AVOC case, i.e., the symbols would intersect the horizontal lines on the figures. Thus, these data provide an indication of how well the average ozone and the minimum substitution error metrics perform in null tests for the particular ozone measures shown on the figures. Since the reactivity factors for each episode day and domain are derived from the reactivity data for that day and domain, they should be the optimum factors to use for the particular metric in each case.

Figure 48 shows that the average ozone metric performs essentially perfectly in predicting the optimum factor for a null test calculation of average ozone in the episodes and domains. This follows from the fact that the average ozone metric is defined to measure the effects of the VOCs on this quantity. As discussed above and shown on Figure 28, the minimum substitution error metric always gives lower relative reactivities than the average ozone metric, which means that it would give higher ethane substitution factors for null test calculations. This is why the minimum substitution error metric consistently overpredicts the substitution factor to give the optimum null test result for regional average ozone concentrations.

Figure 49 shows that the average ozone and the minimum substitution metrics perform about equally well (or poorly) in predicting the optimum ethane substitution factors for null test calculations of the regional average daily maximum ozone concentration. The results are quite variable, presumably

Change in Regional Average of 1-Hour Maximum O_3 (ppb) vs. Ethane Substitution Factor (Carbon Basis)

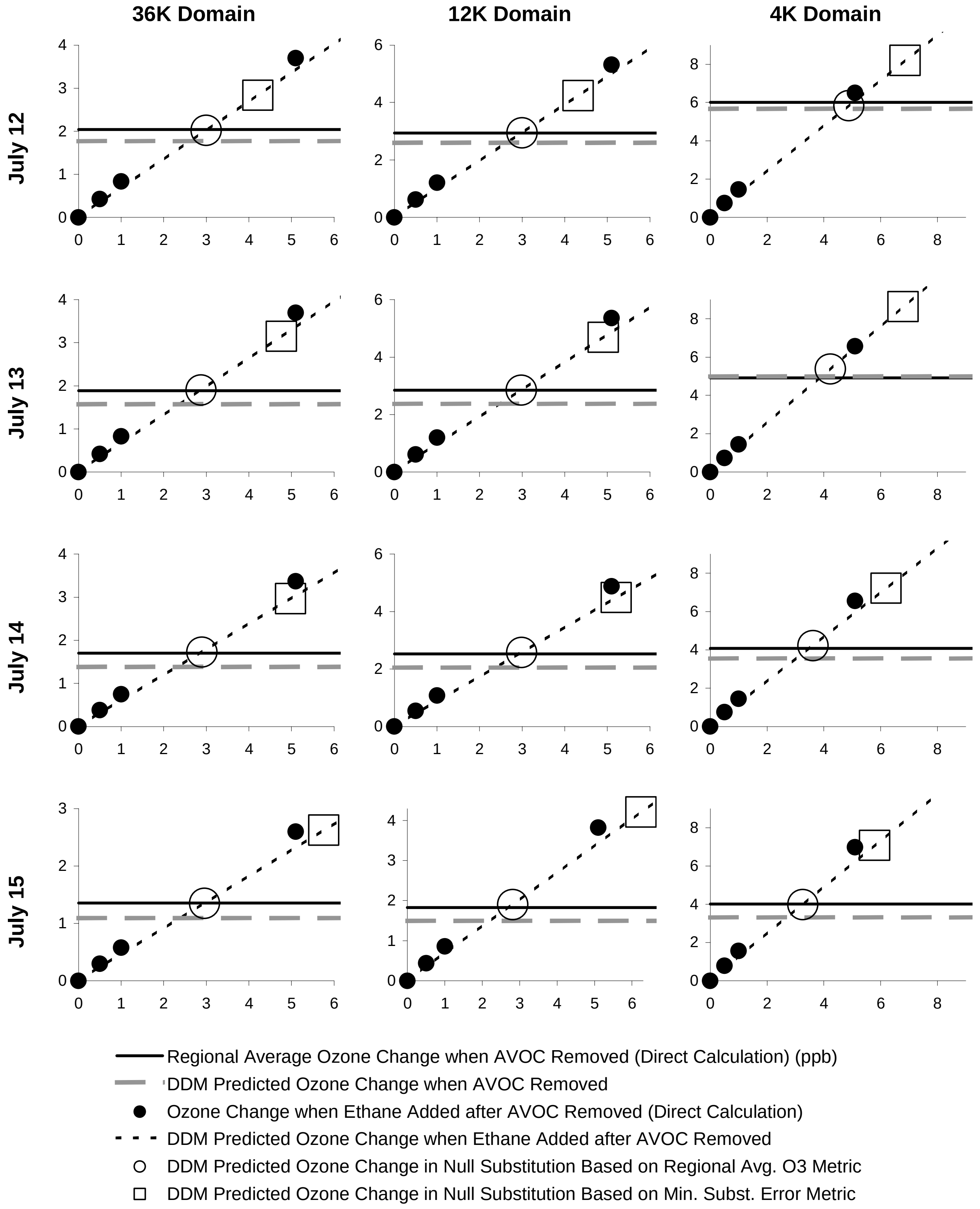

Figure 48. Plots of change in average O_3 caused by adding back ethane after anthropogenic VOCs are removed, against the ethane carbons added relative to the AVOC carbons removed.

Change in Regional 1-Hour Maximum O_3 (ppb) vs. Ethane Substitution Factor (Carbon Basis)

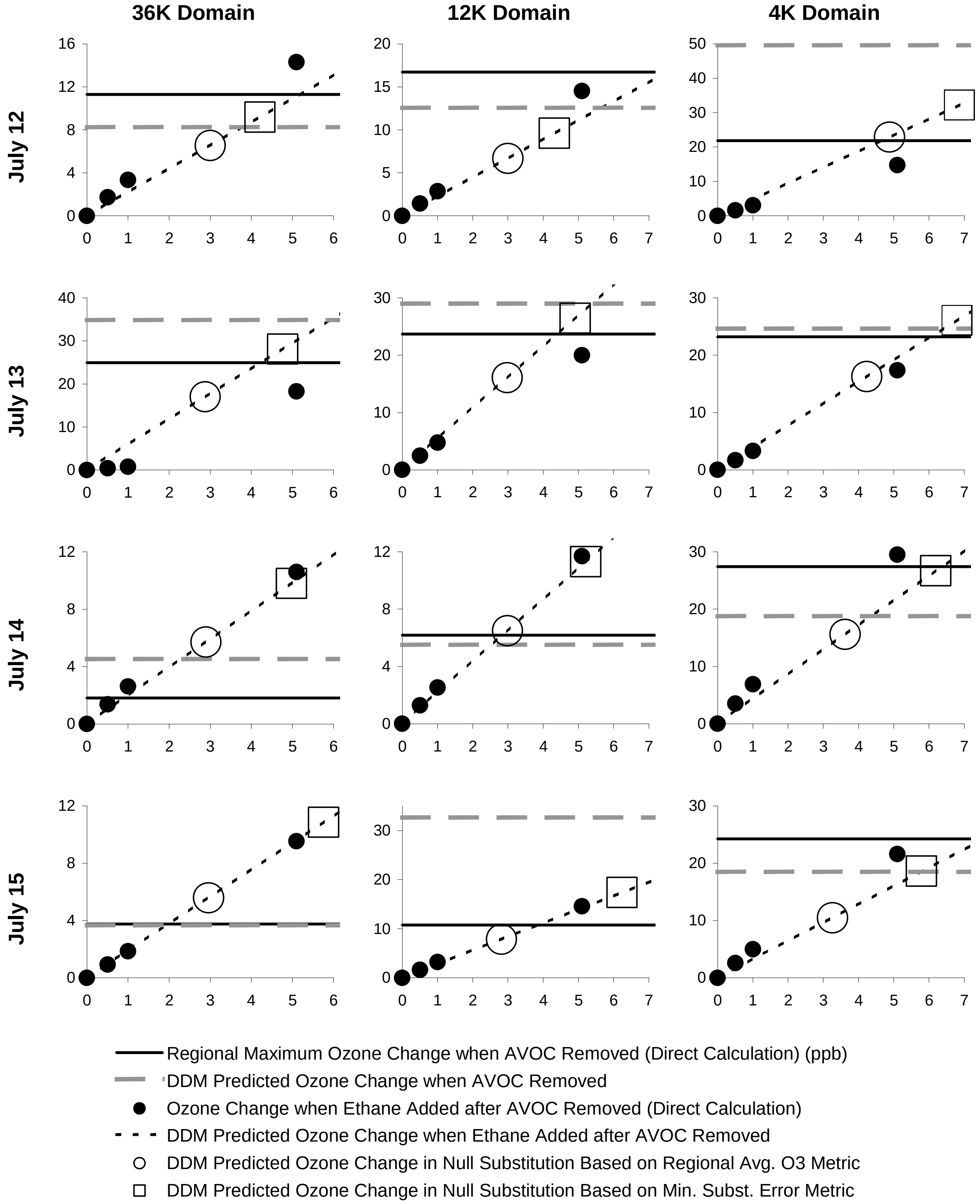

Figure 49. Plots of change in maximum O_3 caused by adding back ethane after anthropogenic VOCs are removed, against the ethane carbons added relative to the AVOC carbons removed.

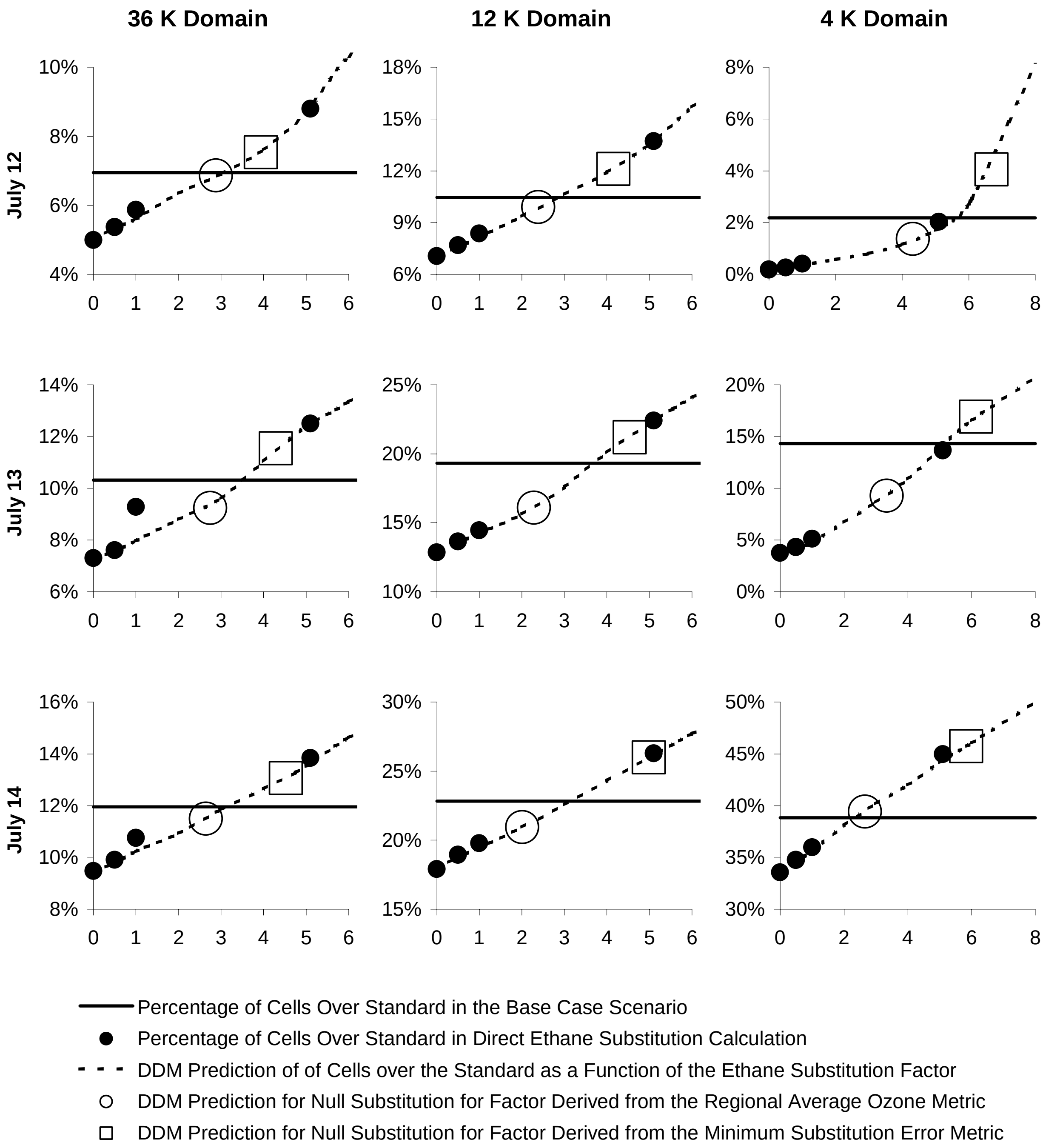

Figure 50. Plots of fractions of cells over the 8-hour standard in base case and large scale substitution calculations against the ethane carbons added relative to the AVOC carbons removed.

because of the variability of conditions at the location of the maximum ozone as discussed above. However, neither metric appears to be strongly biased one way or another in terms of underpredicting or overpredicting the effects of the null test on maximum ozone, though the minimum substitution error metric may perform slightly better in the more urban-dominated 4K domain.

Figure 50 shows that the optimum ethane reactivity factors for predicting fractions of cells over the 8-hour ozone standard in null test simulations of the various episode days and domain are in almost all cases between those predicted by the average ozone and the minimum substitution error metrics. (The 8-hour quantification is used in this case because there are more cells over the 8-hour standard than over the 1-hour standard, so there is somewhat less variability in the data.) The average ozone over the standard metric may give a better prediction of fractions of cells over the standard, since as shown on Figure 30 and Figure 31, above, its relative reactivities for ethane tend to fall between those from the average ozone and minimum substitution error methods.

Classification of Reactivity Scales by Effective Range

An important characteristic of a reactivity scale from a policy perspective is its effective range, i.e., the range of reactivities from the least reactive compound that is of relevance to ozone control to the most reactive. The magnitude of this range measures the maximum effectiveness of a reactivity-based regulatory policy when applied to compounds that would otherwise be regulated on a mass basis, and affects the incentive to substitute to low reactivity compounds should a reactivity-based policy be adopted. If the policy uses a reactivity scale with in an inappropriately high effective range, then some reactivity-based substitutions may lead to unacceptable ozone increases in some regions because the relative ozone impacts of the low reactivity compounds will actually be higher than reflected by the policy. If, on the other hand, the policy uses a reactivity scale with an inappropriately low effective range, then there would be insufficient incentive for at least some beneficial reactivity-based substitutions, and the net result would be less ozone reduction for the available resources. Therefore, it is useful from a policy perspective to have some quantitative measure of this for the various alternative reactivity scales that are discussed in this work.

Since the actual ozone impacts of compounds will range from zero for compounds that do not react at all to some finite value for reactive compounds, strictly speaking the effective range of any reactivity scale is infinite. However, the current mass-based policy in fact does not regulate compounds considered to have “negligible” reactivity, and if their impacts are really negligible then their relative impacts are irrelevant. Therefore, from a policy perspective the relevant measure of effective range is ratio of reactivity of the most reactive compound of significance to the least reactive compound that is considered to have a non-negligible impact and therefore subject to mass-based regulations. Since the current EPA policy uses ethane to define the borderline between reactive and exempt (Dimitriades, 1999), its reactivity is a logical choice for defining the low end of the effective range. However, as discussed below the qualitative results would probably not be greatly different had a lower reactivity compound been used for this purpose.

There are a number of high reactivity compounds that could be used to represent the high end of the range, though obviously the compound used for this purpose should be reasonably representative of the actual distribution of the highly reactive compounds that are currently emitted. The choice is simpler when using a condensed mechanism such as Carbon Bond, since only a limited number of model species are available to choose from. On a carbon basis, the most consistently reactive model species in most metrics is OLE, though formaldehyde is more reactive than OLE in certain metrics and domains. For this discussion, we will choose OLE as the basis for defining the high end of the range. As discussed below, using formaldehydes or even xylenes for this purpose would not give qualitatively different results.

Figure 51 shows plots of ratios of reactivities of various types of reactive model species to ethane against the OLE/ethane reactivity ratio that is being proposed as the measure of the effective ranges of reactivity scales for most[5] of the regional and EKMA reactivity scales that were developed in this work. The multiple points for the regional metrics represent the various episode days and domain sizes for the metrics considered. It can be seen that there is an excellent correlation between the formaldehyde, xylene, or acetaldehyde/ethane ratio to the OLE/ethane ratio for both the EKMA and regional models, with all data being reasonably well fit by straight lines. This indicates that essentially the same results in terms of reactivity scale classifications had these other species instead of OLE been chosen to define the high end of the range, at least in terms of relative differences.

It is interesting to note that although there is a reasonably good near-linear relationship between the OLE/ethane and the formaldehyde or xylene/ethane ratios, this is not the case for the relative reactivities of these compounds themselves. An example of this is shown on Figure 52, which gives plots of relative reactivities of formaldehyde against those for OLE for the same set of reactivity scales as used in Figure 51. It can also be seen that there are significantly nonzero intercepts in both cases. This is also apparent from the reactivity scale comparison plots shown on Figure 26 through Figure 35, above, where it can be seen that in most metrics the relative reactivities of formaldehyde and xylenes are much more variable than the relative reactivities of OLE. Figure 51 indicates that this variability is not random, but reflects the fact that formaldehyde and xylenes tend to have lower relative reactivities in scales with lower effective ranges. This suggests that the “effective range” metric provides a means for classifying the scales in terms of differences in reactivities compounds other than the two used to define the range. Thus, this concept may have more utility than just the policy applications discussed above.

Figure 53 shows plots of the CO/ethane ratio against the OLE/ethane ratio, where it can be seen that the CO/ethane ratio is essentially constant. This indicates that the metric would not have been greatly different had CO rather than ethane been chosen to represent the low end of the range, suggesting that choosing other low reactivity compounds may also give similar results. (Of course, this is only applicable for compounds that have low reactivity because of low atmospheric reaction rates. Compounds that have low reactivity because of inhibiting properties probably would have different reactivity characteristics. However, such compounds are not representative of most low reactivity compounds in use, and in any case they are not represented in the Carbon Bond mechanism.) Note, however, that the CO/ethane reactivity ratio for the EKMA scales are all on the low end of the range for the regional reactivity scales, perhaps because of the relatively short reaction times in the 1-day EKMA scenarios compared to the multi-day regional model. Because of this, that the effective range metric for the EKMA scales may change relative to the regional scales if a lower reactivity cutoff were used.

From the figures it can be seen that the effective ranges of the reactivity scales developed in this work vary from under 20 to around 60, indicating significant differences in the scales in this regard. In other words, the relative ozone impacts of the most reactive to the borderline exempt compounds in this mechanism range from ~20 to almost 70, depending on the scale employed. Although the lowest effective range of ~20 is considerably lower than the effective range of 61 for the MIR scale adopted in the regulatory programs in California, it still reflects a significant difference in ozone impact between the most reactive and the least reactive VOC species represented in this mechanism.

The values of this effective range metric for the major regional and EKMA reactivity scales developed in this work are summarized on Figure 54, where the regional values for the various domains are based on averages for the different episode days. The scales are sorted in order of increasing effective range. Consistent with the discussion in the sections above, the scales with the greatest effective ranges

---

[5] The regional maximum ozone metric is considered to be too variable to be useful and is not included in this analysis.

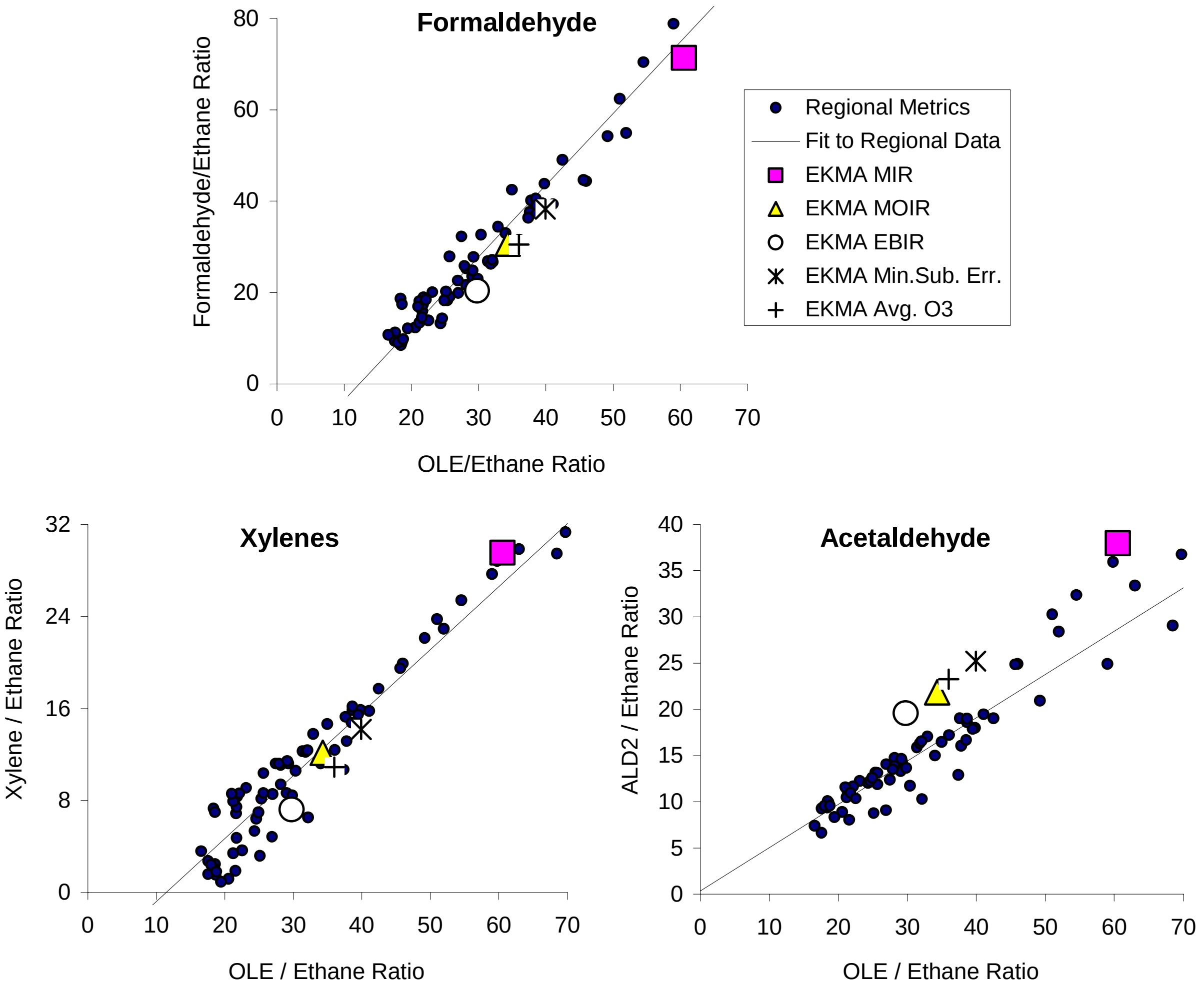

Figure 51. Plots of ratios of formaldehyde, xylenes, or acetaldehyde, to ethane against the OLE/ethane ratio for the major regional and EKMA reactivity scales developed in this work, based on the daily maximum 1-hour average ozone quantification.

are those, such as MIR or MIR-MOIR that are most sensitive to the VOC-sensitive, urban-dominated regions that tend to have the lowest relative reactivities for the slowly reacting compounds and the highest relative reactivities for at least some of the more reactive species. The lowest effective ranges are the average ozone metrics that give greater weight to the NO_x-limited cells with relatively low anthropogenic VOC sensitivity. For a given type of domain, the ordering of effective ranges for the scales in terms of type of metric is MIR > MIR-MOIR ≈ Minimum Substitution Error > Average O_3 over the standard > Average ozone. However, the effective range also depends on the type of domain or model, with the regional scales derived for the urban-dominated 4K domain having consistently higher effective ranges than those derived from the larger domains. This causes overlap in effective range with scales derived using different metrics. For most metrics the EKMA scales give very similar effective ranges as the corresponding regional scales for the 4K domain. The exception is the average ozone metric, where the regional metrics reflect impacts on regions that are not well represented in the EKMA scenarios.

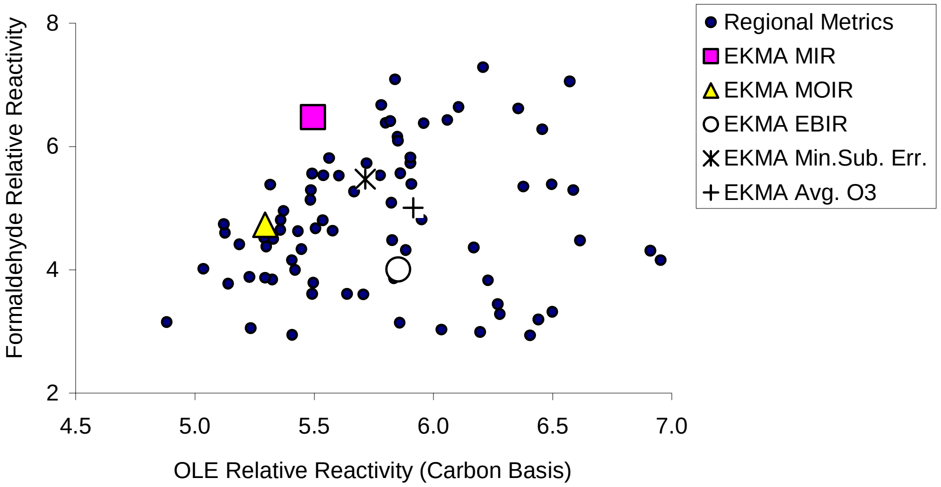

Figure 52. Plots of relative reactivities of formaldehyde against relative reactivities of the OLE model species for the major regional and EKMA reactivity scales developed in this work, based on the daily maximum 1-hour average ozone quantification.

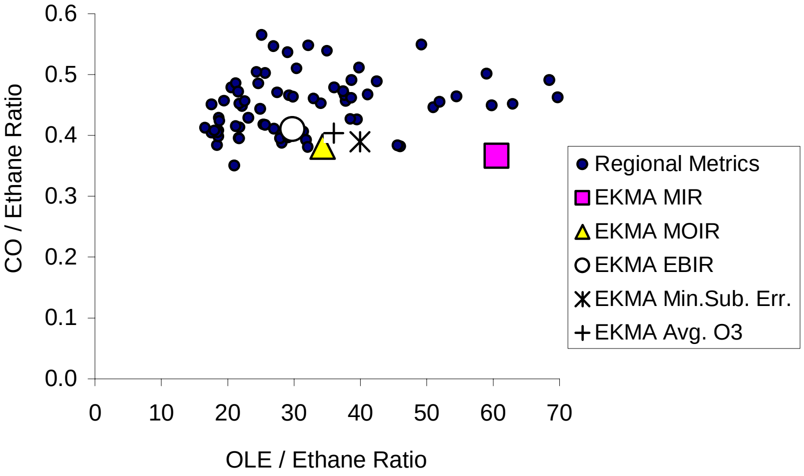

Figure 53. Plots of ratios of CO to ethane against the OLE/ethane ratio for the major regional and EKMA reactivity scales developed in this work, based on the daily maximum 1-hour average ozone quantification.

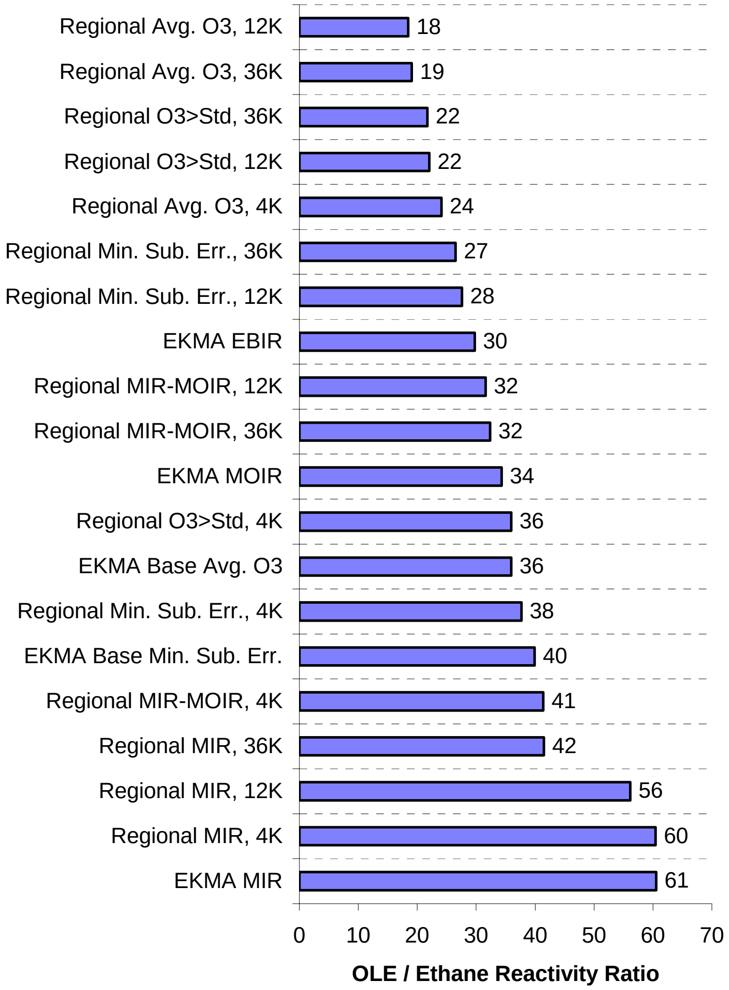

Figure 54. Summary of effective ranges for major reactivity scales derived in this work for the maximum 1-hour average ozone quantification.

The effective ranges for the reactivity scales derived using the maximum 8-hour average O_3 quantification are generally the same as those derived using the 1-hour quantification, at least for those metrics that reflect impacts on the same regions. This is shown on Figure 55, which gives plots of effective ranges for reactivity scales based on 8-hour averages against corresponding 1-hour scales. The main exceptions are those for the regional MIR metric, where the data are scattered. This is because they reflect impacts in a single cell, and the cells that had the highest base ROG reactivity in the 8-hour quantification are generally not the same as those with the highest 1-hour reactivities. In addition, the effective ranges for the average O_3 over the standard scales are consistently ~20% lower for the 8-hour scales than the corresponding 1-hour scales. This is because the spatial extents of regions that exceed the 8-hour standard are greater than those that exceed the 1-hour standard, and apparently the cells that exceed the 8-hour but not the 1-hour standard are better represented by scales representing lower effective ranges.

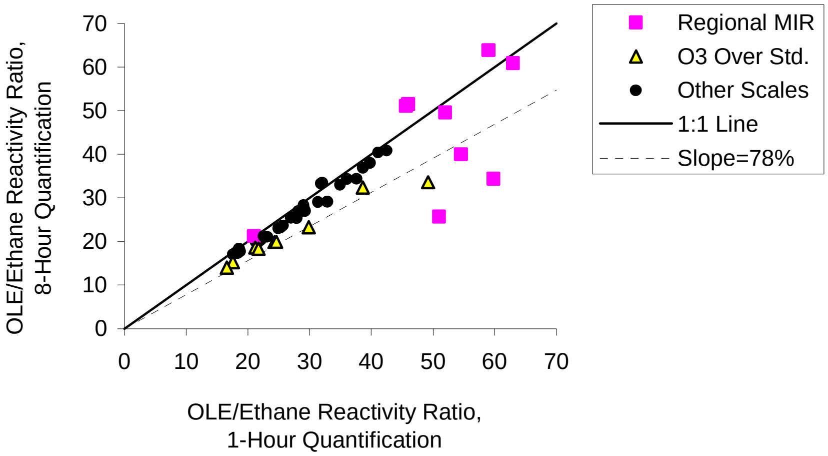

Figure 55. Plots of effective ranges for the major reactivity scales developed in this work for the 8-hour average ozone quantifications against those for the corresponding scale for the 1-hour average quantification.

CONCLUSIONS AND RECOMMENDATIONS

Conclusions

The primary motivation behind this study was to address the concern among policy makers and researchers that relative reactivities of VOCs towards ozone formation may be significantly different on a regional scale than indicated by previous modeling studies of urban scenarios, and that this difference may result in degradation of regional ozone levels should reactivity-based VOC controls be adopted. Previous studies using EKMA and urban scale models have indicated that although relative reactivities in urban scenarios can be variable, most have concluded that it is still possible to derive reactivity scales that can serve as a basis for deriving a more efficient ozone control strategy than regulating all non-exempt VOCs equally. However, there is a concern that this may not be the case in large-domain regional scenarios, where long-range transport and multi-day effects can be more important in affecting ozone formation over wide regions. There is also the concern that the EKMA models cannot represent meteorology, transport and other dynamic processes as realistically as does 3-D regional models.

We believe that this project has achieved its primary objectives of providing modeling data that addresses this concern. This study has shown that although there are some differences between urban and regional-scale relative reactivities, the relative reactivity rankings are generally preserved for the major types of VOC species that contribute to ozone formation. This suggests that it should be possible to develop reactivity scales that appropriately represent both urban and regional impacts. However, choices will have to be made concerning which types of model and reactivity metrics are most appropriate to use when developing reactivity scales for regulatory applications. This is discussed further below.

The results of this and most recent previous modeling studies indicate that most of this Eastern U.S. consists of regions where ozone is much more sensitive to biogenic than anthropogenic VOC emissions, and where ozone is far more responsive to controlling NO_x than VOCs. This study has shown that there are indeed differences in relative ozone impacts of VOCs in those regions compared to those in the urban-dominated regions that have been studied previously, even though orderings of the reactivity rankings are generally similar in a qualitative sense. Probably the most significant finding is the fact that there is less of a range in relative ozone impacts between borderline exempt compounds such as ethane and the most reactive of the VOCs in most of the regional domain than is the case in the urban-dominated areas. This is because slowly reacting compounds will have had more time to react by the time they reach air parcels that are far removed from the primary VOC sources, and also because O_3 formation in such NO_x-limited areas are less sensitive to radical initiating effects of the most reactive VOCs. In addition, compounds with large NO_x sinks in their mechanisms tend to have much more negative effects on O_3 formation in the NO_x-limited areas than in the more VOC-sensitive urban dominated areas of the domain.

A number of different approaches can be used to derive regional reactivity metrics, depending on how ozone impacts are quantified and on how a global reactivity number is derived from the varying impacts in the different regions. The approaches for deriving a global metric from the regional results that were examined in this study are summarized on Table 13. Generally, reasonably consistent results are obtained for different episode days for those metrics that reflect impacts over multiple cells, with more variable results being obtained with metrics that reflect impacts only a single cell with extreme conditions. The latter type of metrics, particularly the highly variable regional maximum O_3 metrics, should probably not be used as the basis for deriving regulatory scales. The major differences among the truly regional scales are the effective reactivity ranges (i.e., the ratio of reactivity of the most to the least

Table 13. Summary of the regional ozone reactivity metrics examined in this work.

Metric	Derivation	Effective Range [a] 4K	Effective Range [a] 36K	Discussion
Regional Average Ozone	Effect of VOCs on domain-wide average O_3	24	19	Reflects impacts over the entire domain, weighting absolute O_3 sensitivities in each cell equally. Most sensitive to impacts in non-urban that are least sensitive to AVOC changes. Not highly sensitive to using a low O_3 cutoff if the cutoff is sufficiently below the ozone standard. Gives the lowest effective reactivity ranges.
Regional O_3 over the standard	Effect of VOCs on average O_3 in cells that exceed the air quality standard	36	22	Reflects impacts only in regions modeled to exceed the standard, not borderline regions that may exceed the standard should O_3 increase slightly. May give the best prediction of effects of VOCs on extent of exceedences. Gives effective reactivity ranges between the average O_3 and minimum substitution error metrics.
Minimum Substitution Error	Minimizes sum of squares O_3 change caused by null test substitutions	38	27	Reflects impacts over the entire domain, but weighs impacts in AVOC-sensitive cells greater than does the average ozone metric. Gives highest effective ranges of all the metrics that reflect the entire domain. Two alternative derivation methods are possible, but one is unsatisfactory because it gives numerically unstable results for NO_x-inhibiting species. Comparable to the base case reactivity scales developed by Carter (1994a).
Regional MIR to MOIR	Effect of VOCs on average O_3 in regions with negative NO_x sensitivity	41	32	Comparable to the MIR and MOIR scales developed by Carter (1994a,b). Reflects ozone impacts in regions with the highest VOC sensitivity, where NO_x control is counter-productive. May be appropriate for use in conjunction with a separate NO_x control policy to reduce O_3 in other regions. Very similar to the minimum substitution error scales.
Regional MIR	Effect of VOCs on the cell with the greatest AVOC sensitivity	60	42	Not a true global metric because only a single cell is used, but not as variable as the maximum O_3 metric because MIR cells have similar chemical conditions. Comparable to the Carter MIR scale (1994a,b). Least sensitive to NO_x-inhibition effects and gives the highest effective ranges. If a MIR metric is to be used, it would be better to derive an alternative based on impacts in multiple cells with MIR-like conditions.
Regional Maximum O_3	Effects of VOCs on the domain-wide ozone maximum	Highly Variable		Not a true global metric because only a single cell is used. Results are highly variable because the chemical conditions of the maximum O_3 cell varies with episode day and sometimes the maximum O_3 level is insensitive to AVOCs. Probably not satisfactory for regulatory use.

[a] Effective reactivity range (carbon basis) for the 4K and 32K domains. Ratio of most consistently reactive to the least reactive VOC model species examined in this work.

reactive of the VOC model species) and the reactivities derived for the highly NO_x-sensitive TOL model species. The effective ranges as defined by the OLE/ethane ratio vary by as much as a factor of 3, with the highest values being for the scales what weigh the urban impacts more greatly, and the lowest for those which weigh the impacts in the various regions more equally. However, even the scales with the lowest effective ranges still have over an order of magnitude difference in ozone impacts between the most and least reactive ofthe VOC species, indicating that substitutions to low reactivity compounds would still reduce ozone according to those scales, though perhaps not as much as in urban areas.

The Carbon Bond TOL model species represents a special case because of its unusually variable ozone impacts, ranging from moderately positive in the relatively high NO_x urban conditions to quite negative in the large portions of the regional domain that are NO_x-limited. This resulted in highly variable reactivity metrics depending on the scale, domain, and episode, ranging from highly negative in the average ozone metrics, near zero in the minimum substitution error metrics, to positive in MIR-MOIR and MIR metrics. If TOL were actually representative of the major classes of emitted VOCs then adaptation of reactivity-based regulatory approaches would be highly problematical. As it is, the TOL model species may not be an accurate representation of the reactivity characteristics of toluene (the compound it is intended to represent), whose qualitative reactivity behavior may be better represented by XYL. However, its reactivity behavior is still of relevance because other compounds, such as styrenes, phenols, and certain alkyl bromides, exhibit highly NO_x-sensitive reactivity characteristics and probably would have qualitatively similar reactivity metrics as TOL. Although such compounds are currently relatively unimportant in emissions inventories, reactivity-based regulations will still need to incorporate a quantification of their impacts. The problem of how best to do this needs to be considered when choosing reactivity scales for regulatory applications. Depending on the reactivity policy that is adopted, emissions of such compounds may well increase, and it needs to be determined whether this is a desirable outcome.

One concern has been whether the adoption of the 8-hour standard for ozone may indicate use of different reactivity scales than those developed for the current 1-hour standard. This study has shown that in most cases the choice of averaging time does not have a significant impact on the reactivity that is derived. With one exception, relative reactivities are either essentially the same, or differ by less than the day-to-day variability with episode day for the more variable single-cell metrics. The one exception is the average ozone over the standard metric, where the effective reactivity ranges are about ~20% less for the 8-hour scales compared to the 1-hour scales for the same episode-days. This is because the spatial extent of regions where the 8-hour standard is exceeded is greater than those with 1-hour exceedences. However, this difference is small compared to differences between the other types of metrics.

Another concern addressed by this study is whether reactivity scales developed using single day EKMA models, such as those of Carter (1994a,b, 2000), can appropriately represent reactivity effects on a regional domain. EKMA models obviously oversimplify conditions of actual airsheds, and the 1-day models used by Carter (1994a,b, 2000) obviously cannot represent multi-day effects. However, the results of this study indicate remarkable similarities between EKMA and regional model scales derived using comparable metrics. The EKMA scales do tend to give higher effective reactivity ranges than do the comparable regional scales, as is expected since they are developed based only on urban conditions and also do not represent multi-day effects. However, the differences in effective ranges between the EKMA scales and the corresponding regional results for the 4K domain for the minimum substitution error or average MIR-MOIR are within the day-to-day variability of the regional scales. The differences between EKMA and regional scales are greater for the larger domains or the for the average ozone metric, where the non-urban impacts are relatively more important. However, since the EKMA scenarios used by Carter (1994a,b) were not intended to represent such non-urban conditions, these differences are perhaps smaller than one might have expected. It may well be that expanding the set of EKMA scenarios to include better representations of non-urban episodes and longer-term irradiations may result in significantly better performance in duplicating regional reactivity scales. The trajectory scenarios used by Derwent and co-workers (e.g., Derwent and Jenkin, 1991), or the multi-day scenarios employed by Stockwell et al (2001) suggest possible approaches that may be used in this regard. It may be appropriate to investigate this further.

The large scale substitution calculations carried out for this study are generally consistent with the expectations based on the DDM sensitivity results discussed above. Removing anthropogenic VOCs but not NO_x was found to give only relatively small O_3 reductions in most of the modeling domain, with many regions still exceeding both 1-hour and 8-hour ozone standards. This is because of the large role of the biogenic VOCs in the Eastern U.S., combined with the related fact that most of the domain is NO_x limited. The spatial distribution and approximate magnitudes of the ozone reductions were reasonably consistent with what is predicted using the DDM sensitivity results, assuming a linear approximation. (The reasonably good performance of the linear approximation may be due in part to the fact that the contributions of AVOCs are relatively small compared to biogenic VOCs in most of the domain.) However, biogenic emissions are uncertain, and thus the actual effects of significantly reducing the mass or reactivity of anthropogenic VOCs may be greater or less than predicted by this model. In any case, it is clear that NO_x control is necessary to address the need to reduce ozone exceedences in non-urban areas, though VOC control will still be necessary to reduce ozone in some urban areas, at least in the near to mid term. The fact that VOC control must necessarily be carried out in conjunction to NO_x controls probably should be considered when determining what reactivity metric is most appropriate for reactivity-based VOC controls (see, for example, CARB, 1993).

The large scale substitution calculations where ethane replaced anthropogenic VOCs on a molar or carbon (i.e., approximately mass) basis resulted in ozone levels that were somewhat higher than the in the calculations where all the AVOCs were removed, which is expected since ethane does have a positive ozone impact. However, the ozone levels in these substitution calculations were much closer to the levels in the no-AVOC calculation than those in the base case simulation. This indicates that either type of substitution would result in almost as much ozone reduction throughout the domain as anthropogenic VOC removal.

Obviously if enough of a low but positive reactivity compound such as ethane is added to replace the current AVOC emissions, the ozone levels would eventually equal or exceed the current levels. Indeed, one test of a reactivity scale is to conduct a “null test” calculation, where the amount of low reactivity is chosen to be sufficient to yield no net change in ozone, according to its relative reactivity in the scale. The null test calculations carried out in this study used substitution factors based on the minimum substitution error method, which gives relatively low relative reactivities compared to the average ozone metric. Because of this, these substitutions resulted in increases in the domain-wide average ozone levels, and also an increase in the number of cells over the air quality standards in most cases, though this was counterbalanced by generally larger ozone decreases in the more urban-dominated areas. Conducting a null test using an average ozone metric or another scale with a lower effective reactivity range would have resulted in less ozone overall because less ethane would be added because of its higher relative reactivities in these metrics. In the case of the average ozone metric, the expected result of a null substitution would be no net change in average ozone, but probably decreased ozone maxima and decreased number of cells over the standards compared to the base case simulation. These results are consistent with the DDM results that indicate that the slowly reacting compounds such as ethane have relatively higher impacts in the non-urban areas compared to their impacts in the more urban dominated regions.

The spatial distribution and approximate magnitudes of the ozone increases in the ethane substitution calculations were also reasonably well predicted by the DDM sensitivity results. This is despite the fact that our calculations employed extremely large changes to AVOC emissions that should produce the most non-linear results. This indicates that DDM first-order sensitivities could be used to give at least approximate predictions of effects of other types of substitutions, such as null tests employed using different metrics (as done in this work) or substitutions involving additions or removals of different VOCs. Dunker at al. (2002) concluded that the CAMx first-order sensitivities were useful for predicting the effects of emission changes of up to 40% in another Eastern U.S. modeling domain. Although the results will not exactly duplicate the direct calculations if very large substitutions are employed, they will probably be close enough to indicate the types of general trends that are of interest in this type of study. The estimates are probably within the uncertainty of the model predictions in any case, particularly considering the uncertainties of the chemical mechanisms and emissions inventories employed. However, the reliability of extrapolating first-order sensitivities decreases as the perturbation to the system increase.

Recommendations

It should be recognized that this study was not intended to develop actual reactivity scales for regulatory applications, since an out-of-date and highly condensed mechanism was employed, the modeling represents only one 4-day episode, and the emissions inventory probably needs to be updated. Comprehensive scales should reflect not only use of an appropriately updated, detailed, and experimentally evaluated mechanism, but also an appropriately comprehensive set of scenarios reflecting the range of conditions of interest, and the best available emission inventory. It may not be necessary to use all the available scenarios when developing the actual scale, but reactivity effects in all the available scenarios need to be understood before determining the appropriate scenarios that should be employed. The work of Russell et al (e.g., Hakami et al, 2002), who used a more current and detailed SAPRC-99 mechanism (Carter, 2000a) to examine reactivity effects in not only this but also several other regional scenarios, represents an important complement to this work and a necessary starting point to examining reactivity effects in multiple scenarios.

The results obtained by Russell and co-workers (e.g., Hakami, 2002) are generally consistent with the results obtained in this study, and tend to support our conclusion that it should be possible to develop reactivity scales that appropriately represent both urban and regional impacts. However, the analysis approach they employed does not permit comparison with all the metrics examined in this work, and it may be useful to independently evaluate these results with a different model. If unexpected results are obtained, a process analysis study may be useful to understand the reason and assess the implications to the general issue of variability in regional reactivity scales, and how this should be taken into account when developing scales for regulatory applications.

While we believe these follow-on assessment studies are useful and probably necessary, we also believe that the general question of whether reactivity will “work” on a regional scale has been answered, and the focus of the RRWG now should shift to how to actually calculate reactivity scales for regulatory applications. This involves work in policy as well as scientific and modeling efforts. Recommended work in these areas is briefly summarized below.

The policy makers need to decide soon which type of reactivity metric is best suited for regulatory applications. Sufficient information should now be available to begin the process of making these decisions. The work carried out thus far has presented a number of options in this regard, and the consequences of these options in terms of relative reactivities of representative types of VOCs and effective reactivity ranges. A choice needs to be made between using a metric with a low effective range that best reflects impacts over wide regions, or a metric with a high effective range that may be more optimal for ozone reductions in urban areas where VOC controls are most needed. The fact that VOC control is being carried out in conjunction with NO_x controls also needs to be considered. How to weigh the relative impacts in the different regions will require political input as well as considerations of economic, health, and other issues. The types of metrics, regions, and episodes chosen based on these policy considerations will to some extent determine the research priorities for deriving the regulatory scale, which is why these policy decisions are best made as soon as possible.

Before making the final decision on the scenarios to use for deriving the general reactivity scale, the evaluation of how reactivity effects vary with different regions, meteorologies, and emissions scenarios needs to be completed. As indicated above, significant progress has been made in this regard by Russell and co-workers, and after the possible problems have been investigated the results need to be summarized in terms of reactivity metrics of interest to the policy community (or, lacking their input, those developed in this work), and extended to other existing scenarios, where possible. The evaluations should all employ consistent mechanisms and reactivity analysis methodologies, though as indicated above at least some of the modeling should be independently verified using implementations in different models by other researchers. The results can then be used as a basis for developing a set of scenarios and modeling approach for deriving a regulatory reactivity scale that will appropriately represent the distribution of conditions of relevance to the regulatory priorities.

Calculating reactivity scales using regional photochemical models is a significant undertaking because of the time and expertise needed to set-up and analyze the results. Computational requirements are less constraining because of the continued rapid advance in technology – indeed the calculations for this study were completed on typical desktop personal computers. It is feasible to calculate reactivity scales using detailed chemical mechanisms in regional models, but it would be a large undertaking to do this for the many hundreds of VOCs whose impacts will need to be quantified.

A lower cost and more practical alternative for the near to mid term may be to develop an improved set of EKMA or trajectory scenarios that can be used to assess reactivities and calculate comprehensive scales using inexpensive computers and currently available software. Although such models cannot represent specific episodes in any detail, they permit use of fully detailed chemical mechanisms and can represent the major chemical conditions that affect VOC reactivity. The results of this study indicate that an appropriate set of such scenarios can give reactivity metrics that are remarkably close to those derived using the regional model. This is despite the fact that the EKMA scenarios employed represent only urban areas, are way out of date, and predict ozone levels far greater than is currently observed[6]. Significantly better agreement should be obtained if scenarios are added to represent the non-urban areas not represented in the current set of scenarios, including scenarios representing multi-day effects. Although box models cannot represent the meteorology of multi-day effects with any accuracy, this does not necessarily mean that they cannot represent the chemical effects. Stockwell et al (2001) has shown that EKMA models can be readily adapted to calculate multi-day effects from a chemical standpoint, and give the lower effective reactivity ranges that are more characteristic of non-urban areas in regional models. Therefore, it should be possible to develop a set of updated EKMA scenarios that gives reactivity scales that are within the range of variability of those derived using regional models, regardless of the metric that is employed. At a minimum, there would be a better documented and more realistic set of scenarios for which to calculate reactivity scales for urban conditions for other applications where EKMA models are well suited. In any case, the amount of time and cost required for this effort will be considerably less than that required to make regional models a practical alternative in this regard.

---

[6] For example, the SAPRC-99 mechanism predicts that the maximum ozone in the base case scenario representing Los Angeles is almost 600 ppb, and predicts over 200 ppb of ozone for over 60% of the other urban areas.

Finally, it must be recognized that regardless of the level of detail of the chemical mechanism and the accuracy of the representation of meteorological conditions and emissions inventories, model predictions of relative reactivity are no more reliable than the chemical mechanism employed. Although significant progress has been made in recent years, there are still many uncertainties in mechanisms for aromatics and other important classes of VOCs, and there are still many types of VOCs whose mechanism have not been experimentally evaluated. In addition, currently available environmental chamber data are not adequate for evaluating mechanisms under the lower pollution, non-urban conditions that are important in affecting predictions of effects of VOCs on regional average ozone and other metrics, and additional funding for the research needed to address this may be needed (Carter, 2002b). Although the basic laboratory research and the more applied environmental chamber research needed to address these uncertainties has not been a priority for the RRWG, once reactivity-based regulations are established, the need to reduce these uncertainties becomes more evident. The RRWG would be well advised to anticipate this need so that when a reactivity scale is eventually adopted by the EPA it will reflect the best mechanistic information possible.

REFERENCES

Baugues, K. (1990): “Preliminary Planning Information for Updating the Ozone Regulatory Impact Analysis Version of EKMA,” Draft Document, Source Receptor Analysis Branch, Technical Support Division, U. S. Environmental Protection Agency, Research Triangle Park, NC, January.

CARB (1993): “Proposed Regulations for Low-Emission Vehicles and Clean Fuels -- Staff Report and Technical Support Document,” California Air Resources Board, Sacramento, CA, August 13, 1990. See also Appendix VIII of “California Exhaust Emission Standards and Test Procedures for 1988 and Subsequent Model Passenger Cars, Light Duty Trucks and Medium Duty Vehicles,” as last amended September 22, 1993. Incorporated by reference in Section 1960.

CARB (2000): “Initial Statement of Reasons for the Proposed Amendments to the Regulation for Reducing Volatile Organic Compound Emissions from Aerosol Coating Products and Proposed Tables of Maximum Incremental Reactivity (MIR) Values, and Proposed Amendments to Method 310, ‘Determination of Volatile Organic Compounds in Consumer Products’,” California Air Resources Board, Sacramento, CA, May 5.

Calvert J.G., R. Atkinson, K.H. Becker, R.M. Kamens, J.H. Seinfeld, T.J. Wallington and G. Yarwood (2002): “The Mechanisms of Atmospheric Oxidation of Aromatic Hydrocarbons,” Oxford University Press, New York, New York.

Carter, W. P. L. (1994a): “Development of Ozone Reactivity Scales for Volatile Organic Compounds,” J. Air & Waste Manage. Assoc., 44, 881-899.

Carter, W. P. L. (1994b): “Calculation of Reactivity Scales Using an Updated Carbon Bond IV Mechanism,” Report Prepared for Systems Applications International Under Funding from the Auto/Oil Air Quality Improvement Research Program, April 12.

Carter, W. P. L. (1996): “Condensed Atmospheric Photooxidation Mechanisms for Isoprene,” Atmos. Environ., 30, 4275-4290.

Carter, W. P. L. and R. Atkinson (1989): “A Computer Modeling Study of Incremental Hydrocarbon Reactivity”, Environ. Sci. Technol., 23, 864.

Carter, W. P. L., D. Luo, and I. L. Malkina (1997a): “Environmental Chamber Studies for Development of an Updated Photochemical Mechanism for VOC Reactivity Assessment,” Final report to the California Air Resources Board, the Coordinating Research Council, and the National Renewable Energy Laboratory, November 26. Available at http://www.cert.ucr.edu/~carter/absts.htm #rct3rept

Carter, W. P. L., D. Luo, and I. L. Malkina (1997b): “Investigation of the Atmospheric Ozone Formation Potential of Selected Alkyl Bromides,” Report to Albemarle Corporation, November 10.

Carter, W. P. L. (2000a): “Documentation of the SAPRC-99 Chemical Mechanism for VOC Reactivity Assessment,” Report to the California Air Resources Board, Contracts 92-329 and 95-308, May 8. Available at http://www.cert.ucr.edu/~carter/reactdat.htm.

Carter, W. P. L. (2000b): "Implementation of the SAPRC-99 Chemical Mechanism into the Models-3 Framework," Report to the United States Environmental Protection Agency, January 29. Available at http://www.cert.ucr.edu/~carter/absts.htm#s99mod3.

Carter, W. P. L. (2002a): Emissions database work in progress under contract for the University of Houston.

Carter, W. P. L. (2002b): Main Information page for "Development of a Next Generation Environmental Chamber Facility for Chemical Mechanism and VOC Reactivity Research," http://www.cert.ucr.edu/~carter/epacham.

Derwent, R. G. and M. E. Jenkin (1991): "Hydrocarbons and the Long-Range Transport of Ozone and PAN Across Europe," Atmos. Environ., 25A, 1661-1678.

Dimitriades, B. (1999): "Scientific Basis of an Improved EPA Policy on Control of Organic Emissions for Ambient Ozone Reduction," J. Air & Waste Manage. Assoc. 49, 831-838

Dudhia, J. (1993): "A Non-hydrostatic Version of the Penn State/NCAR Mesoscale Model: Validation Tests and Simulation of an Atlantic Cyclone and Cold Front," Mon. Wea. Rev., 12, 1493-1513.

Dunker, A M. (1980). "The Response of an Atmospheric Reaction-Transport Model to Changes in Input Functions." Atm. Env. 14, 671-679.

Dunker, A. M., G. Yarwood, J. Ortmann, and G. M. Wilson (2002). "The Decoupled Direct Method for Sensitivity Analysis in a Three-Dimensional Air Quality Model – Implementation, Accuracy, and Efficiency," Environ. Sci. Technol. 36, 2965-2976.

ENVIRON (2002a). "Photochemical Modeling Study of the July 1995 NARSTO-Northeast Episode CRC Projects A-24 and A-35A," Final Report to the Coordinating Research Council, 3650 Mansell Road, Suite 140, Alpharetta, GA 30022-8246.

ENVIRON (2002b). "User's Guide to the Comprehensive Air Quality Model with Extensions, Version 3.10," available at http://www.camx.com.

EPA (1998). Emissions received by email from Deborah Luecken of EPA on Thu, 31 Dec 1998. The email message indicated that the data were forwarded from nmm@hpcc.epa.gov on 12/30/98 06:58:57 PM. The message also included the following text: "These ASCII files contain SAROAD emission totals for Benjyey's 36km evaluation grid. These attached files …are based on the 1995-NET EPA US inventory. These files contain the emission summaries for the US part of the grid." The comments also note that the emissions have not been completely reviewed and should be regarded as preliminary. Separate totals were given for area and point source totals. These were summed up to get the total emissions.

Gery, M. W., G. Z. Whitten, and J. P. Killus (1988): "Development and Testing of the CBM-IV For Urban and Regional Modeling,", EPA-600/ 3-88-012, January.

Jeffries, H. E. and Crouse, R. (1991): "Scientific and Technical Issues Related to the Application of Incremental Reactivity, Part II: Explaining Mechanism Differences," Final report to the Western States Petroleum Association, Los Angeles, CA.

Hakami, A., R. A. Harley, J. B. Milford, M. T. Odman and A. G. Russell (2002): "Regional, Three-Dimensional Reactivity Assessment of Organic Compounds," Manuscript in preparation. (Personal communication to W. P. L. Carter, April, 2002).

Hales, J. M., M. W. Gery, and Crouse, R. (1993): "VOC Reactivity and its Application for Emission Regulation," Report submitted to the American Petroleum Institute, March.

RRWG (1999): "VOC Reactivity Science Assessment", Prepared by the Reactivity Research Working Group Science Team, May 5, Available at http://www.cgenv.com/Narsto/reactinfo.html.

Stockwell, W. R., H. Geiger, and K. H. Becker (2001): "Estimation of Incremental Reactivities for Multiple Day Scenarios: An Application to Ethane and Dimethyoxymethane," Atmos. Envir., 35 929-939.

APPENDIX A. MECHANISM LISTING

Table A-1. Listing of the version of the Carbon Bond 4 mechanism used in this study.

No.	Rate Parameters [a]			Reactions
	k(300)	A	B	
1	PF=NO2-01			NO2 + HV = NO + O
2	8.38e+4	-1175		O = O3
3	2.64e+3	1370		O3 + NO = NO2
4	1.38e+4			O + NO2 = NO
5	2.30e+2	-687		O + NO2 = NO3
6	3.23e+2	-602		O + NO = NO2
7	1.76e+2	2450		O3 + NO2 = NO3
8	0.0053 x PF=NO2-01			O3 + HV = O
9	PF=O3O1D-1			O3 + HV = O1D
10	1.15e+5	-390		O1D = O
11	3.26e+0			H2O + O1D = 2 OH
12	2.34e+3	940		O3 + OH = HO2
13	2.10e+1	580		O3 + HO2 = OH
14	33.9 x PF=NO2-01			NO3 + HV = 0.89 NO2 + 0.89 O + 0.11 NO
15	1.91e+4	-250		NO3 + NO = 2 NO2
16	3.66e+1	1230		NO3 + NO2 = NO + NO2
17	7.85e+2	-256		NO3 + NO2 = N2O5
18	1.90e-6			N2O5 + H2O = 2 HNO3
19	2.11e+16	10897		N2O5 = NO3 + NO2
20	2.60e-5	-530		NO + NO = 2 NO2
21	1.68e-17	-6348		NO + NO2 + H2O = 2 HONO
22	6.55e+2	-806		OH + NO = HONO
23	0.1975 x PF=NO2-01			HONO + HV = OH + NO
24	9.77e+3			OH + HONO = NO2
25	1.50e-5			HONO + HONO = NO + NO2
26	1.54e+3	-713		OH + NO2 = HNO3
27	7.6	-1000		OH + HNO3 = NO3
28	5.48e+3	-240		HO2 + NO = OH + NO2
29	1.64e+2	-749		HO2 + NO2 = PNA
30	2.88e+15	10121		PNA = HO2 + NO2
31	1.91e+3	-380		OH + PNA = NO2
32	8.74e+1	-1150		HO2 + HO2 = H2O2
33	7.69e-10	-5800		HO2 + HO2 + H2O = H2O2
34	0.189 x PF=HCHOM-1			H2O2 + HV = 2 OH
35	4.72e+3	187		OH + H2O2 = HO2
36	3.22e+2			OH + CO = HO2
37	1.50e+4			HCHO + OH = HO2 + CO
38	PF=HCHOR-1			HCHO + HV = 2 HO2 + CO
39	PF=HCHOM-1			HCHO + HV = CO

Table A-1 (continued)

No.	Rate Parameters [a]			Reactions
	k(300)	A	B	
40	4.30e+4	1550		HCHO + O = OH + HO2 + CO
41	9.30e-1			HCHO + NO3 = HNO3 + HO2 + CO
42	1.74e+4	986		ALD2 + O = C2O3 + OH
43	1.04e+4	-250		ALD2 + OH = C2O3
44	3.70e+0			ALD2 + NO3 = C2O3 + HNO3
45	PF=ALD2R-1			ALD2 + HV = XO2 + 2 HO2 + CO + HCHO
46	5.15e+4	180		C2O3 + NO = NO2 + XO2 + HCHO + HO2
47	3.84e+3	-380		C2O3 + NO2 = PAN
48	1.20e+18	13500		PAN = C2O3 + NO2
49	3.70e+3			C2O3 + C2O3 = 2 XO2 + 2 HCHO + 2 HO2
50	9.60e+3			C2O3 + HO2 = 0.79 HCHO + 0.79 XO2 + 0.79 HO2 + 0.79 OH
51	6.52e+3	1710		OH = XO2 + HCHO + HO2
52	1.20e+3			PAR + OH = 0.87 XO2 + 0.13 XO2N + 0.11 HO2 + 0.11 ALD2 + 0.76 ROR – 0.11 PAR
53	6.25e+16	8000		ROR = 1.1 ALD2 + 0.96 XO2 + 0.94 HO2 - 2.1 PAR + 0.04 XO2N + 0.02 ROR
54	9.55e+4			ROR = HO2
55	2.20e+4			ROR + NO2 =
56	1.76e+4	324		O + OLE = 0.63 ALD2 + 0.38 HO2 + 0.28 XO2 + 0.3 CO + 0.2 HCHO + 0.02 XO2N + 0.22 PAR + 0.2 OH
57	7.74e+3	-504		OH + OLE = HCHO + ALD2 + XO2 + HO2 - PAR
58	2.10e+1	2105		O3 + OLE = 0.5 ALD2 + 0.74 HCHO + 0.33 CO + 0.44 HO2 + 0.22 XO2 + 0.1 OH - PAR
59	1.14e+1			NO3 + OLE = 0.91 XO2 + 0.09 XO2N + HCHO + ALD2 - PAR + NO2
60	1.54e+4	792		O + ETH = HCHO + 0.7 XO2 + CO + 1.7 HO2 + 0.3 OH
61	3.00e+3	-411		OH + ETH = XO2 + 1.56 HCHO + HO2 + 0.22 ALD2
62	1.86e+1	2633		O3 + ETH = HCHO + 0.42 CO + 0.12 HO2
63	3.11e+3	-322		OH + TOL = 0.08 XO2 + 0.36 CRES + 0.44 HO2 + 0.56 TO2
64	1.20e+4			TO2 + NO = 0.9 NO2 + 0.9 HO2 + 0.9 OPEN
65	2.50e+2			TO2 = CRES + HO2
66	6.10e+4			OH + CRES = 0.4 CRO + 0.6 XO2 + 0.6 HO2 + 0.3 OPEN
67	3.25e+4			NO3 + CRES = CRO + HNO3
68	2.00e+4			CRO + NO2 =
69	8.4 x PF=HCHOR-1			OPEN + HV = C2O3 + HO2 + CO
70	4.40e+4			OPEN + OH = XO2 + 2 CO + 2 HO2 + C2O3 + HCHO
71	8.03e-2	500		OPEN + O3 = 0.03 ALD2 + 0.62 C2O3 + 0.7 HCHO + 0.03 XO2 + 0.69 CO + 0.08 OH + 0.76 HO2 + 0.2 MGLY
72	2.453+04	-116		OH +XYL = 0.7 HO2 + 0.5 XO2 + 0.2 CRES + 0.8 MGLY + 1.1 PAR + 0.3 TO2
73	2.60e+4			OH + MGLY = XO2 + C2O3
74	P8.96 x F=HCHOR-1			MGLY + HV = C2O3 + HO2 + CO
79	1.20e+4			XO2 + NO = NO2
80	2.55e+1	-1300		XO2 + XO2 =
81	1.20e+4			XO2N + NO =
86	1.13e+2	-1300		XO2 + HO2 =
87	1.13e+2	-1300		XO2N + HO2 =

Table A-1 (continued)

No.	Rate Parameters [a] k(300)	A	B	Reactions
88	2.55e+1	-1300		XO2N + XO2N =
89	5.10e+1	-1300		XO2N + XO2 =
90	7.03e+4	-250		HO2 + OH =
91	2.78e-4			CRO =
75	5.32e+4			O + ISOP = 0.75 ISPD + 0.5 HCHO + 0.25 XO2 + 0.25 HO2 + 0.25 C2O3 + 0.25 PAR
76	1.48e+5			OH + ISOP = 0.912 ISPD + 0.629 HCHO + 0.991 XO2 + 0.912 HO2 + 0.088 XO2N
77	1.90e-2			O3 + ISOP = 0.65 ISPD + 0.6 HCHO + 0.2 XO2 + 0.066 HO2 + 0.266 OH + 0.2 C2O3 + 0.15 ALD2 + 0.35 PAR + 0.066 CO
78	9.96e+2			NO3 + ISOP = 0.2 ISPD + 0.8 NTR + XO2 + 0.8 HO2 + 0.2 NO2 + 0.8 ALD2
96	2.20e-4			NO2 + ISOP = 0.2 ISPD + 0.8 NTR + XO2 + 0.8 HO2 + 0.2 NO + 0.8 ALD2 + 2.4 PAR
92	4.97e+4			OH + ISPD = 1.565 PAR + 0.167 HCHO + 0.713 XO2 + 0.503 HO2 + 0.334 CO + 0.168 MGLY + 0.273 ALD2 + 0.498 C2O3
93	1.05e-2			O3 + ISPD = 0.114 C2O3 + 0.15 HCHO + 0.85 MGLY + 0.154 HO2 + 0.268 OH + 0.064 XO2 + 0.02 ALD2 + 0.36 PAR + 0.225 CO
94	1.48e+0			NO3 + ISPD = 0.357 ALD2 + 0.282 HCHO + 1.282 PAR + 0.925 HO2 + 0.643 CO + 0.85 NTR + 0.075 C2O3 + 0.075 XO2 + 0.15 HNO3
95	PF=ISPD-01			ISPD + HV = 0.333 CO + 0.067 ALD2 + 0.9 HCHO + 0.832 PAR + 1.033 HO2 + 0.7 XO2 + 0.967 C2O3
84	4.88e+3	380		MEOH + OH = HCHO + HO2
85	6.06e+3	70		ETOH + OH = 0.078 HCHO + 0.961 ALD2 + HO2 + 0.05 XO2
100	2.01e+3	498	1	ETHA + OH = ALD2 + XO2 + HO2

[a] For thermal reactions, data rate constant is given by k = A exp(-Ea/300) $(T/300)^{B}$, where A is in ppm, minute units and Ea is in degree K. Photolysis reactions are indicted by “PF = photolysis set” or “fac x PF = photolysis set”, where “photolysis set” refers to an array of photolysis rates given as a function of solar zenith angle as given on Table A-2, and “fac” refers to a factor that is multiplied by the photolysis rate given on Table A-2, if applicable.

Table A-2. Photolysis rate constants used for the airshed simulations used in this work.

Zenith Angle	Rate Constant for Photolysis Set (min^{-1}) NO2-01	O3O1D-01	HCHOR-01	HCHOM-01	ALD2R-01	ISPD-01
0	0.578	2.79e-3	2.38e-3	3.43e-3	4.44e-4	1.18e-4
10	0.575	2.70e-3	2.34e-3	3.39e-3	4.34e-4	1.17e-4
20	0.563	2.44e-3	2.23e-3	3.28e-3	4.04e-4	1.13e-4
30	0.543	2.04e-3	2.05e-3	3.09e-3	3.56e-4	1.08e-4
40	0.510	1.53e-3	1.78e-3	2.80e-3	2.90e-4	9.87e-5
50	0.460	9.90e-4	1.42e-3	2.38e-3	2.11e-4	8.58e-5
60	0.386	5.04e-4	9.89e-4	1.82e-3	1.28e-4	6.78e-5
70	0.273	1.67e-4	5.21e-4	1.10e-3	5.43e-5	4.35e-5
78	0.150	4.07e-5	2.06e-4	5.13e-4	1.68e-5	2.14e-5
86	0.035	5.40e-6	3.93e-5	1.19e-4	2.43e-6	5.07e-6

APPENDIX B. MODEL SPECIES REACTIVITY TABULATIONS

Table B-1. Summary of relative reactivity metrics for the PAR model species.

Domain and Episode Day		Relative Reactivities of PAR Model Species (Carbon Basis)						
		Avg O_3 (All Cells)	Avg O_3 (O_3 > Std)	Regional Max. O_3	Min. Subst. Error #1	Min. Subst. Error #2	Avg O_3 (MIR-MOIR)	Regional MIR
EKMA		0.60	-	-	0.55	0.59	0.51	0.40
36K 1 Hr	7/12	0.84	0.99	1.03	0.74	0.81	0.64	0.75
	7/13	0.85	0.84	0.78	0.71	0.76	0.63	0.41
	7/14	0.90	0.88	1.26	0.71	0.76	0.64	0.51
	7/15	0.90	0.85	1.23	0.62	0.70	0.56	0.36
	Average	0.87 (4%)	0.89 (7%)	1.07 (21%)	0.69 (8%)	0.76 (6%)	0.62 (6%)	0.51 (34%)
36K 8 Hr	7/12	0.83	0.99	0.94	0.75	0.81	0.65	0.73
	7/13	0.85	0.86	0.73	0.74	0.78	0.65	0.64
	7/14	0.92	0.92	1.31	0.73	0.79	0.63	0.47
	Average	0.87 (6%)	0.92 (7%)	0.99 (30%)	0.74 (1%)	0.79 (2%)	0.64 (2%)	0.61 (21%)
12K 1 Hr	7/12	0.84	0.92	0.65	0.72	0.80	0.63	0.36
	7/13	0.86	0.82	0.84	0.71	0.76	0.65	0.43
	7/14	0.90	0.83	1.23	0.69	0.74	0.64	0.50
	7/15	0.93	0.79	0.45	0.57	0.67	0.56	0.38
	Average	0.88 (4%)	0.84 (7%)	0.79 (42%)	0.67 (10%)	0.74 (7%)	0.62 (6%)	0.42 (15%)
12K 8 Hr	7/12	0.84	0.99	0.53	0.75	0.81	0.66	0.36
	7/13	0.86	0.84	0.79	0.73	0.77	0.66	0.67
	7/14	0.92	0.90	2.94	0.71	0.77	0.62	0.47
	Average	0.88 (5%)	0.91 (8%)	1.42 (93%)	0.73 (3%)	0.78 (3%)	0.65 (4%)	0.50 (31%)
4K 1 Hr	7/12	0.62	0.47	0.41	0.51	0.55	0.49	0.37
	7/13	0.65	0.55	0.63	0.54	0.56	0.54	0.38
	7/14	0.80	0.69	0.79	0.60	0.65	0.56	0.47
	7/15	0.90	0.75	0.70	0.63	0.70	0.56	0.39
	Average	0.75 (18%)	0.61 (21%)	0.63 (26%)	0.57 (9%)	0.62 (12%)	0.54 (6%)	0.40 (11%)
4K 8 Hr	7/12	0.60	0.59	0.66	0.51	0.55	0.49	0.34
	7/13	0.66	0.59	0.64	0.56	0.58	0.55	0.56
	7/14	0.81	0.78	0.61	0.61	0.65	0.56	0.49
	Average	0.69 (15%)	0.65 (16%)	0.64 (4%)	0.56 (9%)	0.59 (9%)	0.53 (7%)	0.46 (24%)

Table B-2. Summary of relative reactivity metrics for ethene.

Domain and Episode Day		Relative Reactivities of ETH Model Species (Carbon Basis)						
		Avg O_3 (All Cells)	Avg O_3 (O_3 > Std)	Regional Max. O_3	Min. Subst. Error #1	Min. Subst. Error #2	Avg O_3 (MIR-MOIR)	Regional MIR
EKMA		3.05	-	-	2.93	2.96	2.73	2.64
36K 1 Hr	7/12	3.49	3.63	4.57	2.96	3.12	2.83	2.59
	7/13	3.54	3.31	3.09	2.99	3.08	2.84	2.87
	7/14	3.65	3.48	2.69	2.90	3.04	2.75	2.64
	7/15	3.98	3.99	2.52	3.03	3.21	2.82	2.59
	Average	3.66 (6%)	3.60 (8%)	3.22 (29%)	2.97 (2%)	3.11 (2%)	2.81 (2%)	2.67 (5%)
36K 8 Hr	7/12	3.47	3.54	3.82	2.92	3.08	2.74	2.48
	7/13	3.51	3.45	2.97	2.99	3.09	2.78	3.01
	7/14	3.72	3.57	2.91	2.97	3.14	2.74	2.56
	Average	3.57 (4%)	3.52 (2%)	3.23 (16%)	2.96 (1%)	3.10 (1%)	2.75 (1%)	2.69 (11%)
12K 1 Hr	7/12	3.41	3.11	4.11	2.94	3.08	2.90	2.79
	7/13	3.46	3.19	3.13	2.97	3.05	2.84	2.91
	7/14	3.54	3.22	2.76	2.85	2.95	2.71	2.65
	7/15	3.95	3.76	3.76	2.99	3.14	2.85	2.79
	Average	3.59 (7%)	3.32 (9%)	3.44 (18%)	2.94 (2%)	3.05 (3%)	2.83 (3%)	2.79 (4%)
12K 8 Hr	7/12	3.42	3.30	3.51	2.90	3.04	2.80	2.82
	7/13	3.44	3.32	3.01	2.96	3.04	2.79	2.62
	7/14	3.62	3.39	14.85	2.90	3.02	2.70	2.58
	Average	3.49 (3%)	3.34 (1%)	7.12 (94%)	2.92 (1%)	3.03 (0%)	2.76 (2%)	2.67 (5%)
4K 1 Hr	7/12	3.51	3.28	3.20	3.19	3.25	3.11	3.10
	7/13	3.31	3.14	3.13	3.05	3.07	3.01	2.81
	7/14	3.57	3.24	3.06	3.07	3.13	2.94	2.72
	7/15	3.78	3.65	3.60	3.13	3.27	2.93	2.72
	Average	3.54 (5%)	3.33 (7%)	3.25 (7%)	3.11 (2%)	3.18 (3%)	3.00 (3%)	2.83 (6%)
4K 8 Hr	7/12	3.49	3.27	3.32	3.14	3.20	3.05	2.74
	7/13	3.27	3.17	3.16	3.01	3.04	2.94	3.01
	7/14	3.52	3.42	2.91	3.00	3.08	2.80	2.72
	Average	3.43 (4%)	3.29 (4%)	3.13 (6%)	3.05 (3%)	3.10 (3%)	2.93 (4%)	2.82 (6%)

Table B-3. Summary of relative reactivity metrics for the OLE model species.

Domain and Episode Day		Relative Reactivities of OLE Model Species (Carbon Basis)						
		Avg O_3 (All Cells)	Avg O_3 (O_3 > Std)	Regional Max. O_3	Min. Subst. Error #1	Min. Subst. Error #2	Avg O_3 (MIR-MOIR)	Regional MIR
EKMA		5.91	-	-	5.71	5.76	5.39	5.50
36K 1 Hr	7/12	6.20	5.64	6.18	5.14	5.48	5.13	4.50
	7/13	6.41	5.41	5.09	5.32	5.51	5.29	5.66
	7/14	6.44	5.71	3.07	5.42	5.58	5.30	5.65
	7/15	6.95	6.59	3.93	5.90	6.11	5.72	6.22
	Average	6.50 (5%)	5.84 (9%)	4.57 (30%)	5.45 (6%)	5.67 (5%)	5.36 (5%)	5.51 (13%)
36K 8 Hr	7/12	6.35	5.94	5.99	5.22	5.59	5.16	4.61
	7/13	6.56	5.85	5.20	5.42	5.64	5.34	5.55
	7/14	6.73	6.06	3.58	5.61	5.80	5.51	5.91
	Average	6.55 (3%)	5.95 (2%)	4.92 (25%)	5.42 (4%)	5.68 (2%)	5.33 (3%)	5.36 (13%)
12K 1 Hr	7/12	5.86	4.88	7.66	5.04	5.32	5.12	6.04
	7/13	6.03	5.23	5.02	5.23	5.36	5.19	5.57
	7/14	6.28	5.49	3.07	5.41	5.54	5.33	5.64
	7/15	6.91	6.38	6.72	6.06	6.21	5.85	6.39
	Average	6.27 (7%)	5.50 (12%)	5.62 (36%)	5.43 (8%)	5.60 (7%)	5.37 (6%)	5.91 (6%)
12K 8 Hr	7/12	6.06	5.38	6.96	5.07	5.37	5.07	6.10
	7/13	6.19	5.62	5.07	5.33	5.48	5.29	4.89
	7/14	6.61	5.90	15.27	5.60	5.76	5.54	5.91
	Average	6.29 (5%)	5.63 (5%)	9.10 (60%)	5.33 (5%)	5.54 (4%)	5.30 (4%)	5.63 (12%)
4K 1 Hr	7/12	5.95	5.82	5.98	5.80	5.84	5.78	6.16
	7/13	5.88	5.49	5.57	5.54	5.56	5.49	5.72
	7/14	6.23	5.83	5.40	5.82	5.86	5.78	5.77
	7/15	6.62	6.50	6.49	6.46	6.57	6.36	7.21
	Average	6.17 (5%)	5.91 (7%)	5.86 (8%)	5.90 (7%)	5.96 (7%)	5.85 (6%)	6.22 (11%)
4K 8 Hr	7/12	6.23	5.63	5.34	5.94	5.98	5.89	6.14
	7/13	6.15	5.66	5.72	5.72	5.75	5.67	5.72
	7/14	6.48	6.28	5.60	6.07	6.10	6.00	5.95
	Average	6.29 (3%)	5.86 (6%)	5.55 (3%)	5.91 (3%)	5.94 (3%)	5.86 (3%)	5.94 (4%)

Table B-4. Summary of relative reactivity metrics for the TOL model species.

Domain and Episode Day		Relative Reactivities of TOL Model Species (Carbon Basis)						
		Avg O_3 (All Cells)	Avg O_3 (O_3 > Std)	Regional Max. O_3	Min. Subst. Error #1	Min. Subst. Error #2	Avg O_3 (MIR-MOIR)	Regional MIR
EKMA		-0.63	-	-	-0.24	-3.03	0.19	0.57
36K 1 Hr	7/12	-1.33	-1.27	-1.47	-0.13	-8.07	0.27	0.29
	7/13	-1.57	-0.64	-0.09	-0.14	-6.44	0.23	0.45
	7/14	-1.71	-1.11	-1.01	-0.15	-7.94	0.21	0.43
	7/15	-1.91	-1.41	-1.40	-0.09	-14.64	0.27	0.44
	Average	-1.6 (0.2)	-1.1 (0.3)	-1.0 (0.6)	-0.13 (0.03)	-9 (4)	0.24 (12%)	0.40 (19%)
36K 8 Hr	7/12	-1.46	-1.82	-1.10	-0.25	-5.20	0.21	0.23
	7/13	-1.69	-1.14	0.08	-0.29	-4.08	0.16	0.32
	7/14	-2.04	-1.54	-1.60	-0.35	-4.87	0.17	0.39
	Average	-1.7 (0.3)	-1.5 (0.3)	-0.9 (0.9)	-0.30 (0.05)	-5 (1)	0.18 (16%)	0.31 (25%)
12K 1 Hr	7/12	-1.13	-0.60	-0.93	-0.03	-29.98	0.27	0.48
	7/13	-1.32	-0.43	-0.28	-0.06	-10.64	0.22	0.47
	7/14	-1.57	-0.76	-0.85	-0.07	-12.03	0.20	0.45
	7/15	-2.05	-0.97	-0.03	-0.02	-54.85	0.18	0.45
	Average	-1.5 (0.4)	-0.7 (0.2)	-0.5 (0.4)	-0.04 (0.03)	-27 (21)	0.22 (19%)	0.46 (3%)
12K 8 Hr	7/12	-1.33	-1.45	-0.29	-0.16	-6.13	0.20	0.43
	7/13	-1.46	-0.90	-0.10	-0.19	-4.22	0.13	0.28
	7/14	-1.94	-1.34	-17.27	-0.27	-4.78	0.15	0.41
	Average	-1.6 (0.3)	-1.2 (0.3)	-5.9 (9.9)	-0.21 (0.05)	-5 (1)	0.16 (23%)	0.37 (22%)
4K 1 Hr	7/12	-0.27	0.36	0.43	0.21	1.00	0.31	0.41
	7/13	-0.39	0.29	0.26	0.27	0.88	0.34	0.50
	7/14	-1.04	-0.32	-0.34	-0.01	-51.01	0.21	0.42
	7/15	-1.57	-0.74	-0.65	-0.24	-3.67	0.07	0.34
	Average	-0.8 (0.6)	-0.1 (0.5)	-0.1 (0.5)	0.06 (0.23)	-13 (25)	0.23 (53%)	0.42 (15%)
4K 8 Hr	7/12	-0.43	0.10	0.06	0.11	2.20	0.22	0.41
	7/13	-0.62	0.01	0.10	0.11	2.41	0.23	0.11
	7/14	-1.26	-0.97	0.06	-0.17	-3.64	0.09	0.28
	Average	-0.8 (0.4)	-0.3 (0.6)	0.1 (0.0)	0.01 (0.16)	0 (3)	0.18 (44%)	0.27 (56%)

Table B-5. Summary of relative reactivity metrics for the XYL model species.

Domain and Episode Day		Relative Reactivities of XYL Model Species (Carbon Basis)						
		Avg O_3 (All Cells)	Avg O_3 (O_3 > Std)	Regional Max. O_3	Min. Subst. Error #1	Min. Subst. Error #2	Avg O_3 (MIR-MOIR)	Regional MIR
EKMA		1.79	-	-	2.03	2.19	2.28	2.68
36K 1 Hr	7/12	0.82	0.50	0.15	1.63	2.06	2.02	1.83
	7/13	0.74	1.18	1.58	1.71	2.05	2.07	2.64
	7/14	0.53	0.92	0.23	1.72	2.17	2.03	2.41
	7/15	0.40	0.83	0.30	1.95	2.47	2.24	2.79
	Average	0.62 (31%)	0.86 (33%)	0.57 (120%)	1.75 (8%)	2.19 (9%)	2.09 (5%)	2.42 (17%)
36K 8 Hr	7/12	0.83	0.37	0.62	1.58	2.00	1.97	1.85
	7/13	0.73	0.96	1.75	1.60	1.95	1.98	2.04
	7/14	0.37	0.67	-0.18	1.57	2.17	2.02	2.47
	Average	0.64 (37%)	0.66 (44%)	0.73 (132%)	1.58 (1%)	2.04 (6%)	1.99 (1%)	2.12 (15%)
12K 1 Hr	7/12	0.91	1.05	1.35	1.73	2.11	2.06	2.86
	7/13	0.82	1.36	1.36	1.76	2.05	2.04	2.59
	7/14	0.60	1.20	0.31	1.81	2.18	2.05	2.44
	7/15	0.33	1.14	2.52	2.11	2.53	2.24	2.75
	Average	0.67 (39%)	1.19 (11%)	1.38 (65%)	1.85 (9%)	2.22 (10%)	2.10 (5%)	2.66 (7%)
12K 8 Hr	7/12	0.85	0.56	2.11	1.61	1.98	1.95	2.80
	7/13	0.77	1.09	1.54	1.65	1.95	1.95	2.07
	7/14	0.42	0.81	-10.89	1.67	2.15	2.04	2.48
	Average	0.68 (34%)	0.82 (33%)	-2.42 (-304%)	1.64 (2%)	2.03 (5%)	1.98 (3%)	2.45 (15%)
4K 1 Hr	7/12	1.77	2.62	2.83	2.31	2.44	2.41	2.89
	7/13	1.65	2.25	2.02	2.25	2.33	2.30	2.76
	7/14	1.01	1.65	1.39	2.00	2.25	2.22	2.55
	7/15	0.58	1.31	1.48	1.84	2.29	2.16	2.62
	Average	1.25 (45%)	1.96 (30%)	1.93 (34%)	2.10 (10%)	2.33 (4%)	2.27 (5%)	2.70 (6%)
4K 8 Hr	7/12	1.72	2.03	1.85	2.24	2.37	2.34	2.82
	7/13	1.54	2.00	1.93	2.12	2.22	2.21	2.12
	7/14	0.91	1.15	2.06	1.90	2.17	2.15	2.41
	Average	1.39 (31%)	1.73 (29%)	1.95 (6%)	2.09 (8%)	2.25 (5%)	2.23 (4%)	2.45 (14%)

Table B-6. Summary of relative reactivity metrics for formaldehyde.

Domain and Episode Day		Relative Reactivities of HCHO Model Species (Carbon Basis)						
		Avg O_3 (All Cells)	Avg O_3 (O_3 > Std)	Regional Max. O_3	Min. Subst. Error #1	Min. Subst. Error #2	Avg O_3 (MIR-MOIR)	Regional MIR
EKMA		5.01	-	-	5.47	5.92	5.60	6.47
36K 1 Hr	7/12	2.99	3.61	3.91	3.77	5.13	4.60	3.62
	7/13	2.94	2.95	2.88	3.84	4.67	4.52	7.31
	7/14	3.19	3.60	0.76	4.00	4.63	4.37	5.52
	7/15	4.16	5.29	1.81	5.73	6.64	5.73	8.70
	Average	3.32 (17%)	3.86 (26%)	2.34 (58%)	4.33 (22%)	5.27 (18%)	4.81 (13%)	6.29 (35%)
36K 8 Hr	7/12	3.11	2.83	3.81	3.79	5.11	4.67	4.18
	7/13	3.12	3.40	3.30	3.79	4.60	4.64	3.94
	7/14	3.34	3.54	0.94	4.14	4.86	4.80	6.58
	Average	3.19 (4%)	3.25 (11%)	2.68 (57%)	3.91 (5%)	4.86 (5%)	4.70 (2%)	4.90 (30%)
12K 1 Hr	7/12	3.14	3.15	7.92	4.02	5.38	4.74	7.84
	7/13	3.03	3.05	2.58	3.88	4.65	4.41	6.81
	7/14	3.28	3.61	0.77	4.15	4.80	4.50	5.44
	7/15	4.31	5.35	8.47	6.43	7.28	6.16	8.51
	Average	3.44 (17%)	3.79 (28%)	4.93 (78%)	4.62 (26%)	5.53 (22%)	4.95 (16%)	7.15 (19%)
12K 8 Hr	7/12	3.16	2.72	7.73	3.91	5.26	4.71	8.47
	7/13	3.18	3.36	2.90	3.90	4.68	4.61	4.12
	7/14	3.47	3.48	6.20	4.36	5.10	4.91	6.46
	Average	3.27 (5%)	3.19 (13%)	5.61 (44%)	4.05 (6%)	5.01 (6%)	4.74 (3%)	6.35 (34%)
4K 1 Hr	7/12	4.82	6.41	7.18	6.38	7.09	6.67	8.22
	7/13	4.32	5.29	4.70	5.53	5.81	5.56	7.82
	7/14	3.83	4.48	3.05	5.09	5.56	5.53	6.10
	7/15	4.48	5.39	5.81	6.28	7.05	6.61	9.51
	Average	4.36 (9%)	5.39 (15%)	5.18 (34%)	5.82 (11%)	6.38 (13%)	6.09 (10%)	7.91 (18%)
4K 8 Hr	7/12	4.98	5.33	4.46	6.62	7.45	7.03	9.43
	7/13	4.43	5.40	5.07	5.69	5.97	5.92	5.69
	7/14	4.25	4.62	4.83	5.55	5.95	6.02	6.32
	Average	4.56 (8%)	5.12 (8%)	4.79 (7%)	5.96 (10%)	6.46 (13%)	6.32 (10%)	7.15 (28%)

Table B-7. Summary of relative reactivity metrics for acetaldehyde.

Domain and Episode Day		Relative Reactivities of ALD2 Model Species (Carbon Basis)						
		Avg O_3 (All Cells)	Avg O_3 (O_3 > Std)	Regional Max. O_3	Min. Subst. Error #1	Min. Subst. Error #2	Avg O_3 (MIR-MOIR)	Regional MIR
EKMA		3.83	-	-	3.61	3.69	3.41	3.45
36K 1 Hr	7/12	3.31	2.13	1.19	2.62	2.87	2.53	2.47
	7/13	3.50	2.68	2.51	2.76	2.94	2.67	3.36
	7/14	3.30	2.82	2.20	2.82	2.94	2.72	3.08
	7/15	3.01	2.30	2.20	2.61	2.83	2.59	3.28
	Average	3.28 (6%)	2.48 (13%)	2.03 (28%)	2.70 (4%)	2.90 (2%)	2.63 (3%)	3.05 (13%)
36K 8 Hr	7/12	3.52	3.12	1.77	2.75	3.02	2.61	2.67
	7/13	3.60	2.95	2.48	2.76	2.97	2.61	2.34
	7/14	3.47	2.98	2.42	2.85	2.99	2.72	3.19
	Average	3.53 (2%)	3.02 (3%)	2.22 (18%)	2.78 (2%)	2.99 (1%)	2.65 (2%)	2.73 (16%)
12K 1 Hr	7/12	3.09	2.18	1.40	2.51	2.70	2.48	3.20
	7/13	3.20	2.61	2.44	2.67	2.80	2.60	3.30
	7/14	3.21	2.77	2.12	2.83	2.93	2.75	3.06
	7/15	2.96	2.15	1.86	2.57	2.79	2.53	2.71
	Average	3.11 (4%)	2.42 (13%)	1.95 (23%)	2.65 (5%)	2.81 (3%)	2.59 (5%)	3.07 (8%)
12K 8 Hr	7/12	3.34	2.90	2.02	2.64	2.84	2.57	3.16
	7/13	3.31	2.83	2.51	2.67	2.81	2.58	2.71
	7/14	3.39	2.95	5.14	2.86	2.98	2.79	3.16
	Average	3.35 (1%)	2.90 (2%)	3.22 (52%)	2.72 (4%)	2.88 (3%)	2.65 (5%)	3.01 (9%)
4K 1 Hr	7/12	2.72	2.48	2.58	2.62	2.75	2.59	2.60
	7/13	2.98	2.64	2.07	2.80	2.88	2.70	3.44
	7/14	2.86	2.67	2.60	2.78	2.88	2.74	3.15
	7/15	2.47	2.08	2.22	2.23	2.54	2.26	2.08
	Average	2.76 (8%)	2.46 (11%)	2.37 (11%)	2.61 (10%)	2.76 (6%)	2.57 (8%)	2.82 (21%)
4K 8 Hr	7/12	2.98	2.44	2.33	2.78	2.90	2.70	3.32
	7/13	3.17	2.74	2.04	2.84	2.93	2.73	2.84
	7/14	3.00	2.78	2.79	2.84	2.92	2.84	3.08
	Average	3.05 (3%)	2.65 (7%)	2.39 (16%)	2.82 (1%)	2.92 (1%)	2.76 (3%)	3.08 (8%)

Table B-8. Summary of relative reactivity metrics for ethanol.

Domain and Episode Day		Relative Reactivities of ETOH Model Species (Carbon Basis)						
		Avg O_3 (All Cells)	Avg O_3 (O_3 > Std)	Regional Max. O_3	Min. Subst. Error #1	Min. Subst. Error #2	Avg O_3 (MIR-MOIR)	Regional MIR
EKMA		1.12	-	-	1.02	1.10	0.91	0.76
36K 1 Hr	7/12	1.30	1.04	0.74	0.95	1.10	0.81	0.83
	7/13	1.34	0.83	0.65	0.84	0.98	0.73	0.60
	7/14	1.24	0.97	1.40	0.83	0.94	0.74	0.66
	7/15	1.15	0.82	1.53	0.69	0.84	0.64	0.45
	Average	1.26 (7%)	0.91 (12%)	1.08 (41%)	0.83 (13%)	0.96 (11%)	0.73 (9%)	0.64 (25%)
36K 8 Hr	7/12	1.37	1.35	0.83	1.01	1.17	0.83	0.85
	7/13	1.41	1.07	0.63	0.90	1.06	0.75	0.52
	7/14	1.34	1.12	1.55	0.87	1.01	0.73	0.60
	Average	1.38 (3%)	1.18 (13%)	1.00 (48%)	0.93 (8%)	1.08 (7%)	0.77 (7%)	0.66 (26%)
12K 1 Hr	7/12	1.30	0.99	0.74	0.92	1.07	0.80	0.55
	7/13	1.27	0.80	0.68	0.82	0.92	0.75	0.63
	7/14	1.20	0.94	1.30	0.81	0.90	0.75	0.67
	7/15	1.21	0.77	0.36	0.63	0.79	0.63	0.44
	Average	1.24 (4%)	0.88 (12%)	0.77 (50%)	0.79 (15%)	0.92 (13%)	0.73 (10%)	0.57 (17%)
12K 8 Hr	7/12	1.40	1.34	0.62	1.00	1.16	0.86	0.56
	7/13	1.35	1.03	0.68	0.87	1.00	0.78	0.78
	7/14	1.33	1.13	1.51	0.85	0.98	0.74	0.60
	Average	1.36 (3%)	1.17 (14%)	0.94 (53%)	0.91 (9%)	1.05 (9%)	0.79 (7%)	0.65 (18%)
4K 1 Hr	7/12	0.89	0.56	0.51	0.69	0.75	0.67	0.56
	7/13	1.03	0.68	0.70	0.72	0.77	0.70	0.57
	7/14	0.99	0.79	0.94	0.68	0.76	0.63	0.58
	7/15	1.00	0.67	0.62	0.65	0.75	0.59	0.46
	Average	0.98 (6%)	0.68 (14%)	0.69 (26%)	0.68 (4%)	0.76 (2%)	0.65 (7%)	0.54 (10%)
4K 8 Hr	7/12	0.97	0.76	0.80	0.74	0.81	0.70	0.55
	7/13	1.17	0.78	0.78	0.78	0.87	0.73	0.78
	7/14	1.09	0.99	0.73	0.73	0.84	0.67	0.58
	Average	1.08 (9%)	0.84 (15%)	0.77 (4%)	0.75 (4%)	0.84 (4%)	0.70 (5%)	0.64 (20%)

Table B-9. Summary of relative reactivity metrics for ethane.

Domain and Episode Day		Relative Reactivities of ETHA Model Species (Carbon Basis)						
		Avg O_3 (All Cells)	Avg O_3 (O_3 > Std)	Regional Max. O_3	Min. Subst. Error #1	Min. Subst. Error #2	Avg O_3 (MIR-MOIR)	Regional MIR
EKMA		0.16	-	-	0.14	0.16	0.12	0.09
36K 1 Hr	7/12	0.33	0.32	0.27	0.24	0.29	0.18	0.21
	7/13	0.35	0.22	0.17	0.21	0.26	0.17	0.10
	7/14	0.34	0.27	0.42	0.20	0.25	0.17	0.12
	7/15	0.34	0.26	0.48	0.17	0.24	0.14	0.09
	Average	0.34 (2%)	0.27 (15%)	0.33 (42%)	0.21 (13%)	0.26 (9%)	0.17 (9%)	0.13 (42%)
36K 8 Hr	7/12	0.35	0.39	0.26	0.25	0.31	0.19	0.22
	7/13	0.36	0.29	0.17	0.23	0.28	0.18	0.14
	7/14	0.38	0.33	0.47	0.22	0.29	0.17	0.12
	Average	0.36 (4%)	0.34 (14%)	0.30 (53%)	0.24 (7%)	0.29 (5%)	0.18 (7%)	0.16 (34%)
12K 1 Hr	7/12	0.33	0.29	0.18	0.23	0.29	0.18	0.10
	7/13	0.34	0.21	0.19	0.20	0.25	0.18	0.11
	7/14	0.33	0.25	0.39	0.19	0.24	0.17	0.12
	7/15	0.36	0.24	0.10	0.16	0.23	0.15	0.09
	Average	0.34 (3%)	0.25 (14%)	0.21 (58%)	0.20 (15%)	0.25 (11%)	0.17 (8%)	0.11 (13%)
12K 8 Hr	7/12	0.36	0.38	0.14	0.26	0.31	0.20	0.10
	7/13	0.36	0.28	0.18	0.23	0.27	0.19	0.19
	7/14	0.37	0.32	0.81	0.21	0.27	0.17	0.11
	Average	0.36 (3%)	0.33 (16%)	0.38 (99%)	0.23 (10%)	0.28 (8%)	0.19 (10%)	0.14 (36%)
4K 1 Hr	7/12	0.20	0.12	0.10	0.15	0.17	0.14	0.10
	7/13	0.24	0.14	0.16	0.15	0.17	0.14	0.10
	7/14	0.28	0.20	0.22	0.16	0.20	0.14	0.11
	7/15	0.31	0.20	0.17	0.17	0.22	0.15	0.10
	Average	0.26 (17%)	0.16 (25%)	0.16 (29%)	0.16 (8%)	0.19 (13%)	0.14 (3%)	0.10 (6%)
4K 8 Hr	7/12	0.22	0.17	0.18	0.16	0.18	0.14	0.10
	7/13	0.27	0.17	0.18	0.17	0.20	0.15	0.17
	7/14	0.31	0.27	0.16	0.18	0.23	0.15	0.12
	Average	0.26 (16%)	0.20 (28%)	0.18 (6%)	0.17 (6%)	0.20 (11%)	0.15 (3%)	0.13 (28%)

Table B-10. Summary of relative reactivity metrics for carbon monoxide.

Domain and Episode Day		Relative Reactivities of CO Model Species (Carbon Basis)						
		Avg O_3 (All Cells)	Avg O_3 (O_3 > Std)	Regional Max. O_3	Min. Subst. Error #1	Min. Subst. Error #2	Avg O_3 (MIR-MOIR)	Regional MIR
EKMA		0.07	-	-	0.06	0.06	0.05	0.03
36K 1 Hr	7/12	0.14	0.14	0.15	0.09	0.12	0.07	0.07
	7/13	0.14	0.11	0.09	0.09	0.11	0.07	0.05
	7/14	0.15	0.13	0.17	0.08	0.11	0.07	0.05
	7/15	0.16	0.15	0.17	0.08	0.12	0.06	0.04
	Average	0.15 (8%)	0.13 (12%)	0.15 (28%)	0.09 (8%)	0.11 (5%)	0.07 (6%)	0.05 (28%)
36K 8 Hr	7/12	0.14	0.17	0.13	0.10	0.12	0.07	0.07
	7/13	0.14	0.13	0.08	0.10	0.11	0.07	0.07
	7/14	0.16	0.15	0.19	0.09	0.13	0.07	0.05
	Average	0.15 (7%)	0.15 (10%)	0.13 (42%)	0.09 (3%)	0.12 (5%)	0.07 (5%)	0.06 (23%)
12K 1 Hr	7/12	0.13	0.12	0.10	0.09	0.11	0.07	0.04
	7/13	0.14	0.10	0.10	0.08	0.10	0.07	0.05
	7/14	0.14	0.11	0.16	0.08	0.10	0.06	0.05
	7/15	0.16	0.13	0.07	0.07	0.11	0.06	0.05
	Average	0.14 (9%)	0.12 (10%)	0.11 (34%)	0.08 (10%)	0.11 (4%)	0.07 (7%)	0.05 (5%)
12K 8 Hr	7/12	0.14	0.16	0.08	0.10	0.12	0.08	0.05
	7/13	0.14	0.13	0.09	0.09	0.11	0.07	0.07
	7/14	0.15	0.14	0.75	0.09	0.12	0.06	0.05
	Average	0.14 (5%)	0.14 (11%)	0.31 (125%)	0.09 (6%)	0.11 (4%)	0.07 (10%)	0.05 (22%)
4K 1 Hr	7/12	0.11	0.07	0.06	0.07	0.09	0.07	0.05
	7/13	0.10	0.07	0.08	0.07	0.08	0.07	0.04
	7/14	0.13	0.09	0.08	0.08	0.09	0.07	0.05
	7/15	0.14	0.11	0.09	0.08	0.11	0.07	0.05
	Average	0.12 (15%)	0.08 (25%)	0.08 (18%)	0.08 (7%)	0.09 (14%)	0.07 (1%)	0.05 (8%)
4K 8 Hr	7/12	0.12	0.09	0.09	0.08	0.10	0.07	0.04
	7/13	0.11	0.09	0.09	0.08	0.09	0.07	0.08
	7/14	0.13	0.12	0.07	0.08	0.10	0.07	0.06
	Average	0.12 (8%)	0.10 (20%)	0.08 (13%)	0.08 (3%)	0.09 (7%)	0.07 (4%)	0.06 (28%)

APPENDIX C. DOWNLOADABLE MODEL DATA TABULATIONS

The daily maximum 1-hour and 8-hour average concentrations and the corresponding DDM sensitivity data were used for this study can be downloaded by ftp in either Excel or CSV format. The files are available ftp://ftp.cert.ucr.edu/pub/carter/RRWG/CAMxDDM1. The files and the data they contain are listed in Table C-2. Note that the Excel files with the base case O_3 and sensitivity data contain several sheets, one for each episode day, while the CSV files contain the same data, only with one file per episode day. The Excel files with the O_3 data from the substitution calculations contain two sheets, one for the daily maximum 1-hour averages and one for the 8-hour data, while the CSV files contain the same data, one for each ozone quantification.

Table C-1 give the column headings and the corresponding data in the files for the base case O_3 and O_3 sensitivity data. For the files with the substitution calculation results, the first two columns give the grid locations, and the subsequent sets of 3 or 4 columns give the daily maximum 1-hour or 8-hour average O_3 for the various episode days and cases, as indicated in the column headings.

Table C-1. Data columns in the files with the base case O_3 and O_3 sensitivity results.

Label	Description
Grid Loc col, row	The grid location for the data
Max O_3 Hr	The hour that the O_3 maximum occurred. Note that for the 8-hour data this is the *starting* hour.
Max O_3 Conc.	The daily maximum 1-hour or 8-hour average ground-level ozone concentration, in ppm, for that grid location.
O_3 Sensitivities	DDM sensitivities of the ground-level daily maximum 1-hour or 8-hour O_3 data in the grid cell to the various types of emissions. Labels for types of emissions are as follows:
VOC	Total VOC emissions (biogenic + anthropogenic)
NO_x	Total NO_x emissions
AVOC	Total anthropogenic VOC emissions
MOBL	Total mobile source portion of anthropogenic VOC emissions
AREA	Total area source portion of anthropogenic VOC emissions
PNT	Total point source portion of anthropogenic VOC emissions
BIO	Total biogenic VOC emissions
ROG	Base ROG mixture, computed using the sensitivities for the CB4 model species constituents
PAR … CO	CB4 model species, as indicated on Table 1.

Table C-2. Summary of files containing ozone and DDM data used in this report

File Name	Format	O_3 Quantification	Domain Size	Episode Day
		Base Case O_3 and O_3 Sensitivity Data		
1hr4kdat.xls	Excel	1 Hour	4K	7/12 – 7/15
8hr4kdat.xls	Excel	8 Hour	4K	7/12 – 7/14
1hr12kdat.xls	Excel	1 Hour	12K	7/12 – 7/15
8hr12kdat.xls	Excel	8 Hour	12K	7/12 – 7/14
1hr36kdat.xls	Excel	1 Hour	36K	7/12 – 7/15
8hr36kdat.xls	Excel	8 Hour	36K	7/12 – 7/14
1hr4k12.csv	CSV	1 Hour	4K	7/12
8hr4K12.csv	CSV	8 Hour	4K	7/12
1hr4k13.csv	CSV	1 Hour	4K	7/13
8hr4K13.csv	CSV	8 Hour	4K	7/13
1hr4k14.csv	CSV	1 Hour	4K	7/14
8hr4K14.csv	CSV	8 Hour	4K	7/14
1hr4k15.csv	CSV	1 Hour	4K	7/15
1hr12k12.csv	CSV	1 Hour	12K	7/12
8hr12k12.csv	CSV	8 Hour	12K	7/12
1hr12k13.csv	CSV	1 Hour	12K	7/13
8hr12k13.csv	CSV	8 Hour	12K	7/13
1hr12k14.csv	CSV	1 Hour	12K	7/14
8hr12k14.csv	CSV	8 Hour	12K	7/14
1hr12k15.csv	CSV	1 Hour	12K	7/15
1hr12k12.csv	CSV	1 Hour	36K	7/12
8hr36k12.csv	CSV	8 Hour	36K	7/12
1hr36k13.csv	CSV	1 Hour	36K	7/13
8hr36k13.csv	CSV	8 Hour	36K	7/13
1hr36k14.csv	CSV	1 Hour	36K	7/14
8hr36k14.csv	CSV	8 Hour	36K	7/14
1hr36k15.csv	CSV	1 Hour	36K	7/15
		O_3 Data from Substitution Calculations		
Subst4kdat.xls	Excel	1 and 8 Hour	4K	7/12 – 7/15
Subst12kdat.xls	Excel	1 and 8 Hour	12K	7/12 – 7/15
Subst36kdat.xls	Excel	1 and 8 Hour	36K	7/12 – 7/15
1hr4ksubst.csv	CSV	1 Hour	4K	7/12 – 7/15
8hr4ksubst.csv	CSV	8 Hour	4K	7/12 – 7/14
1hr12ksubst.csv	CSV	1 Hour	12K	7/12 – 7/15
8hr12ksubst.csv	CSV	8 Hour	12K	7/12 – 7/14
1hr36ksubst.csv	CSV	1 Hour	36K	7/12 – 7/15
8hr36ksubst.csv	CSV	8 Hour	36K	7/12 – 7/14